"Music is pleasing not only because of the sound but because of the silence that it is in it"

- Thomas Merton

University of Alberta

Theoretical Considerations For Biological Control: A case study with Scentless Chamomile

by

Tomas de-Camino-Beck 

A thesis submitted to the Faculty of Graduate Studies and Research in partial fulfillment of the requirements for the degree of **Doctor of Philosophy**.

in

Environmental Biology and Ecology

Department of Biological Sciences

Edmonton, Alberta
Fall 2006

Your file Votre référence
ISBN: 978-0-494-23013-8
Our file Notre référence
ISBN: 978-0-494-23013-8

Abstract

The introduction of invasive species is a significant driving force of global change. Weed scientists, resource managers, conservation and restoration biologists have focused their attention on the control of invasive species trying to understand, mitigate and prevent impacts of biological invasions. Biological control, the control of invading organisms by means of their natural enemy, is one way to prevent impacts of biological invasions. Mathematical models are a useful tool for the design of biological control strategies. These models allow for the analysis of population growth and spread, and for determination of aspects of the life cycle of the organisms which can be manipulated to control populations. In this dissertation I use matrix models to study the life history of invading organisms. First, a new method for the calculation of an analytical net reproductive rate formula is derived. I show with examples how this formula can be applied to study the control of invading organisms, particularly weeds. I extend these results, to calculate a mean and variance of the generation time. Later in the thesis, I use coupled map lattice models, a time and space discrete formalism, to calculate rate of spread for scalar and matrix population models. I derive formulae for the wave speed for constant and stochastic environments for coupled map lattices. I then apply these to scentless chamomile, an invasive weed distributed all across North America. The methods for calculation of net reproductive rate and generation time, and formulae for rate of spread in coupled map lattices, are new to biological invasions and biological control.

Acknowledgements

First I would like to thanks my supervisor Mark Lewis. He took me as a student unconditionally when I was going through difficult times. He also encouraged me to find my way as a student, researcher and scientist. No idea was too crazy for him. I would also specially thank Mark Dale, for giving me good advice at a critical time.

I would like to thanks my committee members Alec McClay and Jens Roland for support and comments on early drafts. Also a special thanks to Marjorie Wonham who gave me a lot of support and gave me useful comments on my drafts. Also thanks to Caroline Bampfylde for giving me quick feedback before submitting my thesis to the committee members.

Thanks to the Biology department for providing my studentship, and MITACS for financial support. The Alberta Research Council for providing me with the tools and space to do my fieldwork.

Thanks to Eric Noonburg, Pauline van den Driessche and Alex Potapov for thorough revisions on my manuscripts and advice in solving some mathematical and biological issues.

Thanks also to Chris Jerde for help doing fieldwork and statistical advice. Darcy Visscher, Marty Krkosec, Jungmin Lee and Raluca Eftimie for help in my field work, and the Lewis lab for all the support on presentations. Jason Young for providing classified maps.

A very special thanks to my wife Marcela Vega. She left aside her career, and left her beloved country so I could get my PhD. She also helped me with manuscripts, field work, lab work and all the things that made my time as a student easier. Thanks to my parents who always gave me support in whatever I was doing.

This thesis is dedicated to my wife, my daughter and my parents

Contents

List of Tables

List of Figures

Chapter 1

Introduction

The introduction of invasive species is a significant driving force of global change, affecting biodiversity, serving as a vector of diseases, altering ecosystem function and having considerable economical impacts on production lands (Vitousek et al., 1996). Weed scientists, resource managers, conservation and restoration biologists have focused their attention on the control of invasive species, trying to understand, mitigate and prevent impacts of biological invasions (Sakai et al., 2001). Biological invasions are complex, and successful control involves the understanding of the invader's population dynamics during the arrival, establishment and spread phases of invading species (Williamson, 1996).

One way to control invading organisms is the introduction of natural enemies to control the host. This method is known as biological control by natural enemies (Huffaker and Messenger, 1976). The first successful documented case of biological control was the introduction of the vedalia beetle (*Rodalie cardinalis*) in 1888 to control cottony-cushion scale (*Icerya purchasi*), which was affecting citrus plantations in California. Biological control as a field of study became formal with the work of Varley and Gradwell (1970) and Huffaker and Messenger (1976), which incorporated ecological theory in the study of host-control agent dynamics.

Biological control is a field where mathematical modelling of invasions has a lot to offer (Fagan et al., 2002; Shea, 2004). The study of biological control is a two-fold problem. On the one hand, control agents need to be host specific, produce effective damage on the host, and capable of establishing a permanent population (McFadyen, 1998). On the other hand, detailed biology and life history information of the host are needed, in order to determine if growth and spread can be controlled (Shea et al., 2005). Both of these can be studied using mathematical models. In this thesis, I study how a weed can be controlled by analyzing its life history and population spread.

Biological control of invasive species, alone or combined with other strategies, can be an effective method for the reduction of unwanted invasive species. However,

a biocontrol system is complicated and methods for quantifying how much of an impact a control strategy can cause are essential for the successful application of this method. One way of modelling and analyzing potential effects of biocontrol, is using matrix population models (Murdoch and Briggs, 1996). Matrix models are discrete time models, that incorporate age or stage population structure, to model population dynamics (Caswell, 2001). They were first introduced by Leslie (1945) to model age-structured populations. Because some biological and physiological stages are a better representation of the life cycle of organisms, Leslie models were later extended to stage classified life cycles by Lefkovitch (1965). Matrix models are simple, intuitive and allow for a realistic representation of the life cycle of the organism (Murdoch and Briggs, 1996).

Matrix models have been widely used for the study of biological control of weeds (Shea, 2004). Using a method called elasticity/sensitivity analysis of the population growth rate, it is possible to establish which events in the life cycle of the organism, when perturbed, have the most impact on population growth (Caswell, 2001). Hence, those events should be the target of biocontrol efforts (e.g. Parker, 2000; Shea and Kelly, 1998; Krivan and Havelka, 2000).

The net reproductive rate (R_0), the number of newborn individuals that one individual can produce over its lifetime, can also be calculated from a simple decomposition of the projection matrix in matrix models (Cushing and Zhou, 1994). R_0 is measured over a generation time, and thus is related to population growth rate. This parameter is a simplistic descriptor of the life cycle of an organism, but its study has vital implications for control (Myers and Bazely, 2003).

The calculation of population growth can be done directly on the graph representation of the life cycle (Caswell, 2001). Methods for working on graphs, to solve systems of linear equations, were pioneered by Mason and Zimmermann (1960). This graph theoretic approach has been little applied currently being used mostly in loop analysis (Caswell, 2001). I show in this thesis that these methods allow for the calculation of an analytical formula for the net reproductive rate, and further analysis of the life cycle graph is possible, shifting the focus of life cycle graph analysis to the analysis of pathways that contribute to the net reproductive rate.

The emerging discipline of biological invasions is also a fertile new ground for the development of new theoretical tools. Elton (1958) was the first to describe the ecology of invasive species and since his work was published, there has been substantial progress in the formalization of processes involved in arrival, establishment and spread of invasive organisms. The use of mathematics to describe the spread of invading organisms had a groundbreaking start with works of Fisher (1937) and Skellam (1951), who predicted the asymptotic rate of spread of populations using diffusion equations. Not only were these models interesting and mathematically robust, but they allowed the integration of empirical data and the prediction of population spread (Andow

et al., 1990; Hastings et al., 2005; Shigesada and Kawasaki, 1997). Many years later, Kot et al. (1996) introduced integro-difference equations to invasions theory and showed how the rate of spread can be calculated by using a dispersal kernel that describes the probability of an individual moving in a continuous space and discrete time, while the population grows locally.

Environmental and demographic variability can also have an effect on spread. Thus models of spread that incorporate stochasticity in diffusion models, integro-difference equation and others, have also been developed that account for variation in environmental or demographic parameters (Hastings et al., 2005; Lewis and Pacala, 2000; Neubert et al., 2000).

At certain scales, and because of landscape heterogeneity, it is often appropriate to replace continuous space with a discrete one (Keitt et al., 2001; Levin, 1992). Discrete space is usually done by coupling differential equations on a discrete lattice (Keitt et al., 2001; Owen and Lewis, 2001), using cellular automata (Wang et al., 2003; Sondgerath and B., 2002; Cannas et al., 2003; Marco et al., 2002) or using coupled map lattices (Bevers and Flather, 1999). Coupled map lattice models are discrete-space and time models (Ouchi and Kaneko, 2000), similar to integro-difference equations. The rate of spread equation, derived for integro-difference models, can also be used in discrete space (Weinberger, 1982). However, to my knowledge, this has not been done explicitly before. In this thesis, I work with these models and derive analytical calculations of the rate of spread, relate them to integro-difference equations, and show how they can be applied to study the spread of an invasive species.

Matrix models can also be extended to incorporate space (Neubert and Caswell, 2000). Spatial matrix population models are useful to estimate the rate of spread and determine which transitions in the life cycle can be potential targets for control, to reduce the rate of spread (e.g Neubert and Parker, 2004; Buckley et al., 2005). These matrix integro-difference models combine the analysis of life history of organisms with their ability to spread (Shea, 2004), effectively linking invasion theory with biological control. I also extend these results to coupled map lattices.

The study of invasions, and particularly the analysis of spread rate, are essential to biological control. Fagan et al. (2002) and Owen and Lewis (2001), for example, showed how, by calculating rates of spread of host and control agent, it can be determined if the control agent will be successful in controlling the spatial spread of its host. Invasion theory can contribute to biological control in (Fagan et al., 2002): 1) studying the spread of hosts and control agents, 2) understanding of role of long-distance dispersal, 3) analysis of structured population dynamics, 4) detectability of invasive species, and 5) incorporating stochasticity.

1.1 Thesis objectives

The main motivation of this thesis research is to formalize ideas that can solve problems in biological control and biological invasions research at both theoretical and practical levels. Using scentless chamomile (*Matricaria perforata*, Family: Asteraceae) as a case study, I develop a method for obtaining the net reproductive rate and generation time, based on the life cycle. I also derive rate of spread formulae for application to matrix coupled map lattices. The general objectives are: 1) derive a formula for the net reproductive rate based on the life cycle of organisms , 2) use the net reproductive rate to analyze control of invading organisms, 3) analyze the spread using matrix coupled map lattices.

1.2 Thesis outline

Through the thesis, I develop a theoretical framework, based on matrix population models, for the analysis of invasive species, using scentless chamomile as an example. Chapter 2 and 3 are background and data description chapters, and Chapters 4, 5 and 6 are theoretical.

Chapter 2 is a general review of biological control. Historical, economical and ecological issues of biocontrol are presented. This provides an introductory context for the remainder of the thesis. In Chapter 3, field data on scentless chamomile collected in Vegreville, Alberta, Canada, are described and using matrix models and classic demographic analysis some implications for biological control are drawn.

In Chapter 4, the derivation of a new method for the calculation of the net reproductive rate is developed and all mathematical background is provided. This method is then applied to scentless chamomile and other weeds, to illustrate the applicability of the method.

Chapter 5 uses the method derived in Chapter 4, and expands it by deriving a formula for the calculation of the generation time. Starting with some general description of life cycle graphs, I then derive some general principles from these examples.

The focus of Chapter 6 is the derivation of the rate of spread formulae for matrix coupled map lattices. This chapter includes models for constant and stochastic environments and heterogeneous landscapes. Throughout the chapter, scentless chamomile is used as an example, and the rate of spread is estimated.

Chapter 7 discusses general conclusions and integrates the models in a general framework. Implications of the models developed are discussed.

Bibliography

Andow, D., P. Kareiva, S. Levin, and A. Okubo. 1990. Spread of invading organisms. Landscape Ecology **4**:177–188.

Bevers, M. and C. Flather. 1999. Numerically exploring habitat fragmentation effects on populations using cell-based coupled map lattices. Theoretical Population Biology **55**:61–76.

Buckley, Y., E. Brockerhoff, L. Langer, N. Ledgard, H. North, and M. Rees. 2005. Slowing down a pine invasion despite uncertainty in demography and dispersal. Journal of Applied Ecology **42**:1020–1030.

Cannas, S., D. Marco, and S. Paez. 2003. Modelling biological invasions: Species traits, species interactions, and habitat heterogeneity. Mathematical Biosciences **183**:93–110.

Caswell, H. 2001. Matrix Population Models: Construction, Analysis, and Interpretation. 2nd edition. Sinauer Associates.

Cushing, J. and Y. Zhou. 1994. The net reproductive value and stability in matrix population models. Natural Resource Modeling **8**:297–333.

Elton, C. 1958. The Ecology of Invasions by Animals and Plants. Methuen, London.

Fagan, W., M. Lewis, M. Neubert, and P. Van Den Driessche. 2002. Invasion theory and biological control. Ecology Letters **5**:148–157.

Fisher, R. 1937. The wave of advance of advantageous genes. Annals of Eugenics **7**:355–369.

Hastings, A., K. Cuddington, K. Davies, C. Dugaw, S. Elmendorf, A. Freestone, S. Harrison, M. Holland, J. Lambrinos, U. Malvadkar, B. Melbourne, K. Moore, C. Taylor, and D. Thomson. 2005. The spatial spread of invasions: new developments in theory and evidence. Ecology Letters **8**:91–101.

Huffaker, C. and P. Messenger. 1976. Theory and Practice of Biological Control. Academic Press.

Keitt, T. H., M. A. Lewis, and R. D. Holt. 2001. Allee effects, invasion pinning, and species' borders. American Naturalist **157**:203–216.

Kot, M., M. Lewis, and P. Van den driessche. 1996. Dispersal data and the spread of invading organisms. Ecology **77**:2027–2042.

Krivan, V. and J. Havelka. 2000. Leslie model for predatory gall-midge population. Ecological Modelling **126**:73–77.

Lefkovitch, L. 1965. Study of population growth in organisms grouped by stages. Biometrics **21**:1–18.

Leslie, P. 1945. On the use of matrices in certain population mathematics. Biometrika **33**:183–212.

Levin, S. A. 1992. The problem of pattern and scape in ecology. Ecology **73**:1943–1967.

Lewis, M. and S. Pacala. 2000. Modeling and analysis of stochastic invasion processes. Journal of Mathematical Biology **41**:387–429.

Marco, D., S. Paez, and S. Cannas. 2002. Species invasiveness in biological invasions: A modelling approach. Biological Invasions pages 193–205.

Mason, S. and H. Zimmermann. 1960. Electronic Circuits, Signals, and Systems. Wiley.

McFadyen, R. 1998. Biological control of weeds. Annual Review of Entomology **43**:369–393.

Murdoch, W. and C. Briggs. 1996. Theory for biological control: Recent developments. Ecology **77**:2001–2013.

Myers, J. and D. Bazely. 2003. Ecology and Control of Introduced Plants. Cambridge University Press.

Neubert, M. and H. Caswell. 2000. Demography and dispersal: Calculation and sensitivity analysis of invasion speed for structured populations. Ecology **81**:1613–1628.

Neubert, M., M. Kot, and M. Lewis. 2000. Invasion speeds in fluctuating environments. Proceedings of the Royal Society of London Series B-Biological Sciences **267**:1603–1610.

Neubert, M. and I. Parker. 2004. Projecting rates of spread for invasive species. Risk Analysis **24**:817–831.

Ouchi, N. and K. Kaneko. 2000. Coupled maps with local and global interactions. Chaos **10**:359–365.

Owen, M. and M. Lewis. 2001. How predation can slow, stop or reverse a prey invasion. Bulletin of Mathematical Biology **63**:655–684.

Parker, I. 2000. Invasion dynamics of *Cytisus scoparius*: a matrix model approach. Ecological Applications **10**:726–743.

Sakai, A., F. Allendorf, J. Holt, D. Lodge, J. Molofsky, K. With, S. Baughman, R. Cabin, J. Cohen, N. Ellstrand, D. McCauley, P. O'Neil, I. Parker, J. Thompson, and S. Weller. 2001. The population biology of invasive species. Annual Review of Ecology and Systematics **32**:305–332.

Shea, K. 2004. Models for improving the targeting and implementation of biological control of weeds. Weed Technology **18**:1578–1581.

Shea, K. and D. Kelly. 1998. Estimating biocontrol agent impact with matrix models: *Carduus nutans* in New Zealand. Ecological Applications **8**:824–832.

Shea, K., D. Kelly, A. Sheppard, and T. Woodburn. 2005. Context dependent biological control of an invading thistle. Ecology **In press**.

Shigesada, N. and K. Kawasaki. 1997. Biological Invasions : theory and practice. 1st ed edition. Oxford University Press.

Skellam, J. 1951. Random dispersal in theoretical populations. Biometrika **38**:196–218.

Sondgerath, D. and S. B. 2002. Population dynamics and habitat connectivity affecting the spatial spread of populations – a simulation study. Landscape Ecology pages 57–70.

Varley, G. and G. Gradwell. 1970. Recent advances in insect population dynamics. Annual Review of Entomology **15**:1–24.

Vitousek, P., C. Dantonio, L. Loope, and R. Westbrooks. 1996. Biological invasions as global environmental change. American Scientist **84**:468–478.

Wang, J., M. Kropff, B. Lammert, S. Christensen, and P. Hansen. 2003. Using ca model to obtain insight into mechanism of plant population spread in a controllable system: annual weeds as an example. Ecological Modelling **166**:277–286.

Weinberger, H. 1982. Long-time behavior of a class of biological models. Siam Journal on Mathematical Analysis **13**:353–396.

Williamson, M. 1996. Biological Invasions. Springer.

Chapter 2

Biological Control of Weeds

2.1 Introduction

2.1.1 Biological Control Definition

Biological control is the control of host populations using natural enemies (Wilson and Huffaker, 1976). The goal of biological control is to reduce host population growth over an ecologically long period (Murdoch and Briggs, 1996). Strictly, here we refer to biocontrol as the use of parasites, predators and pathogens to regulate pest populations (Harris, 1993; DeBach and Rosen, 1991), although the term has been used for other forms of non-chemical control (Harris, 1993). The premise of biological control is that organisms that become pests in a region, have natural enemies that in their natural habitats keep their hosts under control, hence when the natural enemies are introduced, the pest populations should be controlled (Huffaker and Messenger, 1976). Biological control is an important alternative (to chemical and mechanical techniques) for controlling pests. Biological control is different form other methods (chemical and mechanical) in the following ways (Radosevich et al., 1997): 1) does not necessarily kill the host, 2) slow acting (it takes many generations), 3) relatively inexpensive, 4) selective, 5) has few side effects, and 6) biocontrol is often permanent.

There are several strategies in which biocontrol can be applied (Waage and Greathead, 1988): *Classical biological control*, where an exotic control agent is introduced to obtain long term control of a pest; *Inoculation*, where periodic establishments of the control agents are forced so the control agent persists; *Augmentation*, where supplemental release of indigenous species is included in the biocontrol; and *Inundation* were a large number of control agents are released to control a single pest generation. Although classical biocontrol still is an important part of integrated pest management programs (IPM), a lot of attention has been shifted to innudative methods (Waage and Greathead, 1988).

In this Chapter, I explore the historical, ecological, economical and practical application of biological control. The first section gives a brief historical background. Next I mention some differences in the biological control of weeds as compared to other types of hosts. Later sections talk about the biocontrol research process, and economical considerations of biological control. The section *biological control and ecology* explores some of the fields of ecological research that are relevant to biological control.

2.1.2 Historical Remarks

Although historically biological control was used informally, the introduction of the vedalia bettle *Rodalia cardinalis* was one of the first well documented successful biological control cases (Waage and Greathead, 1988). This bettle was introduced in 1888 from Australia to control the cottony-cushion scale *Icera purchasi* which was threatening to destroy citrus plantations in California and successfully controlled this pest (Huffaker and Messenger, 1976). This successful case generated some enthusiasm about using natural enemies to control pest population (Huffaker and Messenger, 1976; Waage and Greathead, 1988). The fact that pesticides would induce resistance in many pests, and that most of them had residual effects at that time (around 1940) the importance of ecological considerations made biological control a good alternative to classical pest control (Huffaker and Messenger, 1976). For example, the use of insecticides such as DDT was unsuccessful and actually increased the population of pests like the cottony-cushion scale (DeBach and Rosen, 1991).

Another interesting example is the control of the sugarcane leafhopper, *Perkinsiella saccharicida* in 1900, that attacked sugarcane plantations in Hawaii, and was controlled by the introduction of several natural enemies from Australia (Huffaker and Messenger, 1976). A second good example of successful biological control, is the control of the cacti *Opuntia sp.* introduced in Australia in 1925 by the cactus moth *Cactoblastis cactorum* (Huffaker and Messenger, 1976; Knight, 2001). There are many unsuccessful cases as well, including the introduction of toads(*Bufo marinus*) in 1935 in Australia to control sugarcane beetles, that had adverse results on the local biodiversity (Knight, 2001). Biocontrol increased in popularity from 1920-1945, and then declined, due to the newly introduced synthetic organic insecticides, and in 1955 began a new wave of popularity (Perkins and Garcia, 1999).

In the theoretical front, Varley and Gradwell (1970) and Huffaker and Messenger (1976) formalized the understanding of biological control, by incorporating ecological concepts. They suggested that the understanding of density-dependent processes were important to stabilize and control pest populations. Some of the desirable attributes of natural enemies, to achieve control of a pest, were host-specificity, synchrony with pest, ability to increase rapidly and high rate of successful search. All of these

attributes came mainly from the dynamic properties of Nicholson-Bailey models (Murdoch et al., 1985). From these theoretical models, the concept of successful biocontrol was based on the stability of low pest densities. However, it has been argued that a more broad definition of stability of biocontrol system is needed, where simple persistence and bounded stochasticity are considered (Thorarinsson, 1990).

Murdoch and Briggs (1996) reviewed the contributions of ecological theory to biological control. Some of the issues mentioned included: 1) parasitoid aggregation can induce stability to the host-parasitoid system, 2) metapopulation, 3) spatiotemporal refuges and iv) ratio (predator-prey) dependence and density dependence. Most of this issues are specifically related to host-parasitoid systems but should also be applicable to predation and pathogens. They also mention the practical uses of matrix population models, that can incorporate realism and are easy to use and interpret. For example, Shea and Kelly (1998) use matrix population models to determine the susceptibility of different stages of nodding thistle (*Carduus nutans*) in New Zealand. With the sensitivity matrix they conclude that by suppressing germination and reducing seedbank inputs, this thistle can be controlled.

Nowadays there is an increase in the use of modelling tools to study biocontrol systems and the incorporation of spatial considerations in biological control. Barlow (1999) presents a review of modelling techniques used for biological control. In this review, most of the models are applied to host-parasitoid systems followed by weed-herbivore and insect-pathogen; and most of them are applied to classical biocontrol. How valuable models and theory are is still controversial, because many of the deterministic Nicholson-Bailey and Lotka-Volterra types of models are unrealistic (Myers and Bazely, 2003). There is a strong need to link models with field observations as models become more complicated and parameter estimation is needed to give models some realism (Murdoch and Briggs, 1996). Another front that is becoming important are the possible damaging effects that biological control can have, since many of the initial biological control programs have negative impact. This issue is considered in the Section "Problems and Risks".

2.1.3 Biological Control of Weeds

Invasive weeds constitute a major problem since they have direct impact on rangeland and wildland, threatening biodiversity and reducing production in the farming industry (Bangsund et al., 1999; Masters and Sheley, 2001; Ditomaso, 2000). In weed management, organic pesticides have played a major role in crop production. However, the temporary solution of chemical pesticides, weed resistance, safety of food products, in addition to the costs of developing, testing and producing synthetic herbicides, have created a good opportunity for biological control of weeds (Rao, 2000; Goeden and Andres, 1999). Control of invasive plants are an important part of

biological control. For example in Canada 881 exotic plants have become established, representing 28% of the total flora of the country (Parker and Gill, 2002). Many of these have become noxious plants with important consequences for crop production and local biodiversity.

Biological control of weeds has followed a different path than control of other pests (McFadyen, 1998). Less than 400 invertebrates and fungi have been introduced to control weeds as opposed to more than 5000 to control insects (Knight, 2001). About 259 species of invertebrates have been used, most of them insects (254), with about 62% of them becoming established, and 25% of these control agents being successful (Bellows and Headrik, 1999).

In biological control of weeds as opposed to biocontrol of other pests, a considerable part of the research process is focused on host-specificity tests (McFadyen, 1998). As McFadyen (1998) suggests, host-specificity is said to be the "holy grail" of biocontrol. In general the weed biocontrol community has been careful in testing host-range, to avoid non-target impacts, and in this case they have been fairly successful (Bellows and Headrik, 1999). In addition to this, biocontrol of weeds, instead of using mass releases of large numbers of enemies, has focused on the ecological context and the establishment of a stable population of biocontrol agents (Bellows and Headrik, 1999; Harris, 1993).

Another important aspect of biological control of weeds is that weed biocontrol practitioners have compiled a comprehensive catalog of weeds and the use of biological control agents to control them (Julien et al., 1992). Julien et al. (1992), provide a good catalogue of world wide biocontrol research programmes. Mason and Huber (2002) provide a good revision of biocontrol programmes in Canada from 1981 to 2000, and has an important section about control of weeds.

2.2 Biocontrol Research Process

The biocontrol research process starts when a system is elected for biological control. Not all cases of attacks by pests are suitable for biological control and some scoring systems like McClay's (Peschken and McClay, 1992) and others (Goeden, 1983), based on economical and biological factors, are used to choose systems for which biocontrol is a good option and could lead to successful control.

Once a pest has been detected, and biological control is thought to be appropriate, a biological control programme follows. McFadyen (1998) suggests that some of the steps in the research and application of biological control are Overseas exploration, selection and testing of agents (pre-release studies), rearing and release, evaluation and monitoring (see section Evaluation).

2.2.1 Pre-release Studies

Agent selection is a critical step, in terms of finding an appropriate agent with narrow host range because this procedure is costly and time consuming, and the success and risks of the biocontrol programme depend heavily on this step (McFadyen, 1998; Schaffner, 2001). The general process consists of reducing the natural enemy complex to a few species for introduction (Waage, 1990). At this stage, pre-release studies are performed, consisting of verification of the taxonomic status of the pest and associated enemies, evaluation of the host range (list of species used as hosts by the biocontrol agents (Bernays and Chapman, 1994)) of the biocontrol candidates, population ecology of both agent and pest, and study of the potential damage that the agent inflicts on the pest (Schaffner, 2001). Pre-release studies can be considered in the area of origin of the pest, and studies in the target area (Shroeder et al., 1996)

.

The common methods for evaluating control agents and their interaction with their hosts are life-tables and manipulative field experiments (Luck et al., 1999). Life tables track the number of individuals surviving in the life cycle of an organism (Bellows and van Driesche, 1999). Life tables can be used to evaluate the quantitative impact of natural enemies (i.e. trying to reduce $\mathbf{R}_0$) (Bellows and van Driesche, 1999). Experimental manipulations of predator presence/absence allow for the identification of predator species and also the estimation of their impact (Luck et al., 1999). These methods include the use of cages to evaluate pest population changes with and without the control agents and also for host-range tests (Luck et al., 1999). In weed biocontrol, open field tests are used as part of host-specificity determinations (Cristofaro, 1995). In such studies agents exercise free choice of hosts without the use of cages.

2.2.2 Rearing and Release

The initial goal of biocontrol agent releases is to establish its populations effectively in the region where control is desired (Shea et al., 2002). However, effective release its very complicated and a lot of uncertainties (biological and environmental) are involved. Many control agents fail to establish in the field (Memmott et al., 1998). Usually releases involve the release of a small population of control agents. Because these populations are small, they have a high probability of extinction due to demographic stochasticity, environmental variability, and Allee effects (Grevstad, 1999). It has been suggested that large releases can overcome these problems but large releases can have a high probability of extinction (Memmott et al., 1998). A successful release involves a trade-off between size of release and number of releases (Grevstad, 1999; Memmott et al., 1998). Using stochastic simulation models Grevstad (1999) found that for variable environments, a large number of small releases is optimal.

When an Allee effect with constant environment is suspected, one release would be optimal. It has been suggested by Shea et al. (2002) that, because of the uncertainties in biocontrol, active adaptive management, where learning about past experiences is included in the design of agent selection and release strategies, should be an active component of biocontrol programmes.

2.2.3 Evaluation and Monitoring

Evaluation and monitoring is essential in biocontrol programmes. In the past, it was thought unnecessary to follow up and evaluate biocontrol programmes (McFadyen, 1998). This engendered criticism, specifically that the risks associated with biological control were not considered (see the section Problems and Risks). Most evaluations are done after release and establishment of the control agent, but only variables such as spread and presence are recorded, without much consideration of the changes in population dynamics (McFadyen, 1998; Myers and Bazely, 2003). In a literature survey of methods in weed biocontrol, McClay (1995) found that only a small fraction of surveys used formal experimental methods, and only a few of those measure some weed population variables.

It has been reported that about 17% of the insect pest biological control programmes have been successful over the last 100 years (Bellows, 2001). Estimates of success of herbivorous insects for biological control in the United States, for example, show 40% of projects with some success and 20% with significant control (Louda et al., 1997). Conclusions based on success stories are difficult to draw, since a lot of factors are not considered, such as the actual dynamics or the fact that it was the agent which actually controlled the pest (Perkins and Garcia, 1999).

Most of the biological control monitoring studies focus on detecting if the biological control agent is still present or not in a release area, or if it has spread from the release area (e.g Schaad et al., 2001; Suckling et al., 1999; Bidochka et al., 1996). Some advanced techniques, like analysis of remote sensing data, could be used for monitoring, when levels of infestation reach landscape levels, and the pest is spectrally detectable. In a study by Venugopal (1998), they calculated NDVI (Normalized Difference Vegetation Index) from SPOT satellite data to detect water hyacinth geographical expansion in India. With this data, the author was able to detect new areas of infestation and concluded that biological control, although effective locally, had limited effect in controlling re-invasions. Another similar study by Williams and Hunt (2002) used Airborne Visible Infrared Imaging Spectrometer (AVIRIS) imagery to detect leafy spurge distribution and abundance in northeastern Wyoming. These techniques can be useful to estimate the change in weed coverage over time as a result of weed management.

2.3 Critical Issues in Biological Control

2.3.1 Economical Importance

Suppressing pest organisms is not only a biological problem, but also a social and economical one (Perkins and Garcia, 1999). Perkins and Garcia (1999) point out that historically, biocontrol started as a method for controlling agricultural pest problems and that the main application of biocontrol is related to economical factors of increasing profits reducing costs. It has been difficult to quantify the actual economic cost-benefit of biological control (Perkins and Garcia, 1999). Harris (1979), proposed that the costs of biological control should be measured in scientists years, that is, the technical and administrative costs to support one scientist for one year. The USDA reported that in their laboratories and agencies, there are 190 scientist years devoted to biological control (Perkins and Garcia, 1999). In 1976 one scientist-year in biological control cost around US$80,000 (Gutierrez et al., 1999). In order to estimate more accurately the costs of biocontrol we have to consider the costs of: 1. baseline research, 2. foreign exploration, 3. shipping, 4.quarantine, 5. mass rearing, 6. field releases and 7. post release evaluation (Parker and Gill, 2002).

Although it is believed that biocontrol is very expensive, there is no evidence to suggest that biological control using natural enemies is more expensive than alternative forms of control (Perkins and Garcia, 1999). On the contrary, some cases of classical biocontrol seem to be very cost-effective (Perkins and Garcia, 1999; Gutierrez et al., 1999; Bangsund et al., 1999). Biological control is also economically beneficial if one considers that chemical pesticides can increase the populations of secondary pests to unmanageable levels (Gutierrez et al., 1999). As mentioned before, a good example was the use of DDT which increased the population of scales attacking citrus in California (DeBach and Rosen, 1991)

Another good example of the economic benefits of biocontrol is the effective control of cottony cushion in California in 1888. The current citrus crop is producing US$500 million per year (Gutierrez et al., 1999). In a study of the economic impact of leafy spurge in the Great Northern Plains in the US, Bangsund et al. (1999) estimated a beneficial primary and secondary impact of US$58.4 million. These estimations are based on the expected ability of the control agent to reduce leafy spurge, projected to the year 2025. In mango plantations in Benin, biological control was used to control the mango mealybug *Rastrococcus invadens Williams* that was accidentally introduced in West Africa in the 1980's (Vogele et al., 1991; Bokonon-Ganta et al., 2002). It was estimated that economic production was increased by US$50 million in a year due to biocontrol, and a 20 year projection suggests an estimated production of US$ 531 million, with a cost of biocontrol of only US$ 3.66 million (Bokonon-Ganta et al., 2002). A similar result was obtained earlier by Vogele et al. (1991) in

Togo, showing that biocontrol of the mealybug was very cost-effective. Cost-effective biocontrol has also been shown for the biological control of the water hyacinth in Benin(De Groote et al., 2003), and the spiny blackfly in Swaziland (Van den Berg et al., 2000) to name a few.

All these examples project the benefits of biocontrol assuming that the control agent will maintain the pest at low level, or eliminate it entirely. Another problem with some of these estimations is that there are no reports on biocontrol programmes that failed and the resulting economic loses.

In a study by Nordblom et al. (2002) an optimal release strategy was designed constrained by economical variables. They estimated the costs of the effect of Paterson's curse and other weeds (*Echium spp.*) and the effect of the control agent, the crown weevil (*M. larvatus*). To obtain an optimal release strategy, they used simulation models incorporating the benefits of biocontrol expressed as the value of recovered pasture productivity. Incorporating explicitly spatial and temporal dimension they were able to obtain an economically optimal release strategy.

To establish the cost-benefits of biological control, the cost of invasions need also to be estimated, to determine how much these costs are reduced when biocontrol strategies are used. In the US alone, it has been reported losses due to invading species, combined with their control, ranges around US$137 billion dollars per year (Parker and Gill, 2002).

In terms of institutional costs, CIBC, the largest multinational network of biocontrol scientists, has a budget of US$ 1 million per year, and many of their projects are in developing countries and in Canada (Perkins and Garcia, 1999). Innundative biological control has also created new markets (Waage and Greathead, 1988; Strong and Pemberton, 2000), and there are new companies supplying agents (Perkins and Garcia, 1999)

2.3.2 Problems and Risks of Biological Control

One of the problems of biological control is that the deliberate introduction of non-indigenous species is not free of environmental risks (Louda et al., 1997; Hoy, 2000; Simberloff and Stiling, 1996; Schaffner, 2001), the main concern is for the control agent host range stability (Pemberton, 2000), since there is increasing evidence that harm to non-target species is occurring (Pemberton, 2000; Louda et al., 2003*a*). The introduction of generalized predators can result in many non-target species being attacked by the control agent. For example, the introduction of the Indian mongoose (*Herpestes auropunctatus*) to the West Indies and other islands of the Pacific to control rats infesting agricultural fields, had damaging effects on native bird and reptile diversity (Simberloff and Stiling, 1996). The solution to this problem has been host-specificity tests of biocontrol agents. These tests try to ensure that the control

agent has a sufficiently narrow host-range that it will not affect native non-target species. This concept has achieved such relevance that it is driving research and regulation of biocontrol programmes (Secord and Kareiva, 1996). In weed biocontrol, host-specificity is even considered the "holy grail" of biocontrol (McFadyen, 1998). However, it is clear that control agents also interact with competitors with other indirect effects (Secord and Kareiva, 1996), and there is a risk of host-shifts that are not considered when performing host-specificity tests. McEvoy and Coombs (1999) suggests that host range can be constrained based on physiological, genetical, ecological and behavioral properties of the control agents (Cory and Myers, 2000).

An example of the risks is the introduction of the Eurasian weevil *Rhinocyllus conicus* to control musk thistle in Canada and the United States. The weevil expanded its host range reducing some populations of native thistles (genus *Crisium*) and also lowering the density of native flies (Gutierrez et al., 1999; Louda et al., 1997, 2003*a*; Cory and Myers, 2000; Louda et al., 2003*b*; Louda and O'Brien, 2002). Pre-release studies showed that the beetle *Lema cyanella* was limited to the Canada thistle, but open field studies showed that, even though other similar native species were rare, rarity does not guarantee that the beetle would not find and attack other non-target species (Cory and Myers, 2000). Another study reviewing the use of insects, fungi and nematodes established for biological control in Hawaii and United States, give evidence that many of these have expanded their host range, thus affecting native plants (Pemberton, 2000). Some of the possible explanations of host shifting of the Eurasian weevil range from the existence of increased ecological opportunities in the new area, genetic changes in host preference and availability of target and non-target hosts (Schaffner, 2001). Louda et al. (2003*b*) provides a list of cases where non-target effects of biological control have been important.

Understanding the risks of biological control includes the prediction of establishment, geographical expansion (dispersal) and non-target effects (Hoy, 2000), and the knowledge of the control agent interaction with other species (Secord and Kareiva, 1996; Louda et al., 1997). In addition, evolutionary changes and spatial and temporal dynamics of biocontrol agents are important factors to consider when selecting agents (Thomas and Willis, 1998; Simberloff and Stiling, 1996)

Biocontrol practitioners have argued that all these non-target effects are the result of early biocontrol programmes, where some of the procedures were still under development. However, there are also very recent examples that show that even under strong regulation, non-target effects still occur often (Thomas and Willis, 1998). Another reason, is related to the emergency situation in which most biocontrol programmes start, where there is not much time for detailed ecological analysis (Thomas and Willis, 1998).

In general biocontrol should be applied only when the target represents a serious problem, the potential problems of biocontrol are assessed and when the benefits and

costs in economical and ecological dimensions are balanced (Strong, 1997). Thomas and Willis (1998) suggest that the risks of biocontrol programmes can be reduced by:

1. *Evaluation before control.* Quantifying the economical and ecological extent of pest damage. If the economical/ecological damage is estimated to be minimal, and the pest is restricted to small regions, use other methods of control
2. *Improved non-target testing.* Test a wider range of non-target organisms beyond economical and agricultural importance. Include behavioral, physiological and morphological constraints in host range tests.
3. *Post-release studies.* Use these to measure the effectiveness of biocontrol, and the rate and direction of spread of control agents.
4. *Selection of initial control areas.* Selecting priority areas with respect for geographical location, scale and state of the pest attack.
5. *Changes in control policy.* Biocontrol should not be the last resort, but an alternative to control pests.

Protocols for biocontrol introductions are not sufficient to avoid problems, however, improved protocols could reduce some of the non target effects (Simberloff and Stiling, 1996).

2.4 Biological Control and Ecology

The theory of biological control contains elements of predator-prey systems and control theory (Berryman, 1999), but biocontrol has also strong linkages to biological invasions, since pests are invaders and the introduction of natural enemies is a process of invasion; and, because of the spatial nature of biological populations and the scale at which pests attack, some elements of landscape ecology. Here we review some examples and some important results in these areas.

2.4.1 Ecological Theory

Ecological theory has much to offer to biological control. However, since many biocontrol problems need quick solutions, many of the biological control programmes can not test or validate many ecological ideas (Gaugler et al., 1997). In any case, it is clear that ecological theory could solve many problems in biological control. Many of the formal ideas, now common practice in biocontrol, came from ecological theory. For example results of Nicholson-Bailey models and stability analysis of these

kinds of models (Hassell, 2000; Hassell et al., 1991), establish under what conditions a low persistent host density can be obtained. All these contributions dealt mainly with density-dependent processes and the stability of host-natural enemy interactions. However other areas of important research, where ecology can contribute substantially to biological control come from: metapopulation dynamics, spatial aggregation, refugees and stage-structured models (Murdoch and Briggs, 1996). Other issues include spatial dynamics and biological invasions.

2.4.2 Biological Invasions

Biological invasion occurs when an alien species occupies a new geographic region (Shigesada and Kawasaki, 1997). The invasion process occurs when there is an unintentional or intentional introduction of a species, and occurs in several stages: arrival, establishment, spread and integration (Ehler, 1998). Biological control deals with intentional introductions, so it is evident that there is a strong link between biological control and biological invasions (Ehler, 1998; Shigesada and Kawasaki, 1997). Ehler (1998) argues that, although such a strong linkage exists, theory of biological invasions has not provided enough guidelines and generalizations about invasion processes are not useful. On the contrary, Fagan et al. (2002) note that general theory has much to contribute the the general understanding of the dynamics of invasion process. As an example they show how the calculation of rate of spread, of host and control agent, determines if the control agent will "catch-up" with the host, and be able to control the spread of the host. The authors believe that the areas of contact between both disciplines are the importance of spatial spread of both control and pest, long distance dispersal, structured population dynamics, detectability of invading species and stochasticity and complex dynamics under heterogenous environments.

Rates of spread represent a key concept in biological invasions (Fagan et al., 2002; Shigesada and Kawasaki, 1997). As discussed in the next section, spatial dynamics of host and control agent play an important role in the biocontrol dynamics. However, historically, biocontrol research has payed little attention to rates of spread (Fagan et al., 2002). Many of the unwanted effects of biological control come from the ability of the control agents to expand their geographic range from the new introduced region. For example, the Argentine caterpillar *Cactoblastis cactorum* that was introduced in the Caribbean for control, expanded to the continental United states in a matter of 20 years (Strong and Pemberton, 2000). Probably, this would have been prevented if consideration of spread of the control had been considered.

Rates of spread are important, since in addition to trying to reduce host populations under biological control, we would also like to control the spread of the pest (i.e. a control agent that is capable of catching up with the spread of the pest) (Fagan et al.,

2002). As an example of studies incorporating rate of spread for biocontrol, Grewal et al. (2002) study the biological control of white grubs (Coleoptera: Scarabaeidae) using nematodes. White grub beetles cause damage in turfgrass, ornamental flowers and fruit trees in urban landscapes in North America. In their study they considered the ability of the control agent to reduce the spread of withe grubs. Their results suggest that using one of the native nematode species (*Heterorhabditis bacteriophora*) could delay and reduce the spread of the pest, enhancing biological control.

2.4.3 Spatial Considerations and Landscape Ecology

Habitat fragmentation is usually only considered in the context of conservation, but such heterogeneous spatial configurations also determine how effective biological control can be (Tscharntke and Kruess, 1999). Many of the studies that consider host-enemy interactions do not consider the spatial dimension and heterogeneity of the host and control agent distributions (Kareiva, 1990*a*). Although this simplifying assumption (spatial homogeneity) facilitates the study of such complex dynamic interactions, it omits important changes in the dynamics due to spatial configuration. For example, Kareiva (1990*a*, 1987) showed that the ability of a ladybug to control aphid prey is substantially reduced if the ladybug's dispersal ability is hampered. Kareiva found that increasing patchiness caused local explosions of aphids leading to unstable dynamics. In general, the response to habitat fragmentation of host-enemy interactions will depend largely on the behavioral characteristics of both host and control agent (Kareiva, 1987). Understanding the spatial response of the biocontrol agent to variation in host density is crucial for biocontrol success (Kareiva, 1990*b*). With et al. (2002), in a recent study of ladybugs controlling aphids at a landscape scale, showed that landscape fragmentation affected the aggregation and searching ability of ladybugs, and that changes in the pest-enemy dynamics are related to fragmentation thresholds. Jonsen et al. (2001), showed that the ability of two *Aphthona* flea beetles to control leafy spurge is highly affected by matrix structure, hence, metapopulation dynamics is largely affected by landscape structure. Similar results exist for the host-parasitoid dynamics of the forest tent caterpillar, *Malacosoma disstria* in relation to forest cover (Roland and Taylor, 1997). Other studies like Rees and Hill (2001) on the biological control of gorse (*Ulex europaeus*), show how broad scale disturbances that change the spatial configuration of infested areas (like fire used as control or herbicide application) are important on improving the effect of biological control agents.

On the theoretical front, for host-parasitoid systems, it has been shown that when space is incorporated explicitly (in coupled map lattices or cellular automata), a broad range of behaviors appear in the models (Hassell et al., 1991; Comins and Hassell, 1987). These include global persistence of both species and a parameter space where

host extinction is possible (under conditions of low host dispersal and high parasitoid dispersal). Using this type of model, White et al. (1996) found that increasing pathogen dispersal reduced host metapopulation levels and increased the period of host population fluctuations. Similar results were found by Kean and Barlow (2001) for the biological control of the weevil *Sitona discoideus* by the parasitoid *Microctonus aethiopoides* in a coupled map lattice model, and Bjornstad and Bascompte (2001) theoretically studying spatial correlations in host-parasitoid systems.

Bibliography

Bangsund, D., F. Leistritz, and J. Leitch. 1999. Assessing economic impacts of biological control of weeds: the case of leafy spurge in the Northern Great Plains of the United States. Journal of Environmental Management **56**:35–43.

Barlow, N., 1999. Theoretical approaches to biological control, chapter models in biological control: A field guide, pages 43–68 . Cambridge University Press.

Bellows, T. 2001. Restoring population balance through natural enemy introductions. Biological Control **21**:199–205.

Bellows, T. and D. Headrik, 1999. Handbook of biological control: principles and applications of biological control, chapter arthropods and vertebrates in biological control of plants, pages 505–516 . Academic Press.

Bellows, T. and R. van Driesche, 1999. Handbook of biological control: principles and applications of biological control, chapter life table construction and analysis for evaluating control agents, pages 199–223 . Academic Press.

Bernays, E. and R. Chapman. 1994. Host-plant Selection by Phytophagous Insects. Chapman & Hall.

Berryman, A., 1999. Theoretical approaches to biological control, chapter the theoretical foundations of biological control, pages 43–68 . Cambridge University Press.

Bidochka, M., S. Walsh, M. Ramos, R. Stleger, J. Silver, and D. Roberts. 1996. Fate of biological control introductions: Monitoring an australian fungal pathogen of grasshoppers in North America. Proceedings of the National Academy of Sciences of the United States of America **93**:918–921.

Bjornstad, O. and J. Bascompte. 2001. Synchrony and second-order spatial correlation in host- parasitoid systems. Journal of Animal Ecology **70**:924–933.

Bokonon-Ganta, A., H. De Groote, and P. Neuenschwander. 2002. Socio-economic impact of biological control of mango mealybug in Benin. Agriculture Ecosystems & Environment **93**:367–378.

Comins, H. and M. Hassell. 1987. The dynamics of predation and competition in patchy environments. Theoretical Population Biology **31**:393–421.

Cory, J. and J. Myers. 2000. Direct and indirect ecological effects of biological control. Trends in Ecology & Evolution **15**:137–139.

Cristofaro, M. 1995. Open-field tests in host-specificity determination of insects for biological control of weeds. Biocontrol Science and Technology **5**:395–406.

De Groote, H., O. Ajuonu, S. Attignon, R. Djessou, and P. Neuenschwander. 2003. Economic impact of biological control of water hyacinth in Southern Benin. Ecological Economics **45**:105–117.

DeBach, P. and D. Rosen. 1991. Biological Control by Natural Enemies. 2nd ed edition. Cambridge University Press.

Ditomaso, J. 2000. Invasive weeds in rangelands: Species, impacts, and management. Weed Science **48**:255–265.

Ehler, L. 1998. Invasion biology and biological control. Biological Control **13**:127–133.

Fagan, W., M. Lewis, M. Neubert, and P. Van Den Driessche. 2002. Invasion theory and biological control. Ecology Letters **5**:148–157.

Gaugler, R., E. Lewis, and R. Stuart. 1997. Ecology in the service of biological control: the case of entomopathogenic nematodes. Oecologia **109**:483–489.

Goeden, R. 1983. Critique and revision of harris scoring system for selection of insect agents in biological-control of weeds. Protection Ecology **5**:287–301.

Goeden, R. and L. Andres, 1999. Handbook of biological control: principles and applications of biological control, chapter biological control of weeds in terrestrial and aquatic environments, pages 871–890 . Academic Press.

Grevstad, F. 1999. Factors influencing the chance of population establishment: Implications for release strategies in biocontrol. Ecological Applications **9**:1439–1447.

Grewal, P., S. Grewal, V. Malik, and M. Klein. 2002. Differences in susceptibility of introduced and native white grub species to entomopathogenic nematodes from various geographic localities. Biological Control **24**:230–237.

Gutierrez, A., L. Caltagirone, and W. Meikle, 1999. Handbook of biological control: principles and applications of biological control, chapter evaluation of results: Economics of biological control, pages 243–252 . Academic Press.

Harris, P. 1979. Cost of biological-control of weeds by insects in Canada. Weed Science **27**:242–250.

Harris, P. 1993. Effects, constraints and the future of weed biocontrol. Agriculture Ecosystems & Environment **46**:289–303.

Hassell, M. 2000. Host-parasitoid population dynamics. Journal of Animal Ecology **69**:543–566.

Hassell, M., H. Comins, and R. May. 1991. Spatial structure and chaos in insect population-dynamics. Nature **353**:255–258.

Hoy, M. 2000. The david rosen lecture: Biological control in citrus. Crop Protection **19**:657–664.

Huffaker, C. and P. Messenger. 1976. Theory and Practice of Biological Control. Academic Press.

Jonsen, I., R. Bourchier, and J. Roland. 2001. The influence of matrix habitat on aphthona flea beetle immigration to leafy spurge patches. Oecologia **127**:287–294.

Julien, M., A. C. for International Agricultural Research, and C. International. 1992. Biological control of weeds : a world catalogue of agents and their target weeds. 3rd ed edition. CAB International in association with ACIAR.

Kareiva, P. 1987. Habitat fragmentation and the stability of predator prey interactions. Nature **326**:388–390.

Kareiva, P., 1990*a*. Critical issues in biological control, chapter the spatial dimension in pest-enemy interactions, pages 213–227 . Intercept. VCH Publishers.

Kareiva, P. 1990*b*. Population-dynamics in spatially complex environments - theory and data. Philosophical Transactions of the Royal Society of London Series B-Biological Sciences **330**:175–190.

Kean, J. and N. Barlow. 2001. A spatial model for the successful biological control of *Sitona Discoideus* by *Microctonus Aethiopoides*. Journal of Applied Ecology **38**:162–169.

Knight, J. 2001. Alien versus predator. Nature **412**:115–116.

Louda, S., A. Arnett, T. Rand, and F. Russell. 2003*a*. Invasiveness of some biological control insects and adequacy of their ecological risk assessment and regulation. Conservation Biology **17**:73–82.

Louda, S., D. Kendall, J. Connor, and D. Simberloff. 1997. Ecological effects of an insect introduced for the biological control of weeds. Science **277**:1088–1090.

Louda, S. and C. O'Brien. 2002. Unexpected ecological effects of distributing the exotic weevil, *Larinus Planus* (F.), for the biological control of canada thistle. Conservation Biology **16**:717–727.

Louda, S., R. Pemberton, M. Johnson, and P. Follett. 2003*b*. Nontarget effects - the achilles' heel of biological control? retrospective analyses to reduce risk associated with biocontrol introductions. Annual Review of Entomology **48**:365–396.

Luck, R., B. Shepard, and P. Kenmore, 1999. Handbook of biological control: principles and applications of biological control, chapter evaluation of biological control with experimental methods, pages 225–242 . Academic Press.

Mason, P. and J. Huber. 2002. Biological control programmes in Canada, 1981-2000. CABI Pub.

Masters, R. and R. Sheley. 2001. Principles and practices for managing rangeland invasive plants. Journal of Range Management **54**:502–517.

McClay, A. 1995. Beyond before and after: Experimental design and evaluation in classical weed biocontrol. Proceedings of the VIII International Symposium on Biological Control of Weeds pages 213–219.

McEvoy, P. and E. Coombs. 1999. Biological control of plant invaders: Regional patterns, field experiments, and structured population models. Ecological Applications **9**:387–401.

McFadyen, R. 1998. Biological control of weeds. Annual Review of Entomology **43**:369–393.

Memmott, J., S. Fowler, and R. Hill. 1998. The effect of release size on the probability of establishment of biological control agents: Gorse thrips (sericothrips staphylinus) released against gorse (*Ulex Europaeus*) in New Zealand. Biocontrol Science and Technology **8**:103–115.

Murdoch, W. and C. Briggs. 1996. Theory for biological control: Recent developments. Ecology **77**:2001–2013.

Murdoch, W., J. Chesson, and P. Chesson. 1985. Biological control in theory and practice. American Naturalist **125**:344–366.

Myers, J. and D. Bazely. 2003. Ecology and Control of Introduced Plants. Cambridge University Press.

Nordblom, T., M. Smyth, A. Swirepik, A. Sheppard, and D. Briese. 2002. Spatial economics of biological control: Investing in new releases of insects for earlier limitation of paterson's curse in Australia. Agricultural Economics **27**:403–424.

Parker, D. and B. Gill, 2002. Biological control programmes in Canada, 1981-2000, chapter invasive species and biological control, pages 1–4 . CABI Pub.

Pemberton, R. 2000. Predictable risk to native plants in weed biological control. Oecologia **125**:489–494.

Perkins, J. and R. Garcia, 1999. Handbook of biological control : principles and applications of biological control, chapter social and economic factors affecting research and implementation of biological control, pages 993–1009 . Academic Press.

Peschken, D. and A. McClay. 1992. Picking the target: A revision of McClay's scoring system to determine the suitability of a weed for classical biological control. Proceedings of the VIII International Symposium on Biological Control of Weeds pages 137–143.

Radosevich, S., J. Holt, and C. Ghersa. 1997. Weed ecology : implications for management. 2nd ed edition. J. Wiley.

Rao, V. 2000. Principles of Weed Science. 2nd ed edition. Science Publishers.

Rees, M. and R. Hill. 2001. Large-scale disturbances, biological control and the dynamics of gorse populations. Journal of Applied Ecology **38**:364–377.

Roland, J. and P. Taylor. 1997. Insect parasitoid species respond to forest structure at different spatial scales. Nature **386**:710–713.

Schaad, N., W. Song, S. Hutcheson, and F. Dane. 2001. Gene tagging systems for polymerase chain reaction based monitoring of bacteria released for biological control of weeds. Canadian Journal of Plant Pathology-Revue Canadienne de Phytopathologie **23**:36–41.

Schaffner, U. 2001. Host range testing of insects for biological weed control: How can it be better interpreted? Bioscience **51**:951–959.

Secord, D. and P. Kareiva. 1996. Perils and pitfalls in the host specificity paradigm. Bioscience **46**:448–453.

Shea, K. and D. Kelly. 1998. Estimating biocontrol agent impact with matrix models: *Carduus nutans* in New Zealand. Ecological Applications **8**:824–832.

Shea, K., H. Possingham, W. Murdoch, and R. Roush. 2002. Active adaptive management in insect pest and weed control: Intervention with a plan for learning. Ecological Applications **12**:927–936.

Shigesada, N. and K. Kawasaki. 1997. Biological Invasions : theory and practice. 1st ed edition. Oxford University Press.

Shroeder, D., A. Gassmann, and H. Muller-Schraer. 1996. Prerelease studies: syntesis of session 3. Proceedings of the IX International Symposium on Biological Control of Weeds pages 237–239.

Simberloff, D. and P. Stiling. 1996. How risky is biological control? Ecology **77**:1965–1974.

Strong, D. 1997. Ecology - fear no weevil? Science **277**:1058–1059.

Strong, D. and R. Pemberton. 2000. Ecology - biological control of invading species - risk and reform. Science **288**:1969–1970.

Suckling, D., R. Hill, A. Gourlay, and P. Witzgall. 1999. Sex attractant-based monitoring of a biological control agent of gorse. Biocontrol Science and Technology **9**:99–104.

Thomas, M. and A. Willis. 1998. Biocontrol - risky but necessary? Trends in Ecology & Evolution **13**:325–329.

Thorarinsson, K. 1990. Biological-control of the cottony-cushion scale - experimental tests of the spatial density-dependence hypothesis. Ecology **71**:635–644.

Tscharntke, T. and A. Kruess, 1999. Theoretical approaches to biological control, chapter habitat fragmentation and biological control, pages 190–205 . Cambridge University Press.

Van den Berg, M., G. Hoppner, and J. Greenland. 2000. An economic study of the biological control of the spiny blackfly, aleurocanthus spiniferus (hemiptera : Aleyrodidae), in a citrus orchard in swaziland. Biocontrol Science and Technology **10**:27–32.

Varley, G. and G. Gradwell. 1970. Recent advances in insect population dynamics. Annual Review of Entomology **15**:1–24.

Venugopal, G. 1998. Monitoring the effects of biological control of water hyacinths using remotely sensed data: a case study of Bangalore, India. Singapore Journal of Tropical Geography **19**:92–105.

Vogele, J., D. Agounke, and D. Moore. 1991. Biological-control of the fruit tree mealybug *Rastrococcus Invadens* Williams in togo - a preliminary sociological and economic-evaluation. Tropical Pest Management **37**:379–382.

Waage, J., 1990. Critical issues in biological control, chapter ecological theory and the selection of biological control agents, pages 213–227 . Intercept. VCH Publishers.

Waage, J. and D. Greathead. 1988. Biological-control - challenges and opportunities. Philosophical Transactions of the Royal Society of London Series B-Biological Sciences **318**:111–128.

White, A., M. Begon, and R. Bowers. 1996. Host-pathogen systems in a spatially patchy environment. Proceedings of the Royal Society of London Series B-Biological Sciences **263**:325–332.

Williams, A. and E. Hunt. 2002. Estimation of leafy spurge cover from hyperspectral imagery using mixture tuned matched filtering. Remote Sensing of Environment **82**:446–456.

Wilson, F. and C. Huffaker, 1976. Theory and practice of biological control, chapter the philosophy, scope, and importance of biological control, pages 3–15 . Academic Press.

With, K., D. Pavuk, J. Worchuck, R. Oates, and J. Fisher. 2002. Threshold effects of landscape structure on biological control in agroecosystems. Ecological Applications **12**:52–65.

Chapter 3

Population dynamics and control of Scentless Chamomile

3.1 Introduction

Invasive species have a major impact on habitat destruction, displacement of native species and invasion of agricultural lands (Myers and Bazely, 2003). Once invaders have established, often they need to be controlled or eliminated. Biological control, the control of pests by natural enemies, is one potential management strategy. The goal of biocontrol is to reduce host population growth and spatial spread over an ecologically long period (Murdoch and Briggs, 1996). The first step in invasion control is to understand aspects of the life cycle of the invader and how population changes over space and time. Hence, application of ecological theory and control theory (Berryman, 1999), as well as invasion theory (Fagan et al., 2002) is essential in designing successful control strategies.

Due to the complexity of ecological systems, predicting the outcome and success of a potential biocontrol strategy is difficult, therefore a modelling approach can be valuable. Matrix population models are a useful modelling approach for the control of highly seasonal hosts. These models are biologically realistic, and many of the parameter values are easy to obtain from empirical studies (Murdoch and Briggs, 1996; Caswell, 2001). A matrix model summarizes the life cycle of the host in a series of transition coefficients that represent the probability of an individual growing from one life stage to the next, and then reproducing. The dominant eigenvalue of the matrix represents the net per capita population growth rate (frequently denoted λ in mathematical literature, and r in ecological literature). With matrix models, it is possible to integrate the effect of management strategies directly into the life history stages of the invader (Thomson, 2005). Further, by analyzing the sensitivity of this eigenvalue to the different transition coefficients, it is possible to identify critical

stage/age transitions that may be suitable targets for the application of biocontrol (Kean and Barlow, 2000).

In this chapter, demographic analysis is applied to scentless chamomile (*Matricaria perforata*), an annual, biennial or short lived perennial, introduced in western Canada (Douglas et al., 1991; McClay and De Clerck-Floate, 1999). Annual plants are represented by seeds that germinate and produce flowering plants the same year; biennial, by seeds that germinate and grow as rosettes (no flower stage) producing flowers the following year; and perennial, by plants (rosettes or annuals) that produce flowers for more than one year. Scentless chamomile has high seed production, an estimated 6300 seeds per 10g plant (Lutman, 2002), and a maximum of 1.8 million seed/m^2 for a single plant. It can spread rapidly to croplands and waste areas (Woo et al., 1991; McClay and De Clerck-Floate, 1999). This weed invades mostly annual crops, transition areas, field depressions and slough margins (Bowes et al., 1994; Hinz, 1999). Scentless chamomile has been reported to reduce yields of important agricultural crops (wheat) by 30% to 80% (Douglas et al., 1992, 1991; Milberg and Hallgren, 2004). Biological control of scentless chamomile has been attempted using a seed weevil (McClay and De Clerck-Floate, 1999), a gall midge (Hinz and Muller-Scharer, 2000; Hinz, 1998) and a fungi (Peng et al., 2005). Although the control agents have been successful in establishing populations, there is no evidence of their effectiveness in controlling scentless chamomile. However, biocontrol of scentless chamomile has been shown in greenhouse experiments to have some potential only using high densities of control agents and when s. chamomile is under high inter-specific competition (Hinz and Schroeder, 2003).

Some population modelling for scentless chamomile has been developed. Hinz (1999) used matrix population models to estimate population growth rate, and to calculate the elasticity matrix. Buckley et al. (2001) used an unstructured discrete time population model to study population dynamics and control. Both have estimated that a large reduction in fecundity (higher than 98%) would be necessary to control scentless chamomile populations. Peng et al. (2005) suggested that, when used alone, biocontrol could not control scentless chamomile and only the addition of chemical control could result in the control of scentless chamomile populations.

Using matrix models, I study the population dynamics of this weed in Alberta, Canada. By parameterizing the matrix model I address the invasive potential of scentless chamomile and how to control this weed.

3.2 Methods

I set up a 3 year field study to estimate parameters for the transition matrix and calculate population growth of scentless chamomile.

3.2.1 Field plots set-up and treatment application

In July 2003, 32 (4 rows, 8 columns) 2m by 2m plots were established in Vegreville, Alberta, Canada. Each plot was tilled to clear vegetation in a 25m by 30m area where scentless chamomile was not previously present. To create somewhat natural conditions and levels of competition of scentless chamomile, 1kg of Prairie Seeds' Parkland Pasture Mix #2 was sown in the entire area. This mix contains 50% Fleet Meadow Bromegrass "Nutracoat", 20% Glacier brand Orchardgrass, 10% Boreal Creeping Red Fescue, 5% Troy Kentucky Bluegrass and 15% Buffalo brand Timothy. In each plot, approximately 1000 scentless chamomile seeds were sown and the plot was raked to stimulate germination. All emerging scentless chamomile plants in an inner 1m by 1m subplot were counted as they emerged, and marked to avoid double counting. In late autumn, scentless chamomile flowering plants were counted, and all flowers were clipped. This ensured that only seeds from the seed bank and rosettes would remain available for germination or growth in the following year.

In spring 2004, newly emerging plants were counted and marked. At the end of the season, flowering chamomile plants were counted. The number of seeds per flowering head was estimated by counting a sub-sample of seeds from intact flower heads. In August 2004, flower clipping was applied as treatment to 16 randomly chosen plots (4 per row). The treatments were applied to reduce fecundity (number of flower heads) to approximately 50%. Since the total number of flowers per plot was not known, the reduction was done by clipping all flowers in approximately 50% of the total plot area. The treatment was applied using a 2m by 2m frame with 10cm grid lines. This grid line configuration was chosen to facilitate flower cutting, without causing much disturbance. The frame was placed on top of each plot and in 13 of 25 cells of the grid, representing 53% of the area, all chamomile flowers were clipped and placed in bags. These chamomile flower heads were counted and used to estimate fecundity of that year. The following year (2005), in autumn, flowering chamomile plants and rosettes were counted, and the total number of flowering heads were counted. To test differences in fecundities between clipped and un-clipped treatments, a likelihood ratio test was used (Cameron and Trivedi, 1998)

3.2.2 Flower counting using digital images

In 16 of the 32 plots (where the flower cutting treatment was applied), the clipped flowers were counted manually for each plot. To estimate the number of flowers per plot in the remaining 16 plots, a 3.1 mega-pixel resolution picture (Figure 3.1) was taken with a Cannon Powershot G2 in each 1x1m inner plot. An RGB (red-green-blue bands) decompositions allowed for the identification of yellow flower heads in the green background in the picture. A red green difference was applied to enhance yellow

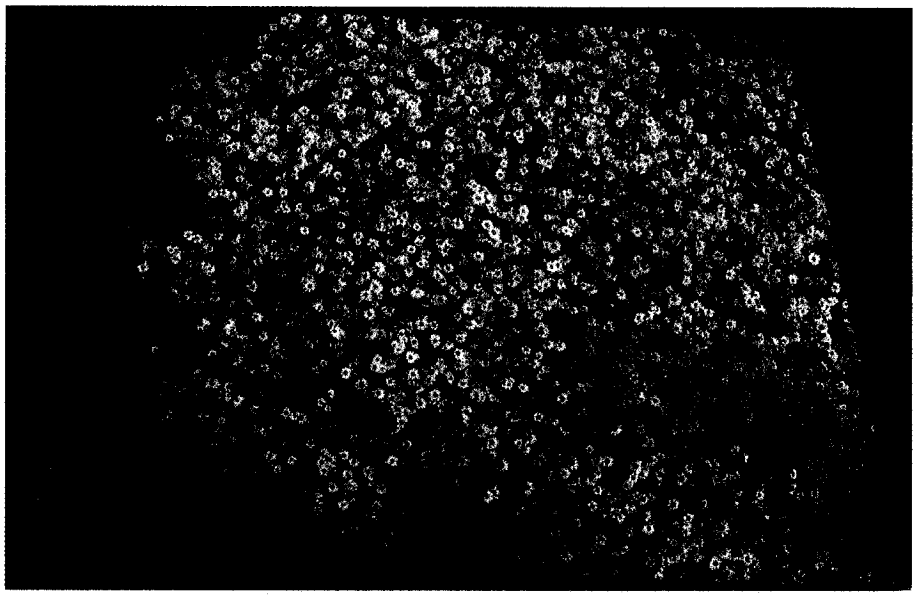

Figure 3.1: 3.1 mega-pixel digital photograph of a scentless chamomile plot taken in August 2004. The 2x2m plot is shown clipped

and each digital image was contoured (a polygon drawn around yellow boundaries) to identify individual seed heads. The identification procedure is shown in Figure 3.4. Using the maximum likelihood estimator, the detection probability was calculated, calibrated with true counts from the clipped treatment, using the procedure described in Borchers et al. (2002). The detection probability is calculated by obtaining the maximum likelihood estimator of the likelihood function,

$$L(p|N,n) = \prod_{i=1}^{m} \binom{N_i}{n_i} p^{n_i}(1-p)^{N_i-n_i}, \tag{3.1}$$

where N_i is the true counted number of flowers in plot i, n_i is the number of flo wers identified in the digital image, in the same plot, $m = 16$ is the number of plots sampled and p is the detection probability to be estimated.

3.2.3 Dispersal kernel

To estimate the dispersal ability of scentless chamomile, two healthy plants where transplanted from the Alberta Research Council (ARC) green house in Vegreville, to a hay field in July 2004. Each plant had 222 and 232 flowering heads with an average of 330 seeds/head. For each plant, 10cm diameter, 10cm deep, seed traps were placed in the North, East, South, West directions at 5m intervals from 0.5m to 20m from the

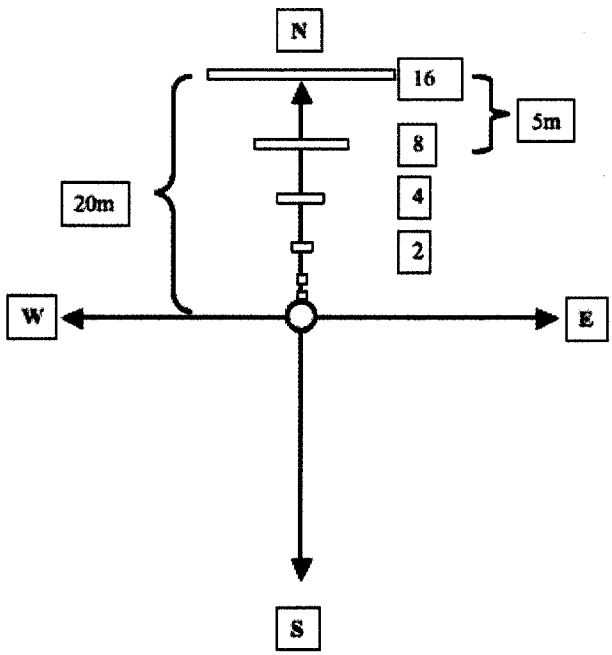

Figure 3.2: Seed trap arrangement at different distances from a source plant. The source plant located at the center, had approximately 50,000 seeds. Seed traps were placed in all 4 directions. The seed traps were place in Vegreville, Alberta, Canada, and left from 2004 to 2005

source plant as shown in Table 3.1 and Figure 3.2. Seeds were collected the following year in late spring and manually counted. To summarize the dispersal ability of chamomile, all cardinal directions were summed and a piecewise linear interpolation was fit to the resultant seed densities.

3.2.4 Matrix model and parametrization

A matrix population model is defined as follows:

$$\mathbf{n}_{t+1} = \mathbf{A}\mathbf{n}_t \tag{3.2}$$

where $\mathbf{n}_t$ is a vector of the abundance of each life stage at time t, and $\mathbf{A}$ is a *population projection matrix* where entries a_{ij} represent transitions from stage j to stage i (Caswell, 2001). With the transition matrix, it is possible to calculate the per capita population growth rate λ, defined as the largest eigenvalue of $\mathbf{A}$. Sensitivity of population growth λ, to entries in the transition matrix can be analyzed by computing

Table 3.1: Total number of seeds collected in seed traps from two plants in the four cardinal directions

Distance(m)	Number of traps	N	S	E	W
0.5	1	6	18	7	5
1	1	6	24	3	1
5	2	1	11	0	0
10	4	1	2	0	0
15	8	1	0	0	0
20	16	0	0	0	0

the sensitivity matrix $\mathbf{S}$,

$$\mathbf{S} = \left[\frac{\partial \lambda}{\partial a_{ij}}\right], \tag{3.3}$$

and elasticity matrix $\mathbf{E}$, defined as,

$$\mathbf{E} = \left[\frac{a_{ij}}{\lambda}\frac{\partial \lambda}{\partial a_{ij}}\right]. \tag{3.4}$$

Elasticities in this matrix can be interpreted as the relative contribution of life stage transitions to population growth. The elasticities can be calculated as (Caswell, 2001),

$$\frac{a_{ij}}{\lambda}\frac{\partial \lambda}{\partial a_{ij}} = \frac{a_{ij}}{\lambda}\frac{v_i w_j}{\langle \mathbf{v}, \mathbf{w} \rangle}, \tag{3.5}$$

where $\mathbf{v}, \mathbf{w}$ are the right and left eigenvectors of $\mathbf{A}$ and $\langle \mathbf{v}, \mathbf{w} \rangle$ is the scalar product.

The year to year life cycle of scentless chamomile is described in Figure 3.3. The first node represents the seed bank stage. Seeds can germinate from early spring to late summer and produce flowering plants (stage 3) or over-wintering rosettes (stage 2). Flowering plants die, and rosettes produce flowering plants the next year (biennial). In matrix notation, Figure 3.3 can be written:

$$\mathbf{A} = \begin{bmatrix} a_{11} & 0 & a_{13} \\ a_{21} & 0 & a_{23} \\ a_{31} & a_{32} & a_{33} \end{bmatrix} \tag{3.6}$$

Parameter estimates of the transition matrix entries a_{ij} were obtained from field work and literature estimates as follows. In the 32 plots established, a cohort in an inner 1m by 1m plot was followed for 3 years. The first year (2003), all emerging scentless chamomile plants were counted, these plants were assumed to have germinated from the seed bank and not from additional sources (dispersal). At the end of the year all rosettes and flowering plants were counted and all flowering plants were clipped,

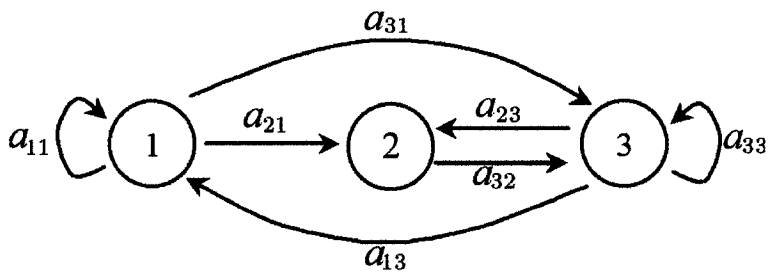

Figure 3.3: Life cycle graph of scentless chamomile. Node 1 represents the seed bank, node 2 rosettes and node 3 flowering plants. a_{ij} edges represent the transition from node j to node i

Table 3.2: Transition matrix parameter estimation. S=seed bank, R=rosettes, F=flowering plants

Transition	Description	Source
a_{11}	SB survival	Hinz (1999)
a_{21}	SB to R	Emerging R year 1
a_{31}	SB to F	Emerging F year 1
a_{32}	R to F	Surviving R to F year 2
a_{13}, a_{23}, a_{33}	F to SB,R, F	Field data. Proportional to Hinz (1999)

transition a_{31} was calculated from the number of flowering plants that year, and a_{21} from all scentless chamomile plants that had no flowers. The second year (2004), only surviving over-wintering rosettes remained. There were no new emerging plants. Transition a_{32} was estimated from the number of rosettes that produced flowers at the end of the year. The number of flowering heads were counted in the clipped treatments (see section 3.2.2). The third year (2005) included rosettes and flowering plants, all flowering heads were removed and counted in September 2005. The total fecundity ($a_{13}+a_{23}+a_{33}$) was obtained from the flower counts and image data for 2004 and from flower counts on 2005 (see Table 3.2). To differentiate between transitions a_{13}, a_{23}, a_{33} the number of seeds for each transition was estimated using the same transition probabilities of seeds going to the seed bank, rosettes or flowering plants, found by Hinz (1999).

Since the distribution of the population growth rate λ is not known, 90 % confidence intervals (CI) were calculated using 30,000 samples obtained by non-parametric bootstrapping. Bootstrapping was done by simulating of the number of new rosettes and flowering plants, starting with 1000 seeds, sampling with replacement from a binomial distribution $\mathrm{B}(a_{ij}, N)$, where a_{ij} is the transition probability from stage j to i, estimated from the data, and N is the initial number of seeds in the interation.

For each bootstrap sample, a projection matrix was estimated, and the population growth rate λ and elasticity matrix were calculated. To analyze the robustness of the elasticity matrix, elasticity was calculated from the same bootstrapped samples used to calculate CI for λ, and the resulting matrices were summarized and counted based on the transitions that had elasticities higher than 2%. The procedure can be outlined as follows: 1) calculate the elasticity matrix, 2) replace elasticities higher than 2% with 1 and put 0 in the rest, 3) Count the resulting matrix structures (matrix structure refers to the positioning of 0 and 1 in the elasticity matrix)

The net reproductive rate R_0 can be calculated using the method described in Chapter 4. For scentless chamomile, R_0 is given by:

$$R_0 = \frac{(a_{31} + a_{21}a_{32})\underline{a_{13}}}{1 - a_{11}} + a_{32}\underline{a_{23}} + \underline{a_{33}}, \tag{3.7}$$

Fecundity transitions are shown underlined.

3.3 Results

3.3.1 Parameter estimation

Number of flowers for the cut and control treatments where both significantly over dispersed (Likelihood ratio test $p < 0.0001$), with a dispersion parameter, of the negative binomial distribution, of $k = 0.48$ for the clipped treatment and $k = 0.38$ for the unclipped, thus a negative binomial distribution was used to test for treatment differences. There was no significant differences between treatments on the number of flowering plants (Likelihood ratio test $p = 0.283$). Hence, the 53% reduction in fecundity had no effect on the number of flowering plants the following year. Because of this, all stage transitions were obtained from averages of all 32 plots. Using the estimated number of flowering heads, and the calculated detection probability $p = 0.41$, flower counts from the remaining 16 plots were estimated. Calibrating the image counts to manual counts resulted in an estimated correlation coefficient of $r = 0.70$ between counted flower heads and estimated flower heads (Figure 3.5).

3.3.2 Model results

The estimated transitions parameters are shown in Table 3.3. In matrix form, Table 3.3 can be written:

$$\mathbf{A} = \begin{bmatrix} 0.08 & 0 & \{36376, 1775\} \\ 0.27 & 0 & \{517, 25\} \\ 0.04 & 0.45 & \{298, 14\} \end{bmatrix} \tag{3.8}$$

Table 3.3: Transition matrix parameter estimates for the scentless chamomile matrix model. Transition a_{11} is taken from Hinz (1999)

Transition	Mean	Variance
a_{11}	0.080	
a_{21}	0.27	0.011
a_{31}	0.04	0.0024
a_{32}	0.45	0.020
$a_{13} + a_{23} + a_{33}$ (year 1)	37192	$4,2 \times 10^8$
$a_{13} + a_{23} + a_{33}$ (year 2)	1816	4046

In the third column, $\{year1, year2\}$ indicates both fecundity estimates for year 1 and year 2. The population growth rate from the matrix model was estimated to be $\lambda(1) = 303.46$ with 90% CI $\{275.93, 331.86\}$ for 2004 and $\lambda(2) = 19.37$ with 90% CI $\{14.97, 24.89\}$ for 2005. The computed elasticity matrices using equation (3.5):

$$\mathbf{E}(1) = \begin{bmatrix} 0.00041 & 0 & \mathbf{1.57} \\ 0.016 & 0 & 0.25 \\ \mathbf{1.55} & 0.26 & \mathbf{96.35} \end{bmatrix}, \mathbf{E}(2) = \begin{bmatrix} 0.071 & 0 & \mathbf{17.16} \\ 2.32 & 0 & 2.36 \\ \mathbf{14.83} & 4.69 & \mathbf{58.56} \end{bmatrix} \tag{3.9}$$

The three highest elasticities are shown in bold face. Using the estimated parameters, for year 1 $R_0 = 6916.24$ and for year 2 $R_0 = 337.51$.

Results from the seed traps are shown on Table 3.1. The density of seeds trapped (in seeds/m^2) are shown in Figure 3.6. The line in Figure 3.6, shows the piecewise linear interpolation applied to the seed density in all directions. Dispersal followed exponential decay, with no seeds being trapped at the 20m seed trap.

3.4 Discussion

As shown by the high population growth rate λ for both years, this plant has a high potential for becoming a weed. However, the large difference in λ between year 1 (2004) and 2 (2005), also suggest some susceptibility of scentless chamomile to local variations in climate and competition. Climatic data from Vegreville, suggests that there was a slight (30%) increase in 20 years standardized rainfall in 2005, triggering high germination and reduced fecundity in 2005. As seen in Figure 3.7, there is a small difference in growing degree days (GDD), the cumulative of difference of average daily temperature and baseline growth temperature of 5 degrees celsius, between 2004 and 2005. The germination and flowering GDD, based on GDD for SC determination by Blackshaw and Harker (1997), was reached earlier in year 1 (2004). It has been suggested that growth of scentless chamomile is not greatly affected by

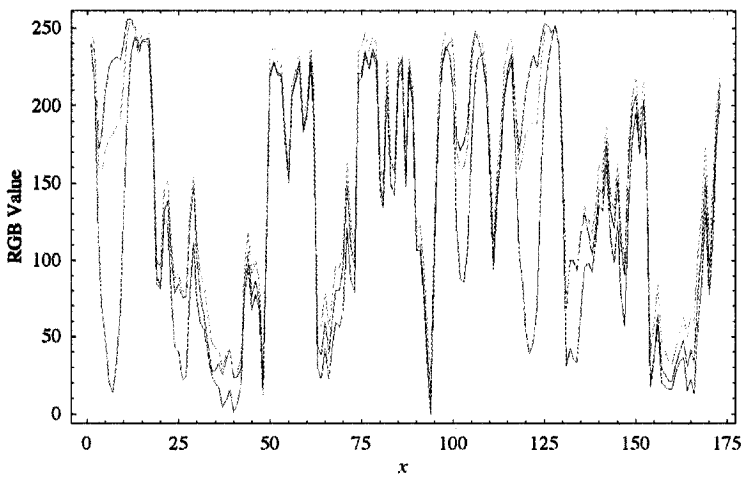

(a) All bands

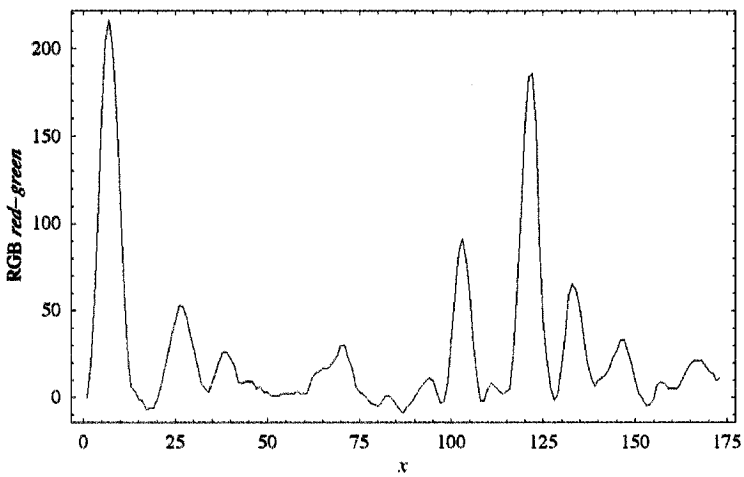

(b) *red-green*

Figure 3.4: Image profile along the middle horizontal section of the image shown in figure 3.5. (a) All RGB bands, (b)Difference between red and green band. The peaks show yellow, which indicates where the scentless chamomile flower heads are located

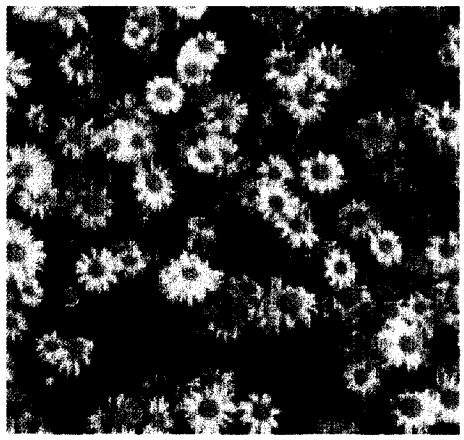

(a) Sample Image

(b) Flowers identified

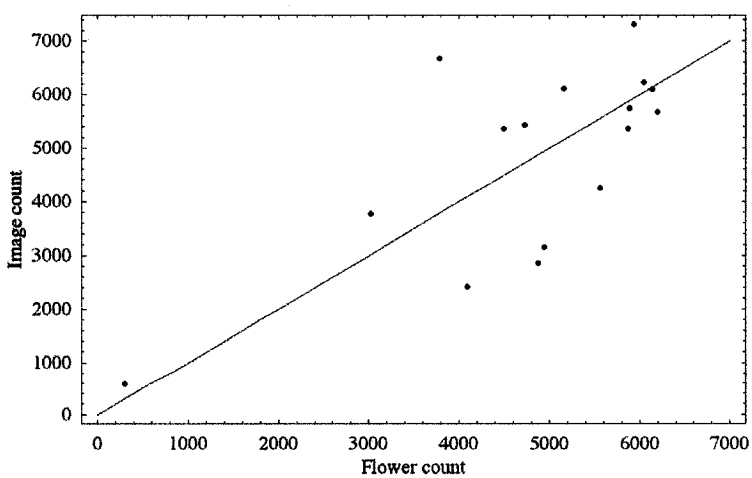

(c) Correlation between true number of flowers per plot and number estimated from imaging analysis

Figure 3.5: (a) Section of the 2x2 plot, (b) Flower contoured using yellow recognition. The identified flowers have a purple contour. (c) Correlation ($r = 0.70$)

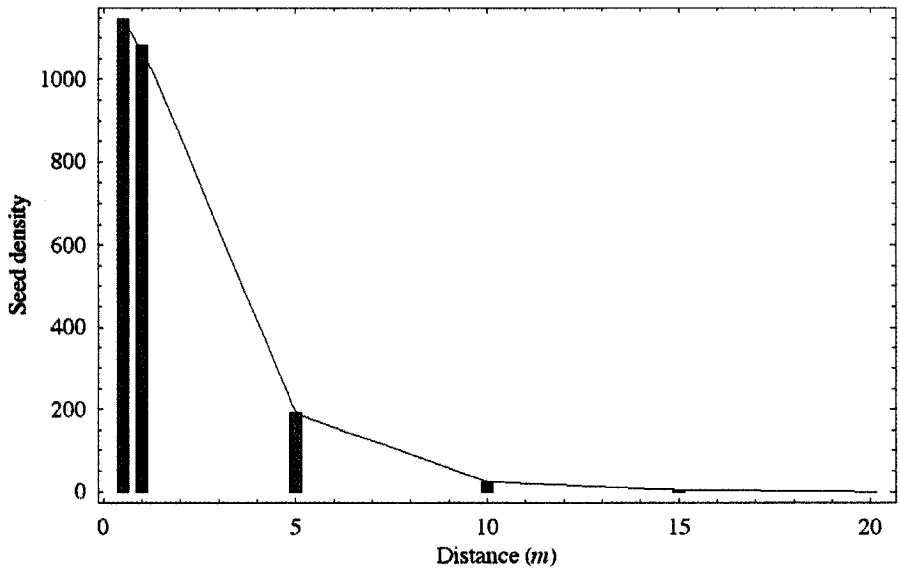

Figure 3.6: Scentless chamomile seed density trapped at different distances from a source plant. All cardinal directions are summed. The line shows a linear interpolation curve

long term climatic conditions (Woo et al., 1991), this is consistent with our results. Differences in growth rates could be explained by inter and intra-specific competition. Year 1 was dominated by stinkweed (*Thlaspi arvense*) and year 2 and 3 dominated by absinth (*Artemisia absinthium*). Depending on the differing competitive ability of these 2 species, this could have had an important impact on survivorship of scentless chamomile. In addition to this, because of the high productivity of scentless chamomile in year 1 (approx. 12,000 seeds in $4m^2$), seedling density was higher at the beginning of year 2, which could have triggered intraspecific competition and hence changes in survivorship and fecundity due to density dependent effects, not considered in the matrix model. Also, since no new SC plants emerged in 2004, as only flowering rosettes remained in the plots, which could have resulted in higher fecundities that year.

These elasticity results are consistent with those of Hinz (1999), indicating that flower to flower transition has the highest impact on population growth. The elasticity matrix from 30,000 bootstrapped matrices (Figure 3.8), shows that 99% of the matrices maintain transition a_{33} (flower to flower) as the entry with highest elasticity, which indicates the robustness of this result. However, looking at the net reproductive rate formula of scentless chamomile given by equation 3.7, it can be seen that flower to flower transition corresponds only to one reproductive pathway in the formula so even if this is reduced to less than 1, there are other two pathways that can make

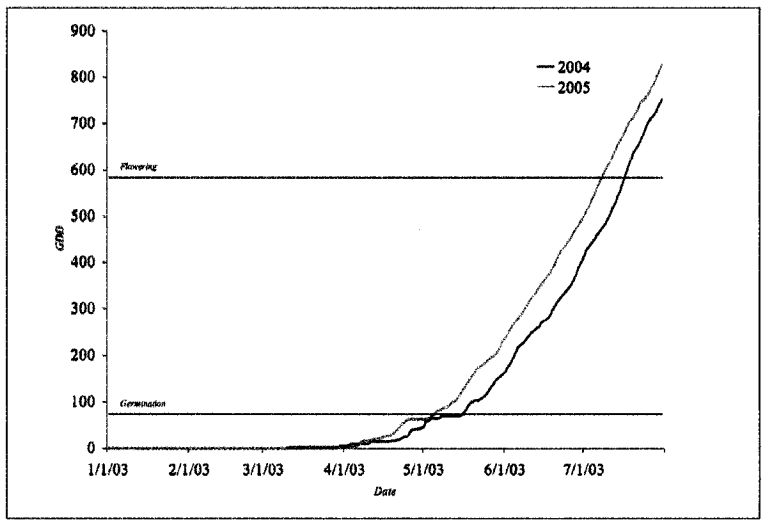

Figure 3.7: Growing degree days from January to August, 2004 and 2005; Vegreville, Alberta, Canada. The horizontal lines show the GDD at which germination and flowering is expected based on Blackshaw and Harker (1997)

the population grow. As an example consider when a_{11} is large and considering that $a_{11}+a_{21}+a_{31} \leq 1$, the first term of the R_0 becomes larger, suggesting that even if a_{33} is reduced to less than 1, the population could still grow, because of other reproductive pathways. This suggests that only reducing fecundity may not be sufficient to reduce scentless chamomile populations. Suppose we could eliminate all seed heads in one year, by analyzing the R_0 equation and looking at the life cycle (Figure 3.3), it can be seen that with enough seeds in the seed bank, scentless chamomile could reinvade in following years.

Our results show that a 53% reduction in fecundity had no measurable effect in densities the following year. Given this result, it seems that scentless chamomile is a difficult weed to control. Most likely a combined strategy with chemical, mechanical and biocontrol measures, would be most successful. The data also suggest that a theoretical approach to study R_0 as shown here, and explored in detail in later chapters for scentless chamomile and other organisms, could be an complementary and important tool to study the control and management of invasive species.

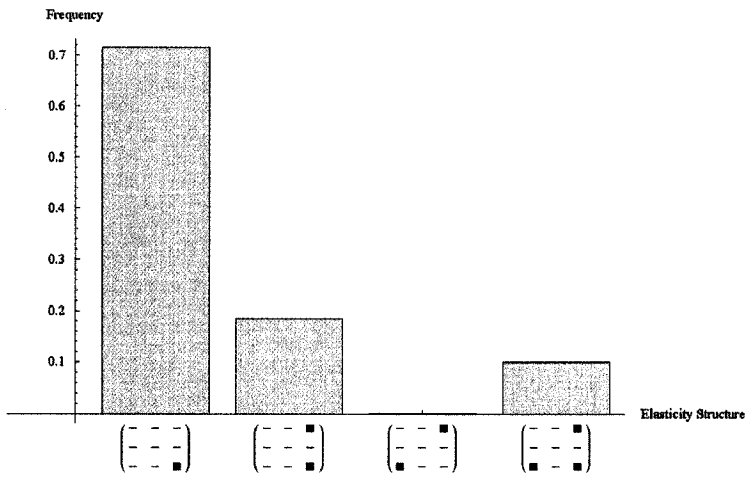

(a) Year 1

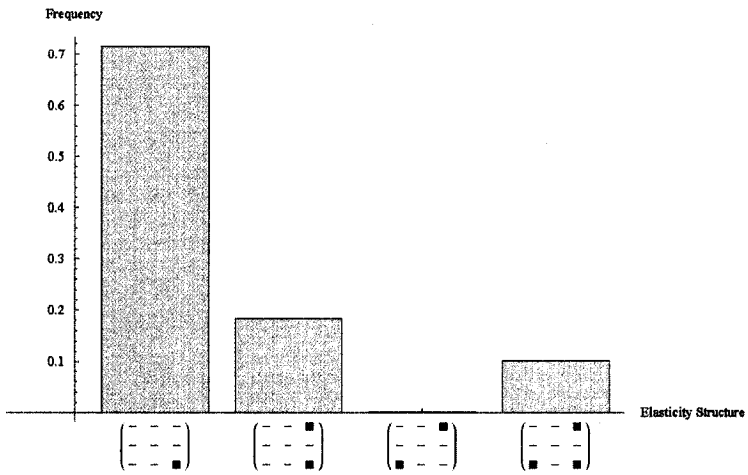

(b) Year 2

Figure 3.8: Frequency of elasticity matrix structure for scentless chamomile, obtained from 30,000 bootstrapped samples. The dark squares in the matrices on the x-axis, indicate elasticities higher than 0.2. The matrix structure with the highest frequencies include the flower to flower transition as the most important

Bibliography

Berryman, A., 1999. Theoretical approaches to biological control, Chapter the theoretical foundations of biological control, pages 43–68 . Cambridge University Press.

Blackshaw, R. and K. Harker. 1997. Scentless chamomile (*Matricaria perforata*) growth, development, and seed production. Weed Science **45**:701–705.

Borchers, D., S. Buckland, and W. Zucchini. 2002. Statistics for Biology and Health. Springer.

Bowes, G., D. Spurr, A. Thomas, D. Peschken, and D. Douglas. 1994. Habitats occupied by scentless chamomile (*Matricaria perforata* Merat) in Saskatchewan. Canadian Journal of Plant Science **74**:383–386.

Buckley, Y., H. Hinz, D. Matthies, and M. Rees. 2001. Interactions between density-dependent processes population dynamics and control of an invasive plant species, *Tripleurospermum perforatum* (scentless chamomile). Ecology Letters **4**:551–558.

Cameron, A. and P. Trivedi. 1998. Regression Analysis of Count Data. Cambridge University Press.

Caswell, H. 2001. Matrix Population Models: Construction, Analysis, and Interpretation. 2nd edition. Sinauer Associates.

Douglas, D., A. Thomas, D. Peschken, G. Bowes, and D. Derksen. 1991. Effects of summer and winter annual scentless chamomile (*Matricaria perforata* Merat) interference on spring wheat yield. Canadian Journal of Plant Science **71**:841–850.

Douglas, D., A. Thomas, D. Peschken, G. Bowes, and D. Derksen. 1992. Scentless chamomile (*Matricaria perforata* Merat) interference in winter-wheat. Canadian Journal of Plant Science **72**:1383–1387.

Fagan, W., M. Lewis, M. Neubert, and P. Van Den Driessche. 2002. Invasion theory and biological control. Ecology Letters **5**:148–157.

Hinz, H. 1998. Life history and host specificity of *Rhopalomyia n. sp.* (Diptera: Cecidomyiidae), a potential biological control agent of scentless chamomile. Environmental Entomology **27**:1537–1547.

Hinz, H., 1999. Prospects for the classical biological control of *Tripleurospermum perforatum* in North America. Ph.D. thesis, Freigurg-Schweiz University.

Hinz, H. and H. Muller-Scharer. 2000. Influence of host condition on the performance of *Rhopalomyia n. sp* (Diptera: Cecidomyiidae), a biological control agent for scentless chamomile, *Tripleurospermum perforatum.* Biological Control **18**:147–156.

Hinz, H. and D. Schroeder. 2003. Impact of competition from wheat and below-ground herbivory on growth and reproduction of scentless chamomile, *Tripleurospermum perforatum* (Merat) Lainz. Journal of Applied Entomology-Zeitschrift Fur Angewandte Entomologie **127**:72–79.

Kean, J. and N. Barlow. 2000. Can host-parasitoid metapopulations explain successful biological control? Ecology **81**:2188–2197.

Lutman, P. 2002. Estimation of seed production by *Stellaria Media, Sinapis Arvensis* and *Tripleurospermum Inodorum* in arable crops. Weed Research **42**:359–369.

McClay, A. and R. De Clerck-Floate. 1999. Establishment and early effects of *Omphalapion hookeri* (Kirby) (Coleoptera: Apionidae) as a biological control agent for scentless chamomile, *Matricaria perforata* Merat (Asteraceae). Biological Control **14**:85–95.

Milberg, P. and E. Hallgren. 2004. Yield loss due to weeds in cereals and its large-scale variability in Sweden. Field Crops Research **86**:199–209.

Murdoch, W. and C. Briggs. 1996. Theory for biological control: Recent developments. Ecology **77**:2001–2013.

Myers, J. and D. Bazely. 2003. Ecology and Control of Introduced Plants. Cambridge University Press.

Peng, G., K. Bailey, H. Hinz, and K. Byer. 2005. *Colletotrichum sp*: A potential candidate for biocontrol of scentless chamomile (*Matricaria perforata*) in Western Canada. Biocontrol Science and Technology **15**:497–511.

Thomson, D. 2005. Matrix models as a tool for understanding invasive plant and native plant interactions. Conservation Biology **19**:917–928.

Woo, S., A. Thomas, D. Peschken, G. Bowes, D. Douglas, V. Harms, and A. Mcclay. 1991. The biology of Canadian weeds .99. *Matricaria perforata* Merat (Asteraceae). Canadian Journal of Plant Science **71**:1101–1119.

Chapter 4

A new method for calculating net reproductive rate

4.1 Introduction

Matrix models are widely used for demographic analysis of age and stage structured population dynamics. Population dynamics of stage structured matrix models can be analyzed by calculating the population growth rate λ, the dominant eigenvalue of the projection matrix, and the net reproductive rate R_0, the mean number of offspring per individual over its lifetime (Caswell, 2001). Here $\lambda = 1$ if and only if $R_0 = 1$. The population grows when λ or R_0 is greater than 1 and shrinks when λ or R_0 is less than 1.

One method for calculating the characteristic equation, and hence the population growth rate λ, for a stage structured model, is directly from the graph representation of a matrix model, known as the life cycle graph. In this approach, a Z-transform is applied to the graph in order to use graph reduction rules and Mason's formula to compute the characteristic equation and corresponding eigenvalues and eigenvectors (Werner and Caswell, 1977; Caswell, 1982*a*, 1984). Graph reduction is used to simplify matrix operations that can be tedious on large and complex matrices. Although these procedures have been well described for calculating λ (e.g Caswell, 2001), no procedure has been developed using this technique to calculate R_0.

In this paper we introduce a new method to calculate the net reproductive rate directly from the life cycle graph; as far as we are aware, no such method has been proposed before. We then show how this method can be applied, with some literature examples, to analyze the control of invading organisms.

4.1.1 Matrix models and life cycle graphs

An age or stage structured matrix model is defined as $\mathbf{n}_{t+1} = \mathbf{A}\mathbf{n}_t$, where $\mathbf{n}_t$ is a vector of ages/stages at time t and $\mathbf{A}$ is a non negative irreducible matrix, describing transitions from one age/stage to another one (Caswell, 2001). Matrix models can be represented by a life cycle graph, where each age/stage is represented as a node in the graph, and transitions are arcs (directed edges) from node to node. More formally, for an $n \times n$ transition matrix $\mathbf{A} = [a_{ij}]$, the associated graph $G_\mathbf{A}$ is a weighted, directed graph, whose nodes are $V = \{1, \ldots, n\}$, such that if $a_{ij} \neq 0$ in $\mathbf{A}$, there is an *arc* from j to i with weight a_{ij} in $G_\mathbf{A}$, for $i, j = 1, \ldots, n$. As an example, the graph from figure 4.1(b) panel A has the projection matrix shown in figure 4.1(a). In a graph $G_\mathbf{A}$ a *path* is a sequence of arcs from one node to another. When the starting and ending nodes of a path are the same, the path is a *loop* (including a self loop at node i if $a_{ii} \neq 0$). Two paths are *disjoint* when they have no nodes in common.

4.1.2 Population growth λ and net reproductive rate R_0

For a non-negative primitive matrix $\mathbf{A}$ the *Perron-Frobenius* theorem ensures that there is a positive and simple dominant eigenvalue λ (Horn and Johnson, 1985). This dominant eigenvalue, or population growth rate, can then be used as a parameter to establish the long-term growth rate of the system described by the matrix. For matrix $\mathbf{A}$, when $\lambda < 1$ the extinction steady state is stable, when $\lambda = 1$ the population is neutrally stable and when $\lambda > 1$ the population grows (Caswell, 2001).

To calculate R_0, the transition matrix is decomposed as $\mathbf{A} = \mathbf{T}+\mathbf{F}$, where $\mathbf{T} = [\tau_{ij}]$ (with $\tau_{ij} \in [0, 1]$ and $\sum_j \tau_{ij} \leq 1$) contains the survivorship transitions and $\mathbf{F} = [f_{ij}]$ (with $f_{ij} \geq 0$) the fecundities. Each entry in $\mathbf{T}$ describes the probability of an individual in stage j surviving to stage i in a single time step. Since individuals in a population eventually die, it is further assumed that $\rho(\mathbf{T}) < 1$ (Li and Schneider, 2002). Once the transition and fecundity matrix are given, $\mathbf{A}$ is uniquely determined. However, decomposition of $\mathbf{A}$ into transition and fecundity matrices is not unique. This decomposition allows for the calculation of the net reproductive rate, R_0, defined mathematically as

$$R_0 = \rho(\mathbf{F}(\mathbf{I} - \mathbf{T})^{-1}), \tag{4.1}$$

where $\mathbf{I}$ is the identity matrix and ρ denotes the spectral radius of the matrix $\mathbf{F}(\mathbf{I} - \mathbf{T})^{-1}$, referred to as the next generation matrix (Li and Schneider, 2002). If $\mathbf{F}(\mathbf{I} - \mathbf{T})^{-1}$ is non-negative and primitive then R_0 is the strictly positive dominant eigenvalue of the matrix. It has been shown (Cushing and Zhou, 1994; Li and Schneider, 2002) that when $R_0 < 1$, the extinction state is stable, when $R_0 = 1$, the extinction state is neutrally stable and when $R_0 > 1$ the population grows. In other words, $\lambda > 1 \iff R_0 > 1$, where λ is the dominant eigenvalue of matrix $\mathbf{A}$.

$$\mathbf{A} = \begin{bmatrix} 0 & a_{12} \\ a_{21} & a_{22} \end{bmatrix}$$

(a) Projection matrix

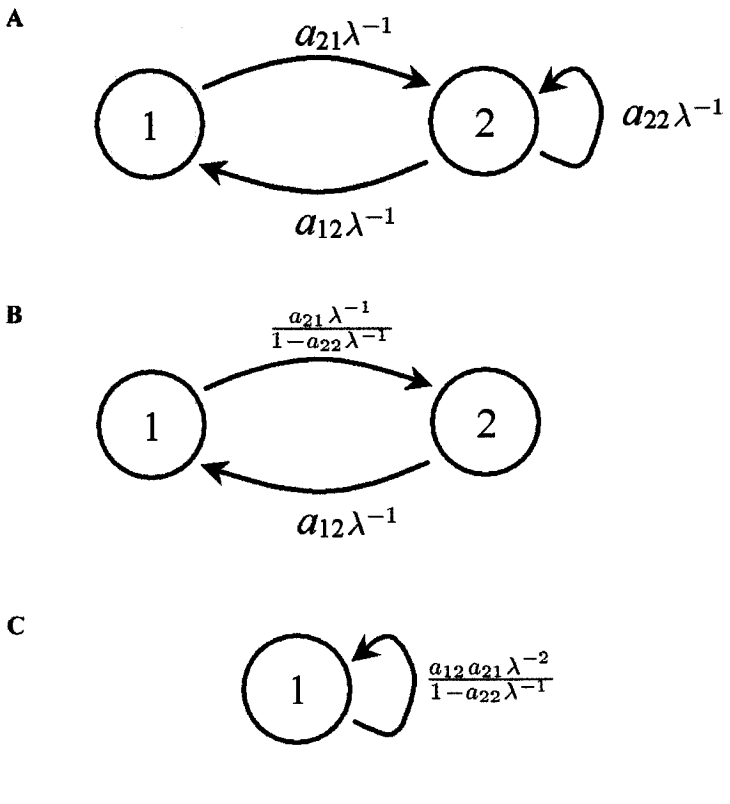

(b) Life cycle graph

Figure 4.1: A. A simple 2 node graph, B. The z-transformed graph $\mathcal{G}_{\mathbf{A}}(\lambda)$, C. Self loop of node 2 is eliminated using rule A of figure 4.2, D. Node 2 is eliminated using rule E of figure 4.2, E. Characteristic equation is calculated from equation (4.2) applied to the single-node graph given in D: $1 - L^{(1)} = 0$, where $L^{(1)} = \frac{a_{12}a_{21}\lambda^{-2}}{1-a_{22}\lambda^{-1}}$

4.2 Graph reduction of matrix models and net reproductive rate

We now introduce our new approach to calculating R_0 directly from a graph, without the need for matrix calculations. First we review an establish graph-based method for the calculation of the characteristic polynomial for a matrix, and then we show, in the following section, the related procedure that can be used to calculate R_0.

4.2.1 Established graph-based method for calculating the characteristic polynomial

To compute the dominant eigenvalue λ or any other eigenvalue from the graph $G_{\mathbf{A}}$, Caswell's formula (Caswell, 1982*b*) for the characteristic equation of the z-transformed graph, denoted $\mathcal{G}_{\mathbf{A}}$, can be used. A z-transformed graph $\mathcal{G}_{\mathbf{A}}(\lambda)$ is defined as the graph obtained from replacing entries a_{ij} in $G_{\mathbf{A}}$, with $a_{ij}\lambda^{-1}$ (Caswell, 2001). Hence the characteristic equation, denoted $P(\mathcal{G}_{\mathbf{A}}(\lambda)) = 0$, yields n possible values for λ, the largest of which is the population growth rate λ and the remaining $n-1$ values are additional smaller eigenvalues. The characteristic polynomial is defined as $P(\mathcal{G}_{\mathbf{A}}(\lambda)) = \det(\mathbf{A}\lambda^{-1} - \mathbf{I})$. If $\lambda = 1$, then $P(\mathcal{G}_{\mathbf{A}}(1)) = \det(\mathbf{A} - \mathbf{I})$. The formula for the characteristic equation, due to Hubbell and Werner (1979) and Caswell (1982*b*), is given by

$$P(\mathcal{G}_{\mathbf{A}}(\lambda)) = 1 - \sum_{i} L^{(i)} + \sum_{i,j}^{*} L^{(i)}L^{(j)} - \sum_{i,j,k}^{*} L^{(i)}L^{(j)}L^{(k)} + \ldots = 0, \tag{4.2}$$

where $L^{(i)}$ is the product of arc coefficients in the i^{th} loop in the graph $\mathcal{G}_{\mathbf{A}}(\lambda)$, and the asterisk indicates that the sum is taken over the product of pairs, triplets, and so forth. See Mason and Zimmermann (1960) and Chen (1976) for a detailed derivation of the formula and Caswell (2001) for applications to life cycle graphs.

By way of example consider the life cycle graph shown in figure 4.1. From the graph shown in figure 4.1A, there are two loops, $L^{(1)} = a_{22}\lambda^{-1}$ and $L^{(2)} = a_{12}a_{21}\lambda^{-2}$. Applying equation (4.2), we get $P(\mathcal{G}_{\mathbf{A}}(\lambda)) = 1 - (a_{22}\lambda^{-1} + a_{21}a_{12}\lambda^{-2}) = 0$.

For a complicated life cycle graph calculation using equation (4.2) can be onerous. However, the same result can be obtained via graph reduction, a procedure that allows for the elimination of paths and nodes from a graph. Since a graph is a representation of a system of linear equations, graph reduction is equivalent to elimination of variables (nodes) by back-substitution. The application of graph reduction simplifies the calculation of equation (4.2). A graph can be reduced using the rules shown in figure 4.2. An important property of graph reduction is that the dynamic properties

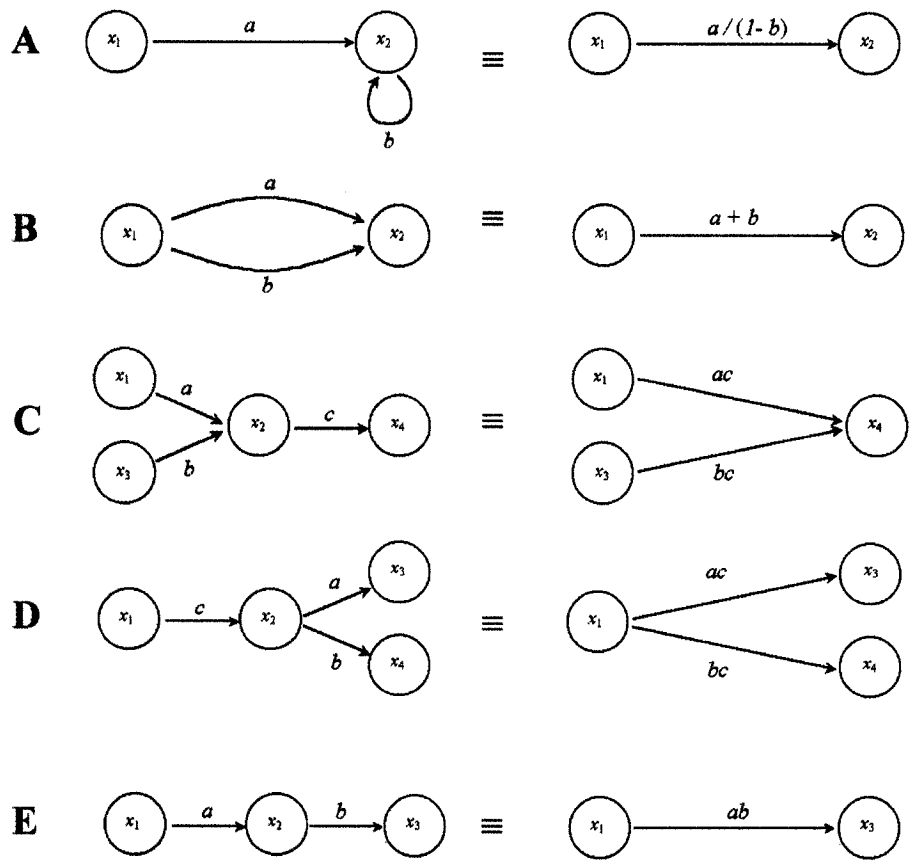

Figure 4.2: Mason equivalence rules for graph reduction (modified from Caswell, 2001). A. Self loop elimination, B. parallel paths elimination, C,D and E. Elimination of node x_2

of the system remain invariant under graph reduction (Caswell, 2001), that is, the characteristic equation remains invariant (Chen, 1976; Lewis, 1977). As shown in figure 4.1, a graph can be reduced completely to one node to obtain the characteristic equation directly. From the previous example (figure 4.1), using graph reduction we obtain the same result (figure 4.1E).

4.2.2 Calculating R_0 from the graph

As mentioned earlier, given a projection matrix, the net reproductive rate can be calculated using equation (4.1). To connect the calculation of R_0 with graph reduction methods we first observe that, for any irreducible and non-negative matrix

$\mathbf{A} = \mathbf{T} + \mathbf{F}$, which can be decomposed into survivorship transitions $\mathbf{T}$ and fecundity $\mathbf{F}$, as defined in Section 4.1.2, the basic reproductive rate can be rewritten implicitly as:

$$\rho(R_0\mathbf{T} + \mathbf{F}) = R_0, \tag{4.3}$$

where ρ denotes the spectral radius. For detailed derivation of equation (4.3) see appendix A. Note that for a non-negative, primitive matrix, there is only one eigenvalue with modulus ρ, so this eigenvalue is called the *dominant eigenvalue* in demographic analysis (Li and Schneider, 2002).

Now, given equation (4.3), we can use the *z-transform* of the matrix $\mathbf{B} = R_0\mathbf{T} + \mathbf{F}$, to calculate using equation (4.2), the characteristic polynomial of $\mathbf{B}$, $P(\mathcal{G}_\mathbf{B}(R_0))$. Note that $\mathcal{G}_\mathbf{B}(R_0)$ can be related to the graph of $\mathbf{A}$, $G_\mathbf{A}$, as follows: each entry $a_{ij} = t_{ij} + f_{ij}$ in $G_\mathbf{A}$ is replaced by $b_{ij}R_0^{-1} = (R_0 t_{ij} + f)R_0^{-1} = t_{ij} + fR_0^{-1}$. In other words $\mathcal{G}_\mathbf{B}(R_0)$ is found by multiplying the fecundity transitions in $G_\mathbf{A}$ by R_0^{-1}.

As we did previously, we can again apply Mason's rules for graph reduction now to solve $P(\mathcal{G}_\mathbf{B}(R_0)) = 0$ for R_0. According to equation (4.3), R_0 is the dominant eigenvalue of $\mathbf{B}$, and hence satisfies $P(\mathcal{G}_\mathbf{B}(R_0)) = 0$.

As an example consider a case where $\mathbf{T}$ and $\mathbf{F}$ are disjoint as shown in figure 4.3(a). Figure 4.3 shows the graph reduction procedure to obtain the characteristic equation for this example. Note that the rank of $\mathbf{F}$ is one and therefore the polynomial $P(\mathcal{G}_\mathbf{B})$ is a polynomial of degree 1; hence there is only one possible value for R_0.

Suppose that $\tilde{\mathcal{G}}_\mathbf{B}$ is the graph obtained from applying Mason's rules to $\mathcal{G}_\mathbf{B}$. We can always apply equation (4.2) to obtain $P(\tilde{\mathcal{G}}_\mathbf{B})$, and then solve for R_0, or we can continue with reduction until there is one node left. In either case, R_0 remains invariant, but the graph reduction method its easier to apply and the result yields a simplified equation.

While typical expressions for R_0 are given explicitly, vegetative reproduction (or clonal reproduction) can lead to more complex reduced graphs, such as the one shown in figure 4.4. Note that all the fecundity transitions in figure 4.4A are multiplied by R_0^{-1}, that in the reduced graph (figure 4.4C) fecundity paths contain the term R_0^{-1}, and that these fecundity loops are not disjoint. To calculate R_0, we apply formula (4.1) on the matrix corresponding to the remaining reduced graph to calculate R_0. This type of graph can occur when there is vegetative reproduction (see for example Dinnetz and Nilsson, 2002), and fecundity pathways in the life cycle graph that reproduce independently from other pathways.

In summary, given the matrix $\mathbf{B} = R_0\mathbf{T} + \mathbf{F}$, and the corresponding graph $\mathcal{G}_\mathbf{B}$, the graph reduction algorithm to calculate R_0 can be applied as follows: 1) Eliminate survivorship self-loops from $\mathcal{G}_\mathbf{B}$, 2) Reduce the graph until only nodes with fecundity self-loops are left, 3) If only one node is left, then eliminate the final node and the result will be R_0; otherwise solve the polynomial that comes from applying equation (4.2) to the reduced graph.

$$\mathbf{T} = \begin{bmatrix} a_{11} & 0 & 0 \\ a_{21} & 0 & 0 \\ a_{31} & a_{32} & 0 \end{bmatrix} \qquad \mathbf{F} = \begin{bmatrix} 0 & 0 & a_{13} \\ 0 & 0 & a_{23} \\ 0 & 0 & a_{33} \end{bmatrix}$$

(a) Projection matrix

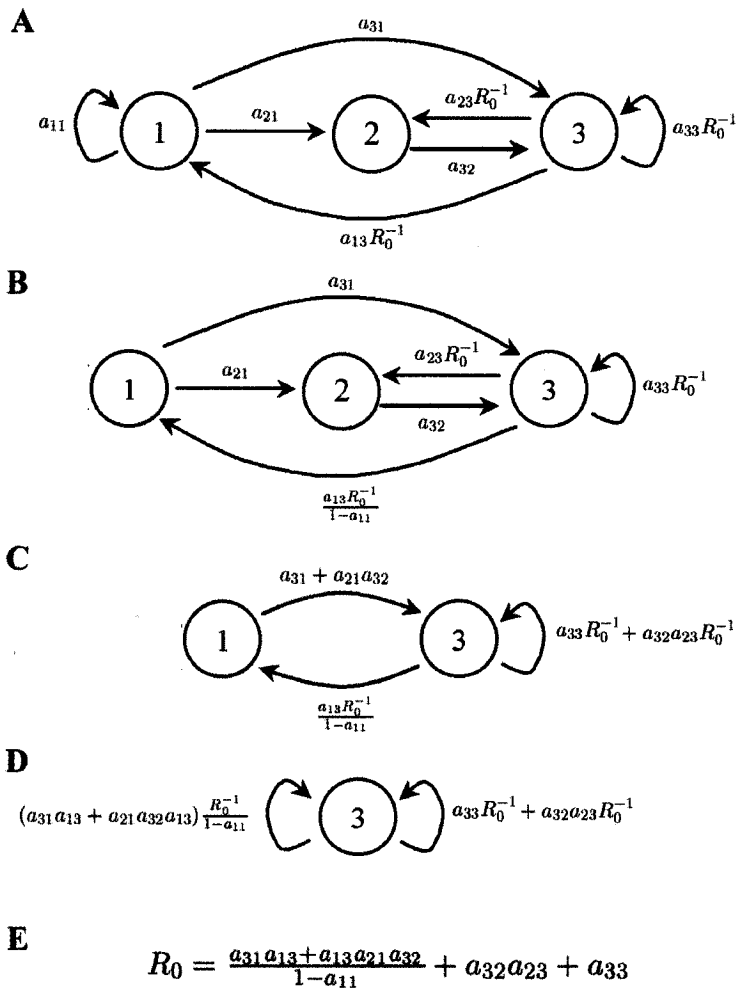

(b) Life cycle graph reduction

Figure 4.3: (a) An example of a transition and fecundity matrix.(b) Graph reduction procedure. A. The full transformed graph (with associated matrices (a)), B. Eliminating self-loop in node 1, C. Eliminating node 2, D. Eliminating node 1, E. Eliminating node 3 and solving for R_0

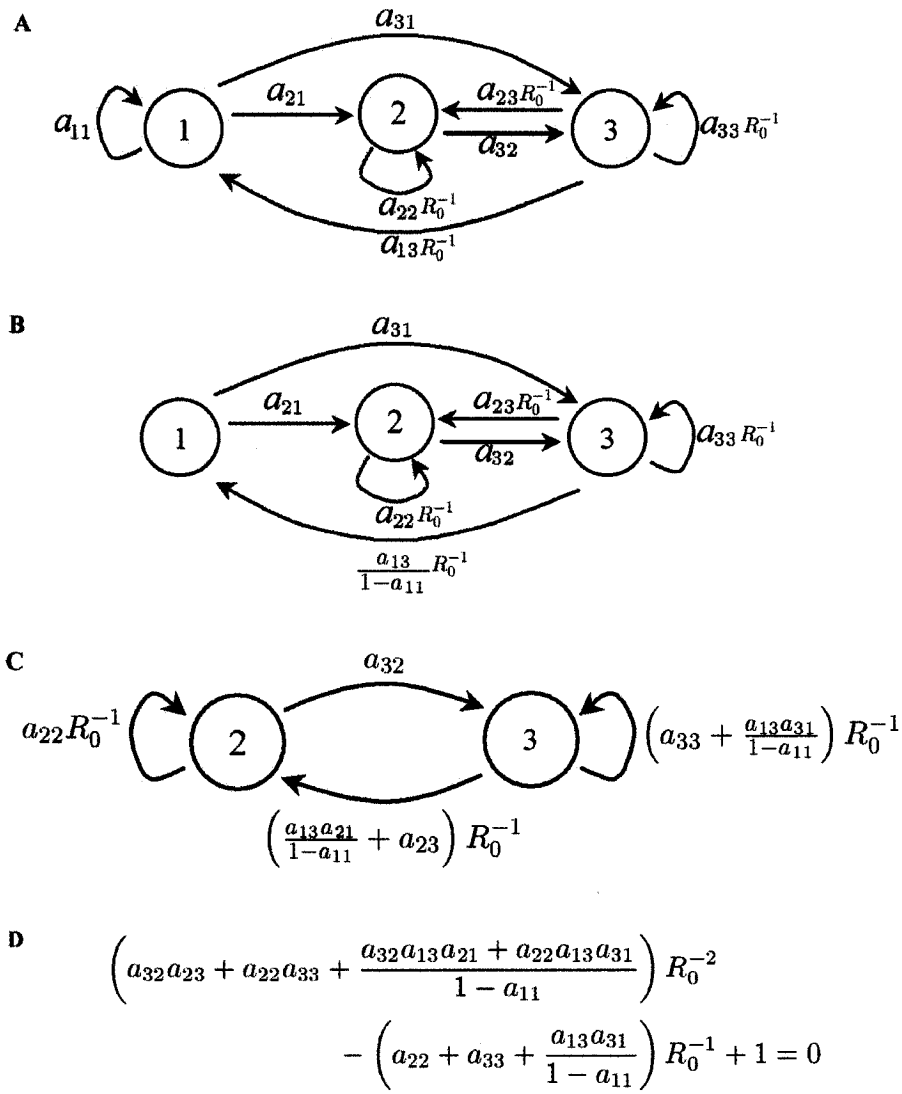

Figure 4.4: Hypothetical life cycle graph with vegetative reproduction. This graph is the same as figure 4.3A, except an additional self loop is added in node 2. A. full graph, B. Elimination of self loop in node 1, C. Elimination of node 1, D. R_0 equation

4.3 Applications

4.3.1 Scentless chamomile (*Matricaria perforata*)

Scentless chamomile is an introduced annual, biennial or short-lived perennial plant that has become a widely distributed weed in cultivated areas in North America (Hinz, 1996; Hinz and McClay, 2000). In Hinz (1996), a stage-structure model is developed, and transition values are compared between different disturbance treatments (soil disturbance and herbivory). The full life cycle is shown in figure 4.3A. Hinz (1996) showed, using elasticity matrices, that in general, transition from rosettes to flowering plants a_{32} and fecundity transitions a_{23} and a_{33} contributed the most to population growth and would therefore be the most effective transitions to control. We calculate R_0 by applying the graph reduction procedure (figure 4.3),

$$R_0 = \frac{a_{31}a_{13} + a_{13}a_{21}a_{32}}{1 - a_{11}} + a_{32}a_{23} + a_{33} \tag{4.4}$$

Examination of R_0 gives additional insight. The fecundity transitions are a_{13}, a_{23}, a_{33}. Note that, if transition a_{33} is larger than one, $R_0 > 1$ regardless of the contributions of other transitions, and population increase will occur. Similarly if the loop $a_{32}a_{23} > 1$ then the population will increase regardless of the other fecundity pathways. This is consistent with Hinz's results (Hinz, 1996), which were based on parameter values, showed elasticity matrices where a_{33} is more important, and other treatments indicated that a_{32} and a_{23} affect population growth the most. This suggests that any control strategy must focus on reducing fecundity below a critical level. However, this action alone would not ensure successful control. For example, as seed bank survival a_{11} gets large, under the restriction that $a_{11} + a_{21} + a_{31} \leq 1$, the term $(1 - a_{11})^{-1}$ becomes large and the population will increase. Hinz (1996) found that transitions a_{13}, a_{31} and a_{21} to be of minor importance. However, it can be seen from the R_0 equation that this situation would probably change as a_{11} increases. With this example we have shown how the analysis of fecundity pathways using R_0 can complement the design of effective control strategies.

4.3.2 Nodding thistle (*Carduus nutans*)

Shea and Kelly (1998) derived a matrix model to study the control of nodding thistle (*Carduus nutans*), a weed that causes economic damage to grazing lands in New Zealand. The authors described the life cycle of *C. nutans* by the graph in figure 4.5A. They concluded using elasticity analysis that seed to seedling and small-plants to seeds transitions contribute the most to λ (g_{21} and r_{12} in the graph). The numerical results indicate that seed losses of 69% are required to reduce the weed populations. A 30%-40% reduction in seed production has been unsuccessful in New Zealand, but

successful in North America, which contradicts the numerical results and suggests regional differences. Their general conclusion was that, to control *C. nutans*, a large reduction in seed bank and suppression of germination is needed. For comparison, using graph reduction we obtained the 2 node graph in figure 4.5C, and further elimination yields:

$$R_0 = r_{22} + g_{42}r_{24} + g_{32}r_{23} + g_{32}g_{43}r_{24} + \frac{g_{21}r_{12} + g_{21}g_{32}r_{13} + g_{21}g_{42}r_{14} + g_{32}g_{43}g_{21}r_{14}}{1 - s_{11}}. \tag{4.5}$$

It is evident from R_0 that if only survivorship g_{21} is reduced by control, but small plant fecundities (r_{12} and r_{22}) are not, then since $r_{22} > 1$ the system is unstable ($R_0 > 1$). As with the previous example, as s_{11} approaches 1, the term $(1 - s_{11})^{-1}$ becomes large, driving R_0 above one. This is consistent with Shea and Kelly (1998), with g_{21} included in all pathways involving a_{11}, but it provides a more general result because we do not require numerical analysis to get to this result. Shea and Kelly (1998) suggest that grazing could contribute substantially to thistle control. We extend the graph reduction procedure to calculate R_0 to explore the combined effects of biocontrol and grazing. To simplify analysis further, we focus on the reproductive pathways, denoting $P_{1,2,\ldots,n}$ as a reproductive path that goes through nodes $1, 2, \ldots, n$. Equation (4.5) can be rewritten as

$$R_0 = \left[P_2 + P_{2,3} + P_{2,4} + P_{2,3,4} + \left(\frac{P_{1,2} + P_{1,2,3} + P_{1,2,4} + P_{1,2,3,4}}{1 - s_{11}}\right)\right] \tag{4.6}$$

where $P_2 = r_{22}, P_{2,3} = g_{32}r_{23}, P_{2,4} = g_{42}r_{24}, P_{2,3,4} = g_{32}g_{43}r_{24}, P_{1,2} = g_{21}r_{12}, P_{1,2,3} = g_{21}g_{32}r_{13}, P_{1,2,4} = g_{21}g_{42}r_{14}$ and $P_{1,2,3,4} = g_{32}g_{43}g_{21}r_{14}$.

Suppose a biocontrol agent is used to control fecundity of reproductive plants (transitions into node 1). The reduction in seed production is represented by scaling variable u_1. The level of grazing, which reduces germination and affects transition g_{21} , is represented by u_2, where $0 \leq u_i \leq 1$ is the proportional reduction in pathways. Note that all the fecundity paths go through node 2 or node 1. So, we can rewrite $P_{i\cdot}^k$ as the pathways of length k that start and end in node i. The R_0 equation can thus be rewritten:

$$R_0 = (1 - u_1)\sum_k \frac{P_{1\cdot}^k}{1 - s_{11}} + (1 - u_2)\sum_k P_{2\cdot}^k \tag{4.7}$$

If $u_1 = 0$, meaning no effort is applied to control germination (i.e. the only control of the path from node 1 to 2 is grazing), then we need a larger proportional reduction in grazing to control the system. Note that in this case control u_2 is chosen based on the number of pathways where transition from 1, 2 is involved. This method confirms analytically the suggestion of Shea and Kelly (1998) that grazing could complement biological control.

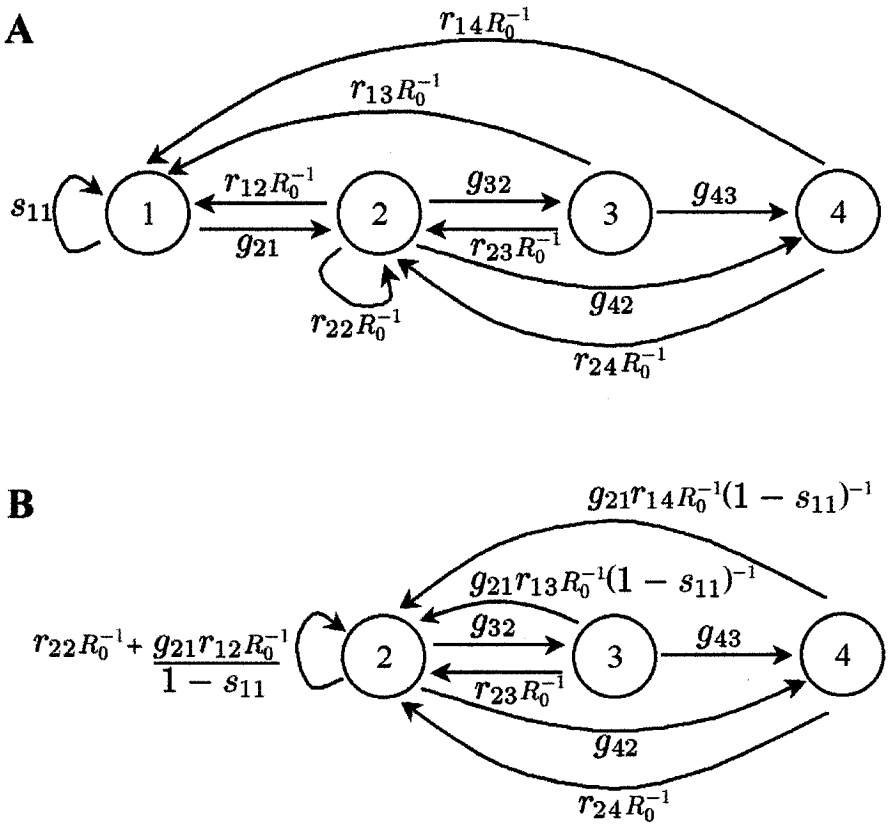

$$\alpha_1 = r_{22} + g_{42}r_{24} + \frac{g_{21}r_{12} + g_{21}g_{42}r_{14}}{1 - s_{11}}$$

$$\alpha_2 = r_{23} + g_{43}r_{24} + \frac{g_{21}r_{13} + g_{21}g_{43}r_{14}}{1 - s_{11}}$$

D

$$R_0 = r_{22} + g_{42}r_{24} + g_{32}r_{23} + g_{32}g_{43}r_{24} + \frac{g_{21}r_{12} + g_{21}g_{32}r_{13} + g_{21}g_{42}r_{14} + g_{32}g_{43}g_{21}r_{14}}{1 - s_{11}}$$

Figure 4.5: Nodding thistle life cycle graph as described by Shea and Kelly (1998). Node 1, seed bank; nodes 2, 3 and 4, small, medium, and large plants. Reproductive transitions are labelled r_{ij} coming out of three nodes $(2, 3, 4)$. A. Full transformed graph, B. Elimination of node 1, C. Elimination of node 4 D. Resulting net reproductive rate.

4.4 Conclusion

Because of their dynamical properties, λ and R_0 are demographic parameters by which optimization can be applied to design a control strategy for unwanted species. As we show here, with the new method given in this paper, it is straightforward to obtain an analytical formula for R_0 using graph reduction methods. The examples show that some analysis of the R_0 equation can aid in biocontrol target selection and more generally in the design of control and conservation strategies. In some cases perturbations in the transition matrix that decrease R_0 may increase λ and vice versa (Caswell, 2001). Nonetheless since $R_0 < 1$ implies $\lambda < 1$, a control strategy that guarantees $R_0 < 1$ for biocontrol, or $R_0 > 1$ for conservation, can be useful in the first stages of planning and can be refined as more data are obtained. In this way, the use of R_0 is a useful alternative to numerical analysis of λ for designing a general control strategy framework that can be customized to accommodate different parameter values in different regions.

Appendix

4.A Derivation of the R_0 equation

Our goal is to show how to derive equation $R_0 = \rho(R_0\mathbf{T} + \mathbf{F})$. The projection matrix $\mathbf{A} = \mathbf{T} + \mathbf{F}$, can be decomposed into survivorship transitions $\mathbf{T}$ and fecundity $\mathbf{F}$. The survivorship matrix contains the probability of stage transitions $\mathbf{T} = [\tau_{ij}]$ with $0 \leq \tau_{ij} \leq 1$, $\rho(\mathbf{T}) < 1$, and $\sum_j \tau_{ij} \leq 1$. The fecundity matrix $\mathbf{F}$ has entries $f_{ij} \geq 0$. We know that $(\mathbf{I} - \mathbf{T})^{-1}$ is nonnegative, because $\mathbf{T}$ is nonnegative, $\rho(\mathbf{T}) < 1$ and $\lim_{k\to\infty} \mathbf{T}^k = 0$ means $(\mathbf{I} - \mathbf{T})^{-1} = \mathbf{I} + \mathbf{T} + \mathbf{T}^2 + \ldots$ is nonnegative. By definition $\mathbf{F} \geq 0$. Hence $\mathbf{F}(\mathbf{I} - \mathbf{T})^{-1}$ is also nonnegative. Let λ_ρ be the eigenvalue of $\mathbf{F}(\mathbf{I} - \mathbf{T})^{-1}$ with $|\lambda_\rho| = R_0$ (equation 4.1). Since $\mathbf{F}(\mathbf{I} - \mathbf{T})^{-1}$ is nonnegative, there is a nonnegative left eigenvector (Perron vector) $\mathbf{u}^T$ corresponding to λ_ρ that satisfies $\mathbf{u}^T\mathbf{F}(\mathbf{I} - \mathbf{T})^{-1} = \lambda_\rho\mathbf{u}^T$. The eigenvalue λ_ρ is real and positive, hence $\lambda_\rho = R_0$ is the dominant eigenvalue of $\mathbf{F}(\mathbf{I} - \mathbf{T})^{-1}$. Now, $\mathbf{u}^T\mathbf{F} = R_0\mathbf{u}^T(\mathbf{I} - \mathbf{T}) = R_0\mathbf{u}^T\mathbf{I} - R_0\mathbf{u}^T\mathbf{T}$. Therefore,

$$\mathbf{u}^T(\mathbf{F} + R_0\mathbf{T}) = \mathbf{u}^T\mathbf{F} + R_0\mathbf{u}^T\mathbf{T} = R_0\mathbf{u}^T \tag{4.8}$$

The matrix $\mathbf{A} = \mathbf{T} + \mathbf{F}$ is irreducible, hence $G_\mathbf{A}$ is strongly connected (see Horn and Johnson, 1985). Since $R_0 > 0$, then the graph corresponding to $R_0\mathbf{T} + \mathbf{F}$ is also strongly connected, hence $R_0\mathbf{T} + \mathbf{F}$ is irreducible. By Theorem 2.1b in Li and Schneider (2002), it follows that R_0 is the unique dominant eigenvalue. From equation (4.8) we can write the formula for R_0 as, $R_0 = \rho(R_0\mathbf{T} + \mathbf{F})$. A similar argument to

that used in this derivation is used by Li and Schneider (2002, Theorem 3.1) as part of the proof that R_0 implies stability of a non-negative irreducible matrix.

Bibliography

Caswell, H. 1982*a*. Optimal life histories and the age-specific costs of reproduction. Journal of Theoretical Biology **98**:519–529.

Caswell, H. 1982*b*. Optimal life histories and the maximization of reproductive value - a general theorem for complex life-cycles. Ecology **63**:1218–1222.

Caswell, H. 1984. Optimal life histories and age-specific costs of reproduction - 2 extensions. Journal of Theoretical Biology **107**:169–172.

Caswell, H. 2001. Matrix Population Models: Construction, Analysis, and Interpretation. 2nd edition. Sinauer Associates.

Chen, W. 1976. Applied Graph Theory; graphs and electrical networks. 2d. rev. ed edition. North-Holland Pub. Co.

Cushing, J. and Y. Zhou. 1994. The net reproductive value and stability in matrix population models. Natural Resource Modeling **8**:297–333.

Dinnetz, P. and T. Nilsson. 2002. Population viability analysis of *Saxifraga cotyledon*, a perennial plant with semelparous rosettes. Plant Ecology **159**:61–71.

Hinz, H., 1996. International Symposium on Biological Control of Weeds: Proceedings of the IX International Symposium on Biological Control of Weeds, Chapter scentless chamomile, a target weed for biological control in Canada: Factors influencing seedling establishment, pages 187–192 .

Hinz, H. and A. McClay. 2000. Ten years of scentless chamomile: Prospects for the biological control of a weed of cultivated land. Proceedings of the X International Symposium on Biological Control of Weeds pages 537–550.

Horn, R. and C. Johnson. 1985. Matrix Analysis. Cambridge University Press.

Hubbell, S. and P. Werner. 1979. Measuring the intrinsic rate of increase of populations with heterogeneous life histories. American Naturalist **113**:277–293.

Lewis, E. 1977. Network Models in Population Biology. Springer-Verlag.

Li, C. and H. Schneider. 2002. Applications of Perron-Frobenius theory to population dynamics. Journal of Mathematical Biology **44**:450–462.

Mason, S. and H. Zimmermann. 1960. Electronic Circuits, Signals, and Systems. Wiley.

Shea, K. and D. Kelly. 1998. Estimating biocontrol agent impact with matrix models: *Carduus nutans* in New Zealand. Ecological Applications **8**:824–832.

Werner, P. and H. Caswell. 1977. Population-growth rates and age versus stage-distribution models for teasel (*Dipsacus sylvestris* Huds). Ecology **58**:1103–1111.

Chapter 5

Analysis of life cycle graph structure: R_0 and generation time

5.1 Introduction

One goal of controlling invading organisms is to reduce population growth. A useful way of achieving this is to identify aspects of the invader's life history that can be targeted for control, using demographic analysis. Demographic analysis is the study of population growth as affected by the explicit life history of individuals. Demographic models follow the fate of organisms, in terms of growth, survival and reproduction; the life history is represented as stages and transition between stages (Wardle, 1998). Demographic analysis can be done using matrix population models, a mathematical formalism that allows for the calculation of intrinsic population growth rate λ and the net reproductive rate R_0. It also allows for analysis of survival, growth and reproduction contributions to population growth, a method known as elasticity analysis (Caswell, 2001). Elasticity analysis is often used in management and control, to determine the transitions in the matrix models that have the most effect on population growth rate λ (Benton and Grant, 1999). In principle, any disturbance will ultimately have consequences in life history pathways (De Kroon et al., 2000). Hence analysis of these transitions is crucial to understand consequences of management and control.

The net reproductive rate R_0 can be calculated for matrix models. The net reproductive rate is the mean number of individuals that one individual will produce over its lifetime (Caswell, 2001). In that sense, R_0 is the per generation rate of increase. Both intrinsic growth rate and net reproductive rate determine if the population will increase or decrease over time (Cushing and Zhou, 1994). As shown in Chapter 4 $\lambda > 1$ if and only if $R_0 > 1$ (Cushing and Zhou, 1994; Li and Schneider, 2002). Therefore, if complete control is desired (eradication of the invader), control

strategies have to be designed that guarantee that λ or R_0 will be less than one. In this chapter I propose the use of the net reproductive rate R_0 to complement elasticity analysis for biocontrol. I use the method proposed on Chapter 4 to derive the R_0 equation of several literature examples. I later show how R_0 can be used to study the control of invading organisms.

Since, R_0 describes generation increments in population, it can be related to the population growth rate λ via the mean generation time (Myers and Bazely, 2003). There are several methods for age classified matrices that calculate generation time as: the time it takes for the population to increase by R_0 individuals, the mean age of the parents of the offspring produced over a cohort lifetime, and the mean age of the parents of the offspring produced by a stable age structure (Caswell, 2001). For stage-classified models, methods are not as direct. The generation time is calculated by relating the stage-classified model with an age-structured one (Cochran and Ellner, 1992; Lebreton, 2005; Houllier and Lebreton, 1986). These methods are not easy to apply and are restricted to certain matrix structures. In this chapter I also derive a new generation time estimate based on the analytic R_0 formula, and show with examples how it can be applied.

I believe the method of life cycle analysis, using R_0 and the calculation of generation time presented here, have implications for the management and control of invasive species.

5.2 Life cycle graphs

5.2.1 Defining the life cycle graph

The life cycle graph is a graphical representation of the life cycle of an organism. As described in Caswell (2001), the life cycle graph is constructed as follows:

1. Define a set of states that describe life stages of the organism.
2. Define the projection interval between stages.
3. For each stage, define a node. This node represents a stage in the life cycle graph.
4. Connect one node to another with an arc only if there is a contribution from that node to the next one within a single projection interval.

More formally, a life cycle graph, denoted $G_{\mathbf{A}}$, is a directed weighted graph whose nodes $V = \{1, \ldots, n\}$ are connected with directed edges $E = \{a_{ij}\}$ for $i, j = 1, \ldots, n$; that represent the projection a_{ij} from node j to node i. An example of a simple two

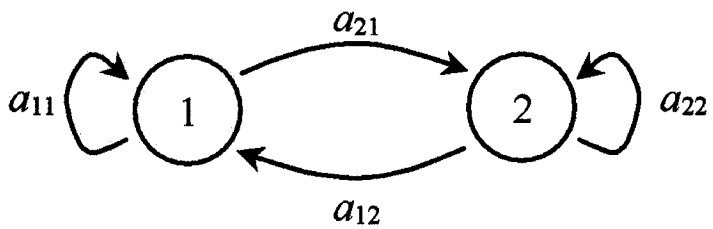

$$\mathbf{A} = \begin{bmatrix} a_{11} & a_{12} \\ a_{21} & a_{22} \end{bmatrix}$$

Figure 5.1: A 2 node life cycle graph and its associated projection matrix.

stage life cycle graph is shown in Figure 5.1. The life cycle graph is isomorphic to the projection matrix in matrix population models (Caswell, 2001). The relation of the graph $G_{\mathbf{A}}$ to the associated matrix $\mathbf{A}$ is as follows. First define an age/stage matrix model as:

$$\mathbf{n}_{t+1} = \mathbf{A}\mathbf{n}_t, \tag{5.1}$$

where $\mathbf{n}_t$ is a vector of ages/stages at time t and $\mathbf{A}$ is a non-negative irreducible matrix whose entries a_{ij} describe transitions from age/stage j to i. For an $n \times n$ projection matrix $\mathbf{A} = [a_{ij}]$, the associated graph $G_{\mathbf{A}}$ is a graph that has n nodes, such that if $a_{ij} \neq 0$ in $\mathbf{A}$, there is a *directed edge* from j to i with weight a_{ij} in $G_{\mathbf{A}}$, for $i, j = 1, \ldots, n$. A projection matrix and the associated life cycle graph is shown in Figure 5.1.

5.2.2 Classes of life cycle graphs

In general matrix models have been classified as age or stage structured matrix models (Caswell, 2001). The distinction is made in the method of classification of states in the matrix. In age classified matrices, each node in the graph represents an age in the life cycle of the organism, and in stage matrix models, each node in the graph is a particular behavioural or physiological state or mode.

Leslie matrices are the standard matrix for age-classified populations. In a Leslie matrix the population is divided in age categories and the width of the age class is the same as the projection interval (Cushing, 1998). A Leslie projection matrix has

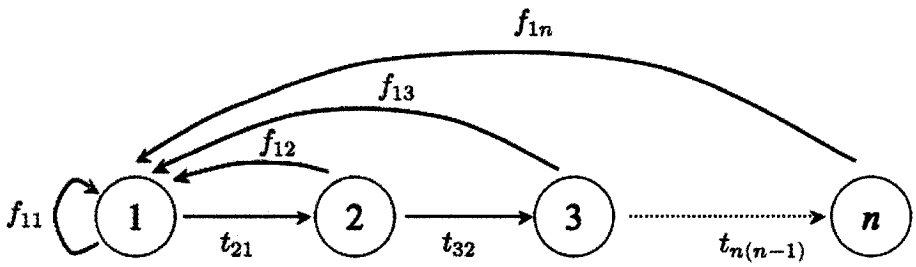

(a) Leslie matrix life cycle graph.

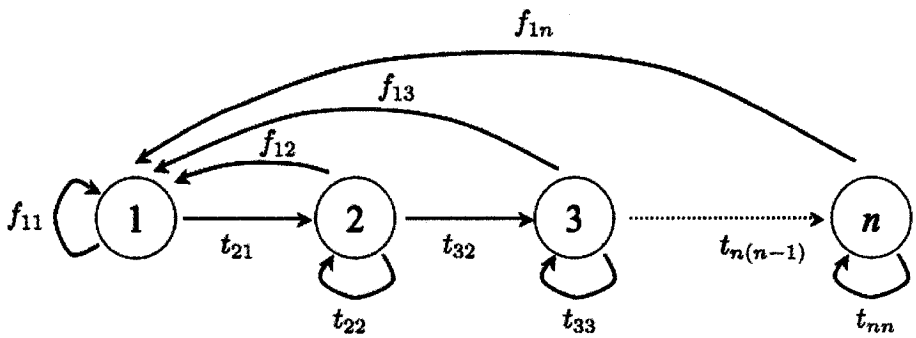

(b) Usher matrix life cycle graph.

Figure 5.2: Generalized Leslie and Usher graphs.

the following matrix structure:

$$\mathbf{A} = \begin{bmatrix} f_{11} & f_{12} & \cdots & f_{1n-1} & f_{1n} \\ t_{21} & 0 & \cdots & 0 & 0 \\ 0 & t_{32} & \cdots & 0 & 0 \\ \vdots & \vdots & \ddots & \vdots & \vdots \\ 0 & 0 & \cdots & t_{nn-1} & 0 \end{bmatrix}. \tag{5.2}$$

Here f_{ij} are fecundity transitions and t_{ij} are survival transitions. The associated life cycle graph is shown in Figure 5.2(a). Leslie matrices are widely used in ecology because of their relation to life table methods and particularly the calculation of generation time (Lebreton, 2005; Cochran and Ellner, 1992).

Another matrix known as the Usher matrix or the standard size classified matrix, is a size classified matrix similar in structure to the Leslie matrix (Cushing, 1998). The difference is that size classes can stay in the class for a period of time before

moving to the next size class. The matrix is given by,

$$\mathbf{A} = \begin{bmatrix} f_{11} & f_{12} & \cdots & f_{1n-1} & f_{1n} \\ t_{21} & t_{22} & \cdots & 0 & 0 \\ 0 & t_{32} & \cdots & 0 & 0 \\ \vdots & \vdots & \ddots & \vdots & \vdots \\ 0 & 0 & \cdots & t_{nn-1} & t_{nn} \end{bmatrix}. \tag{5.3}$$

Note that the diagonal now has t_{ii} entries that allow "stasis", the continuation in a stage for more than one time step. The associated graph is shown in Figure 5.2. Because of the stasis arising from t_{ii} terms, the stage of an individual is not related to age (Lebreton, 2005). The Usher matrix is a special form of a stage-structure matrix where stage is size.

General stage-structure models are more complicated, since stages are defined based on biological states (Caswell, 2001). Matrices for these general stage-structured models are known as Lefkovitch matrices (Silvertown et al., 1993), as they were first introduced by Lefkovitch (1965). Since classes are determined by biological or physiological stages, the matrix can have any entry nonzero, making analysis more complicated, compared to Leslie or Usher matrices (Lebreton, 2005). An example of a stage-structure matrix is shown in Figure 5.4, earlier with the scentless chamomile model and later with literature examples. Stage transitions in these matrices are usually referred to as growth, when an individual in one stage projects to a new stage; stasis, when an individual stays in the same stage; retrogression, when an individual moves to a stage that it had at a previous time step; fission, when an individual splits into two stages; and reproduction when the individual reproduces (Silvertown et al., 1993; Cochran and Ellner, 1992). Stage-structure models have been widely used for invasive plants because in most cases age is not a good indicator of plant demography and different modes of reproduction are easily incorporated as stage classes.

In Usher and Leslie matrices, all pathways (life history pathways) go through the same initial stage (e.g. eggs, newborns, seeds). Looking at Figure 5.2(a) and (b), it can be seen that all pathways that involve fecundities return to node 1 through transitions f_{1i} for $i = 1, \ldots, n$. In a stage-structured model, depending on the stage classification method, any node could potentially be an initial node, and having more than one initial node is also possible.

5.2.3 Weed life cycle graphs

Exploring life cycle structures for stage-classified invasive species can provide information on life history traits and invasibility. Life history traits that make plant species more invasive have been the subject of several studies (e.g. Brock et al., 2005; Mcintyre et al., 2005; Muth and Pigliucci, 2006). Some of the traits that have

been suggested for making a plant more invasive are short juvenile stages, small seed mass and large seed production (Rejmanek and Richardson, 1996; Grotkopp et al., 2002; Hamilton et al., 2005; Sakai et al., 2001). All these traits suggest "r-selective" species (Sakai et al., 2001; Rejmanek and Richardson, 1996), and species that can shift between r- and K- selected strategies(Sakai et al., 2001). These traits affect parameters in the life cycle graph as opposed to the actual structure of the graph. On the other hand, the length of the life cycle in weeds also seems to favour annual and biennial life cycles as opposed to perennial (Mcintyre et al., 2005; Sutherland, 2004). These traits affect the structure of the life cycle graph. Additionally, modes of reproduction (vegetative and seed reproduction), also affect the structure of the graph and may have different advantages in different stages of the invasion process (e.g. Lloret et al., 2005).

In summary, in Lefkovitch graphs, as opposed to Leslie and Usher graphs, fecundity pathways do not necessarily go through the same initial stage, and there are many possible pathways to represent different reproduction modes.

5.3 Life cycle graph analysis

Before I introduce life cycle analysis some definitions are needed. A *pathway* $a_{i_2 i_1} a_{i_3 i_2} \dots a_{i_l i_k}$ is a sequence of transitions that start in node i_1 and end in node i_l. The *length* of a pathway is measured by the number of transitions involved in the product (for example $a_{21}a_{12}$ has length 2). A *loop* is a pathway of any length that starts and ends at the same node. A *self-loop* a_{ii} is defined as a path of length 1 that starts and ends at the same node i. A *fecundity pathway* is a loop of any length where there is only one fecundity transition involved. In this chapter I define *life cycle analysis* as the analysis of the R_0 formula, obtained from a graph using the method described in Chapter 4, using pathways in the life cycle graph.

To simplify notation, a pathway $a_{i_2 i_1} a_{i_3 i_2} \dots a_{i_k i_{k-1}}$ that goes through nodes $i_1, i_2, \dots, i_{k-1}, i_k$, will be denoted $P_{i_1, i_2, \dots, i_{k-1}, i_k}$. Mortality terms $(1 - a_{ii})$ will be denoted m_i.

5.3.1 R_0 formula and the life cycle graph

As mentioned earlier, a life cycle graph $G_{\mathbf{A}}$ can be written in matrix form $\mathbf{A}$. The matrix $\mathbf{A}$ can be decomposed in a survivorship matrix $\mathbf{T}$ (transition matrix), whose elements are transition probabilities, and a fecundity matrix $\mathbf{F}$ (fecundity matrix) that contains fertility values, such that $\mathbf{A} = \mathbf{T} + \mathbf{F}$. For $\mathbf{T} = [\tau_{ij}]$ with $0 \leq \tau_{ij} \leq 1$, $\rho(\mathbf{T}) < 1$, and $\sum_j \tau_{ij} \leq 1$; and $\mathbf{F}$ has entries $f_{ij} \geq 0$, the net reproductive rate R_0

can then be calculated using (Li and Schneider, 2002),

$$R_0 = \rho((\mathbf{I} - \mathbf{T})^{-1}\mathbf{F}). \tag{5.4}$$

As an alternative, the R_0 formula can also be calculated directly from the graph, using graph reduction methods on the transformed graph $\tilde{\mathbf{A}} = \mathbf{T} + \mathbf{F}R_0^{-1}$. The basic procedure is as follows:

1. Multiply all fecundity transitions in the graph by R_0^{-1}.
2. Eliminate survivorship self-loops.
3. Reduce the graph using the graph reduction rules defined in Chapter 4, until only nodes with fecundity self-loops are left.
4. If only one node is left, then eliminate the final node and the result will be R_0.
5. If more that one node is left, then apply the formula $R_0 = \rho((\mathbf{I} - \mathbf{T})^{-1}\mathbf{F})$ on the matrix corresponding to the remaining reduced graph to calculate R_0.

The resulting formula corresponds to the R_0 equation, which can be used to analyze the life cycle graph. The analysis is performed on the derived R_0 formula obtained from the graph. To illustrate the process, first I show how R_0 is calculated for Leslie and Usher matrices, and then we analyze life cycle graphs for several literature examples. Additional examples for scentless chamomile and thistle can be found in Chapter 4.

5.3.2 R_0 formula for classes of the life cycle graph

Cushing and Zhou (1994) have derived explicit R_0 formulae for Leslie and Usher matrices (Figure 5.3(b)). An explicit equation is easy to obtain because all fecundity pathways go to a newborn age. For the Leslie matrix,

$$R_0 = \sum_{i=1}^{m} f_{1i} \prod_{j=1}^{i} t_{j(j-1)}. \tag{5.5}$$

The general reduced Usher life cycle graph is shown in Figure 5.3(c). For Usher matrices,

$$R_0 = \sum_{i=1}^{m} f_{1i} \prod_{j=1}^{i} \frac{t_{j(j-1)}}{1 - t_{jj}}. \tag{5.6}$$

The Leslie graph is obtained when $t_{jj} = 0$. It can be seen in the resulting R_0 equation, that for Leslie and Usher matrices there are a sequence of fecundity

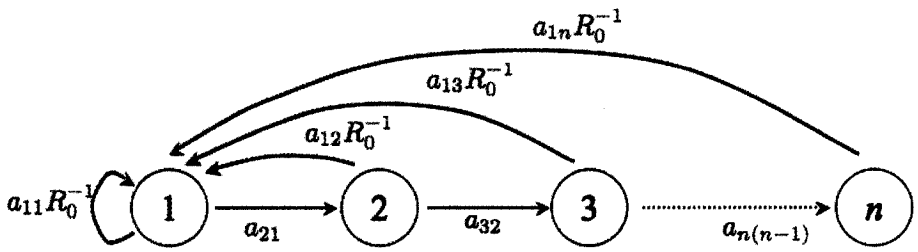

(a) Leslie matrix life cycle.

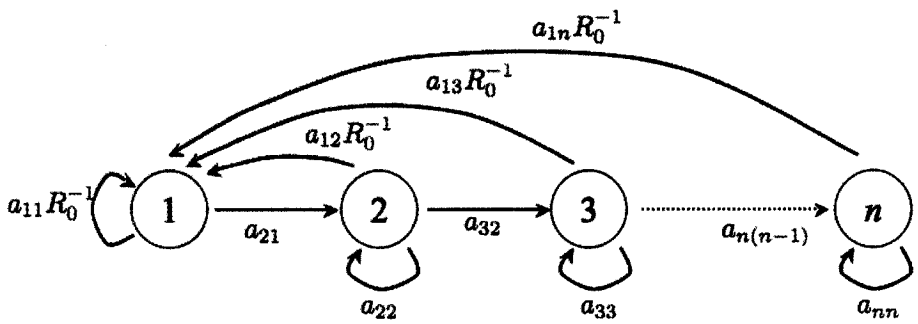

(b) Usher matrix life cycle.

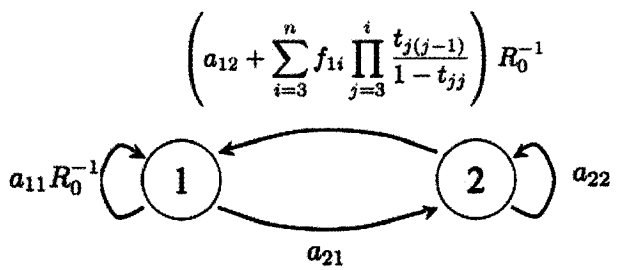

(c) Reduced usher matrix.

Figure 5.3: Generalized transformed Leslie and Usher matrices.

pathways from early reproduction (the first age of reproduction) to the last reproduction.

For general stage-classified graphs, a general formula is hard to obtain, because the life cycle depends on the method of stage classification. However, the graph reduction method R_0 allows for a quick method to calculate R_0. Using examples, I will highlight some common features found in stage-structures models that are applicable to population control, obtained by analyzing the R_0 formula.

In the examples selected, the authors used traditional analysis based on their transition parameter estimates and the estimated λ and corresponding elasticity analysis. The analysis I perform in the examples uses the analytical R_0 formula, without the need for parameter values. The analysis of life cycle graphs is a new approach proposed in this thesis, not used before in matrix population analysis.

Fecundity pathways and stasis: Tansy ragwort (*Senecio jacobaea*)

Consider the life cycle of ragwort (*Senecio jacobaea*) a biennial or short lived perennial weed under successful biocontrol in some parts of North America, due to the use of multiple control strategies (McEvoy and Coombs, 1999). McEvoy and Coombs (1999) analyze the control of ragwort looking at the effect of two biocontrol agents, flea beetle and cinnabar moth, and plant competition. The flea beetle larvae and adults feed on leaves and stems reducing survivorship. The cinnabar moth, whose larvae affects flowering plants, reduces fecundity (McEvoy et al., 1991). Here I use life cycle analysis to study ragwort control. The full life cycle graph is shown in Figure 5.4. The life cycle shows the iteroparus (more than one reproduction) life cycle. Node 1 represent dormant seeds, node 2 and 3 juvenile stages and node 4 the mature stage. The resulting R_0 formula is:

$$R_0 = \left[\frac{a_{21}a_{14}}{1-a_{11}} + a_{24}\right]\left[\frac{a_{32}a_{43}}{(1-a_{33})(1-a_{44})} + \frac{a_{42}}{(1-a_{44})}\right]. \tag{5.7}$$

McEvoy and Coombs (1999) consider a_{24} as the only fecundity transition. However, upon inspection of the graph, the dormant stage (node 1) are seeds produced by an adult plant, hence, transition a_{14} is also here considered a fecundity transition. Although this has no implications for the calculation of λ, it yields different R_0. The rest of the transitions are all survivorship. Using the simplified notation and after some algebra R_0 becomes:

$$R_0 = \frac{P_{1,2,3,4}}{m_1m_3m_4} + \frac{P_{2,3,4}}{m_3m_4} + \frac{P_{1,2,4}}{m_1m_4} + \frac{P_{2,4}}{m_4}. \tag{5.8}$$

The biennial pathway is represented by path $P_{2,4}$, perennial $P_{2,3,4}$, iteroparity P_1 and dormancy $P_{1,2,4}$. Note that all of the pathways are fecundity pathways, pathways

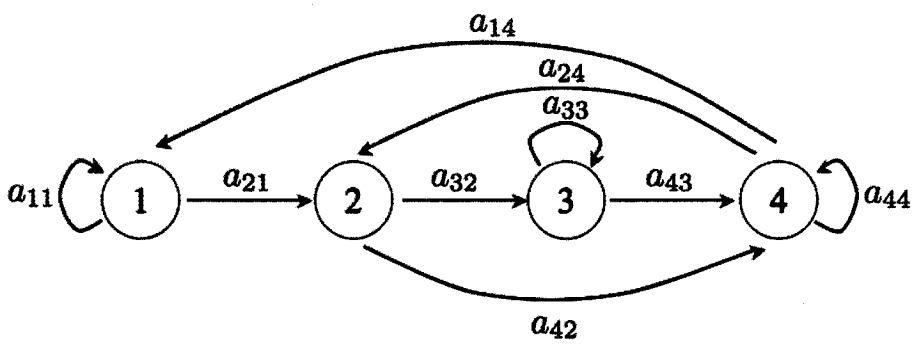

(a) Ragwort life cycle

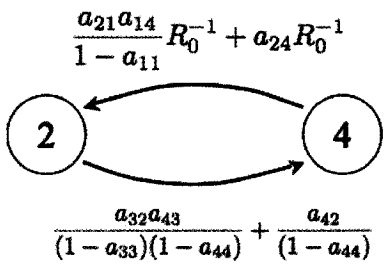

(b) Reduced life cycle

Figure 5.4: Ragwort (*Senecio jacobaea*) life cycle as described in McEvoy and Coombs (1999). Node 1=dormant seeds, node 2=juvenile 1, node 3=juvenile 2, node 4=adult plants.

that involve one fecundity transition. In McEvoy and Coombs (1999) only the case where there is no dormancy ($a_{21} = 0$) and no iteroparity ($a_{44} = 0$) is considered, i.e. reducing disturbance to remove dormant seeds from germination and facilitate adult survivorship, so equation (5.8) simplifies to:

$$R_0 = \frac{P_{2,3,4}}{m_3} + P_{2,4}. \tag{5.9}$$

Since $R_0 < 1$ implies that population will decrease, an effective control strategy is to involve all pathways in the control of this weed. All three control strategies (flea beetle, cinnabar moth and plant competition) affect both terms of equation 5.9. The cinnabar moth only affects a_{24}. The flea beetle affects all transitions including m_3. Note that when m_3 approaches 1, the impact of the first term on R_0 becomes large. Plant competition affect survivorship of first year juveniles (a_{32}, a_{42}). Although some consideration of interaction between strategies is needed when involving multiple control methods, from the R_0 formula it seems reasonable to control both pathways. Additionally, control to reduce m_3 could have a large impact on reducing R_0. Large values of m_3 (high survival of second year juvenile) could trigger a re-invasion in following years. McEvoy and Coombs (1999) suggest selecting the flea beetle over the cinnabar moth, since it affects more pathways, and promote plant competition to disrupt the transitions from node 2 to 3 and 4.

McEvoy and Coombs (1999) focus on elasticity analysis (loop analysis) to investigate the effectiveness of control of ragwort. I have shown how analysis of R_0 can yield similar conclusions. In this example several reproduction modes (semelparity and iteroparity) are included in the life cycle graph. The pathways are clear in the R_0 formula. The success of control is because of the focus on multiple pathways. These pathways can be identified in the R_0 formula as well.

Time of reproduction: Bullfrog (*Rana catesbeiana*)

Bullfrogs (*Rana catesbeiana*) are raised in farms for the use of their legs in gourmet markets (Govindarajulu et al., 2005). Because of escapes, these frogs have invaded many regions in different parts of the world, affecting native fauna (Govindarajulu et al., 2005). Aquatic bullfrogs feed on invertebrates and other amphibians and vertebrates, and have been suspected of being the main cause of other amphibian population decline (Kiesecker and Blaustein, 1997; Kiesecker et al., 2001).

In Govindarajulu et al. (2005) a matrix model for the bullfrog is developed to study population growth and the effect of early metamorphosis in population growth. In general, amphibian population growth rate is more sensitive to post-metamorphic survival than tadpole survival (Govindarajulu et al., 2005). The life cycle graph is shown in Figure 5.5. Node 1 represents eggs, node 2 and 3 first and second year

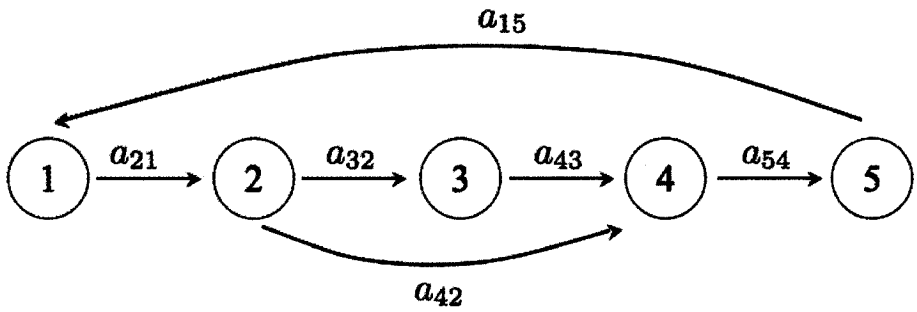

(a) Bullfrog life cycle.

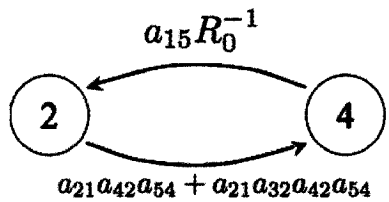

(b) Reduced life cycle.

Figure 5.5: Life cycle of the bullfrog (*Rana catesbeiana*). Node 1=eggs, node 2 and 3=first and second year tadpoles, node 4=metamorphic juveniles and node 5=adults.

tadpoles, node 4 metamorphic juveniles and node 5 adults. There are two possible pathways, a "fast track" where first year tadpoles change into juveniles without going into a second year tadpole stage, and a "slow track" that takes an extra time interval going into the second year tadpoles before metamorphosis occurs. After graph reduction and using pathway notation, the R_0 equation,

$$R_0 = P_{1,2,4,5} + P_{1,2,3,4,5}. \tag{5.10}$$

The "fast track" pathway, is given by $P_{1,2,4,5}$ and the "slow track" by $P_{1,2,3,4,5}$. A full reproductive cycle can be completed in only 4 years (the length of pathway $P_{1,2,4,5}$). Using λ estimates and elasticity analysis, the authors found that early metamorphic tadpoles (node 2) had the highest elasticities and therefore would be a good target for biological control. From the R_0 equation, it can be seen that since node 3 can be "skipped", the control of early tadpoles or juvenile-adults would be better. Because of other factors affecting survival of juveniles and adults, the conclusion that metamorphic juveniles could be the best target for control is clear from the R_0 equation, without necessarily obtaining parameter estimates.

The bullfrog example, shows how time of reproduction is included in the life cycle graph, and the effects on the R_0 equation. The "fast track" and "slow track" are evident in the R_0 equation. Possible control strategies can be studied using the R_0 formula.

Common survival transitions: Common teasel (*Dipsacus sylvestris*)

Teasel is a herbaceous perennial plant introduced from Europe and restricted to disturbed habitats (Werner and Caswell, 1977). Teasel is not a serious problem in agriculture; however it usually invades disturbed areas where it can be a nuisance (Werner, 1975). The matrix model for teasel was derived by Werner and Caswell (1977) and Caswell and Werner (1978), and later modified by Caswell (2001). The full model is shown in Figure 5.6A. Caswell (2001) shows using elasticity analysis on data from Werner and Caswell (1977), that flowering plants-medium rosettes-large rosettes-flowering plants ($a_{46}a_{54}a_{65}$ in the graph), contribute 73% to λ and the pathway flowering plant-seeds-large rosettes ($a_{16}a_{51}$) adds another 13% to population growth.

The reduced graph with only two nodes is shown in Figure 5.6B and the R_0 obtained by eliminating all nodes is shown in Figure 5.6C. Using the same notation introduced for the previous example of nodding thistle, R_0 can be rewritten,

$$R_0 = P_{4,6} + \frac{P_{5,6}}{m_3} + \frac{P_{4,5,6} + P_{3,4,5,6}}{m_4 m_5} + \frac{P_{1,2,3,4,5,6} + P_{1,3,4,5,6}}{m_3 m_4 m_5}. \tag{5.11}$$

From this, it can be seen that nodes 4, 5 and 6 are involved in all the reproductive paths. This suggests that, in addition to targeting fecundity transitions, effective control could be used in those transitions affecting paths from 5 to 6 and 4 to 6. In this life cycle, stasis (self loops at a given node) becomes critical (as evident in all the $1/(1-a_{ii})$ terms). If any of these survivorship transitions are high (approach 1), then R_0 grows quickly, making this system harder to control. From this example it can be seen that studying R_0 is consistent with numerical analysis of λ, but it allows for a more general analytical investigation of the possibilities of control. In Caswell (2001, example 4.1), it is shown that a flawed life cycle graph for teasel derived in Werner and Caswell (1977), a graph that has an extra dormant seed stage (extra node in the graph), yields the same numerical value for R_0 compared to the corrected one (presented in Caswell, 2001), but very different values for λ. However, although R_0 is the same, generation time is longer in the flawed graph, hence an individual would replace itself faster in the corrected graph, resulting also in a higher λ (as shown also in Caswell (2001)).

Finding the best strategy or transition to control in this example, involves finding a common transition that is shared in all pathways in R_0.

Vegetative reproduction: Cat's ear (*Hypochaeris radicata*)

When vegetative reproduction is present, life cycle graph analysis becomes more challenging. The graph cannot be reduced completely because there are more than one self-loop containing the term R_0^{-1}. However, inspection of the reduced graph

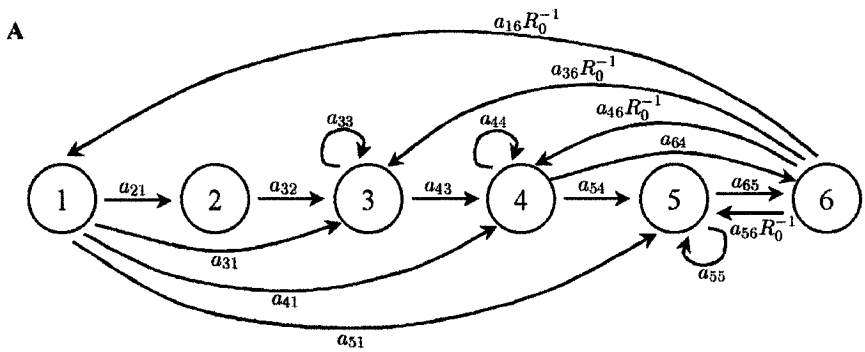

B

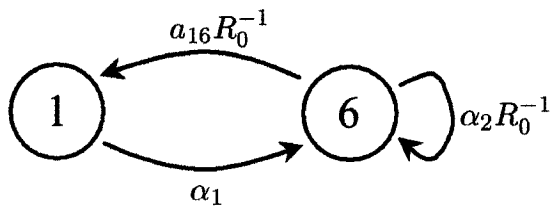

$$\alpha_1 = \frac{(a_{21}a_{32}+a_{31})a_{43}a_{54}a_{65}}{(1-a_{33})(1-a_{44})(1-a_{55})}$$

$$\alpha_2 = a_{64}a_{46} + \frac{a_{65}a_{56}}{(1-a_{55})} + \frac{a_{65}a_{46}a_{54}}{(1-a_{44})(1-a_{55})} + \frac{a_{36}a_{43}a_{54}a_{65}}{(1-a_{44})(1-a_{55})}$$

C

$$R_0 = a_{16}\alpha_1 + \alpha_2$$

Figure 5.6: Common teasel life cycle graph as described by Caswell (2001). Node 1 and 2 represent dormant seeds; 3, 4, 5 rosettes and node 6 large flowering rosettes. A) Full graph, B) Reduced graph, C) R_0.

without explicitly calculating R_0 reveals some vital information. As an example, consider the life cycle of *Hypochaeris radicata*, a short-lived perennial herb that grows on grasslands and wetlands in Europe (Pico et al., 2004; De Kroon et al., 1987). As described in De Kroon et al. (2000) in Figure 5.7(a), the life cycle of this herb contains juvenile plants (node 1) that grow and produce mature plants (node 3). Mature plants can then reproduce vegetatively, producing a side ramification (rosette node 2), or sexually to produce more juvenile plants. In matrix notation,

$$\mathbf{T} = \begin{bmatrix} 0 & 0 & 0 \\ 0 & 0 & 0 \\ a_{31} & a_{32} & a_{33} \end{bmatrix}, \mathbf{F} = \begin{bmatrix} 0 & a_{12} & a_{13} \\ 0 & a_{22} & a_{23} \\ 0 & 0 & 0 \end{bmatrix}. \tag{5.12}$$

Using the graph reduction method on the transformed graph, the reduced graph shows the four possible reproductive pathways (Figure 5.7(b)). As shown in Figure 5.7(c), nodes 1 and 2 contain reproductive self loops. Suppose that, under control, we can eliminate all mature plants. It can be seen from the remaining node 2, that this herb would persist since node 2 has a vegetative reproductive loop.

If one individual is introduced in node 1 (juvenile), then both fecundity pathways are of length 2, meaning that it would take two time intervals for reproduction to occur. On the other hand, if an individual is introduced in node 2, reproduction can occur immediately in one time interval (vegetative reproduction), or in two (also vegetative but maturing).

To calculate R_0, we remove R_0^{-1} from the graph (Figure 5.7(b)), and calculate R_0 using the associated decomposed matrix of the remaining graph:

$$\mathbf{T}' = \begin{bmatrix} 0 & 0 \\ 0 & 0 \end{bmatrix}, \mathbf{F}' = \begin{bmatrix} \frac{a_{31}a_{13}}{1-a_{33}} & a_{12} + \frac{a_{32}a_{13}}{1-a_{33}} \\ a_{31}a_{23} & a_{22} + \frac{a_{23}a_{32}}{1-a_{33}} \end{bmatrix}. \tag{5.13}$$

Consequently, using equation (5.4), the net reproductive rate is calculated as $R_0 = \rho(\mathbf{F}'(\mathbf{I}-\mathbf{0})^{-1} = \rho(\mathbf{F}')$. It can be seen from the reduced graph that different modes of reproduction have also an effect on R_0. For this herb, spatial and temporal variation have consequences on parameter values and therefore consequences on population growth (Jongejans and De Kroon, 2005). Hence, parameter estimates are valid only for the region where data were collected. By looking at the R_0 equation, it is possible to derive general conclusions that do not depend on parameter estimates.

Modes of reproduction make the life cycle graph more complex. However, the reduced life cycle graph seems to provide useful information even when the R_0 equation is not solved explicitly. Distinct reproductive modes appear as disjoint loops in the graph.

5.3.3 Properties of the R_0 equation

After reviewing the examples, some general properties of the R_0 formula are evident:

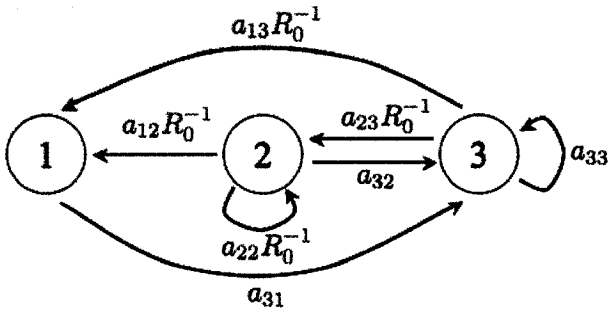

(a) Full transformed life cycle graph.

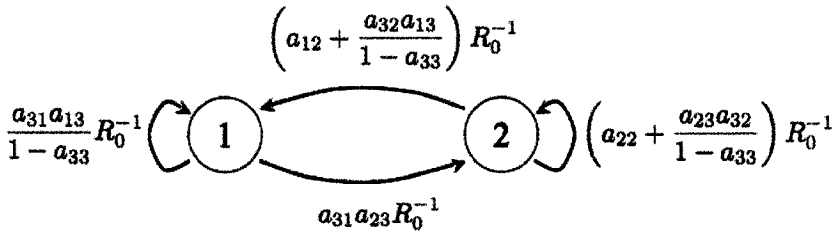

(b) Reduced life cycle

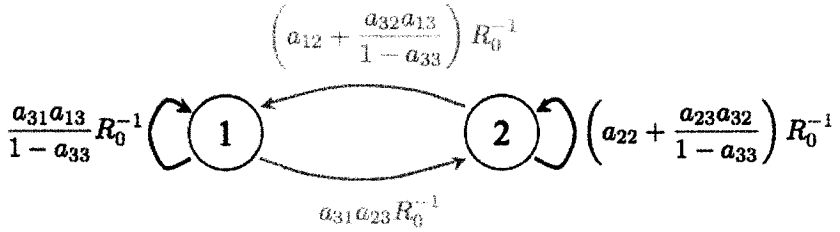

(c) Two disjoint loops are highlighted.

Figure 5.7: Life cycle of *Hypochaeris radicata* as described in (De Kroon et al., 2000). Node 1=juvenile, node 2=side rosette, node 3= mature plant. (a) Full life cycle, (b) Reduced life cycle, (c) Disjoint reproductive pathways are highlighted.

1. The R_0 formula comes from a polynomial of R_0^{-1}, therefore all terms in the formula represent fecundity pathways.

2. If the population has a stable stage distribution, the path length is the time it takes for reproduction to occur in that pathway. This will be explored in the next section.

3. The number of modes of reproduction is equal to the number of disjoint fecundity pathways and hence the order of the polynomial of R_0.

4. Survivorship self loops m_i can have a large impact on fecundity pathways. As they get large, the contribution of the pathways grows large.

5. Some possible control strategies: a) find a control mechanism that controls all pathways, b) target transitions that occur in the most number of pathways, c) target the pathways that potentially can contribute the most to R_0.

5.4 Generation time and time of first reproduction

Since the net reproductive rate defines growth per generation, generation time is also an essential quantity that should be calculated along with R_0. Generation time is the time that it takes the population to increase by a factor of R_0. There are several ways of calculating generation time (Caswell, 2001). The simplest calculation is given by:

$$\tilde{T} = \frac{\log R_0}{\log \lambda}. \tag{5.14}$$

One of the advantages of looking at the explicit graph of a species is that, as seen in the teasel example in Caswell (2001, example 4.1), a different structure in the life cycle graph may have the same R_0 but different generation time and λ.

One of the advantages of looking at the explicit R_0 is that it provides us with information about time of first reproduction just by inspecting the pathways. Consider again the teasel example presented here. If we start with a stable stage distribution, the time of first reproduction is 2 time intervals, since the shortest fecundity pathways are $P_{4,6}$ and $\frac{1}{m_3}P_{5,6}$, I will call this the time of first reproduction. Similarly, the time of the last reproduction is the longest fecundity pathway, in the teasel example $\frac{1}{m_3 m_4 m_5}P_{1,2,3,4,5,6}$. These reproduction times can have implications for control, since short pathways may have large contributions to R_0, hence might be a good target for control.

In stage-structured models, the calculation of generation time is difficult, since stage is not related to age and individuals can stay in a stage for a long period of time (Cochran and Ellner, 1992; Lebreton, 2005). To explore generation time

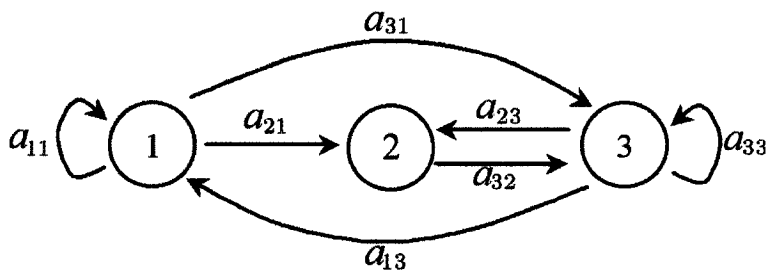

Figure 5.8: Scentless chamomile life cycle.

in a stage-structure model using R_0, the time that it takes to go through each pathway has to be included in the R_0 formula. Associate the weight τ^n with a path $P_{i_1,i_2,\ldots,i_n}$, that take n steps to complete. For a self loop, in a pathway $m_i^{-1} = (1 - a_{ii}\tau)^{-1} = 1 + a_{ii}\tau + a_{ii}^2\tau^2 + \ldots$, where the expansion indicates that a self loop can be visited $1, 2, \ldots, \infty$ times in a pathway. Summing all the fecundity loops that have weight n into a coefficient R_n, and then summing across all possible values of n yields,

$$R(\tau) = \sum_{n=1}^{\infty} R_n \tau^n, \tag{5.15}$$

which will be called the R_0-*generating function.* This generating function originates when taking the *z-transform* of the life cycle graph (see Caswell, 2001), with $\tau = z^{-1}$.

Lets consider the scentless chamomile life cycle graph shown in Figure 6.2 as an example. Nodes 1, 2 and 3 correspond to seed bank, rosettes and flowering plants respectively as described in Chapter 3. The R_0 equation is given by,

$$R_0 = a_{33} + a_{32}a_{23} + \frac{a_{31}a_{13} + a_{13}a_{21}a_{32}}{1 - a_{11}}. \tag{5.16}$$

The R_0-generating function,

$$R(\tau) = a_{33}\tau + a_{32}a_{23}\tau^2 + \frac{(a_{31}a_{13}\tau^2 + a_{13}a_{21}a_{32}\tau^3)}{1 - a_{11}\tau}. \tag{5.17}$$

Suppose we start with one reproductive individual. The number of direct

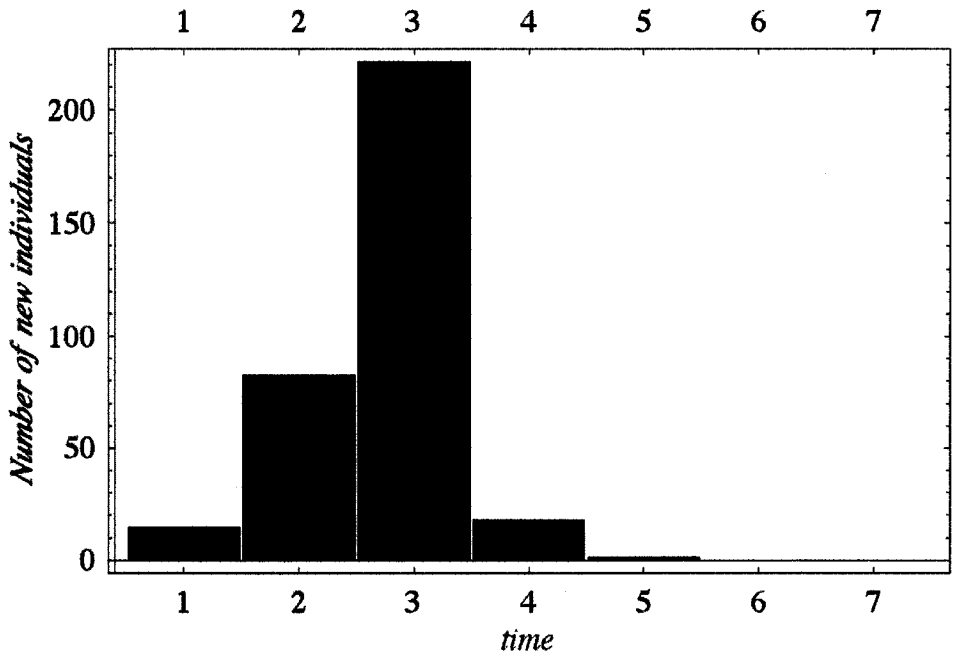

Figure 5.9: Plot of the number of new scentless chamomile flowering plants descendants of the original flowering plant after 7 years.

descendants in $1, 2, \ldots, n$ time steps will be:

$$R_1 = \frac{dR}{d\tau}(0) \tag{5.18}$$

$$R_2 = \frac{1}{2}\frac{d^2R}{d\tau^2}(0) \tag{5.19}$$

$$\vdots$$

$$R_n = \frac{1}{n!}\frac{d^nR}{d\tau^n}(0). \tag{5.20}$$

The total number of new individuals produced that are direct descendants of the original individual is:

$$R_0 = \sum_{n=1}^{\infty} R_n. \tag{5.21}$$

Using a Taylor series representation for $R(\tau)$ about 0, we observe,

$$R(\tau) = R(0) + \tau \frac{dR}{d\tau}(0) + \frac{\tau^2}{2}\frac{d^2R}{d\tau^2}(0) + \ldots \tag{5.22}$$

$$= \sum_{n=1}^{\infty} \tau^n R_n. \tag{5.23}$$

Hence $R(1) = \sum_{n=1}^{\infty} R_n = R_0$ which is the same as the R_0-generating function evaluated at 1 (5.15). Given a randomly selected direct descendant of the original reproducing individual, the year in which the descendant was produced is a random variable T with probability mass function:

$$Pr\{T = n\} = \frac{R_n}{R_0} = Q_n. \tag{5.24}$$

The mean value for T is:

$$\bar{T} = \sum_{n=1}^{\infty} nQ_n = \frac{1}{R_0}\sum_{n=1}^{\infty} nR_n = \frac{1}{R_0}\sum_{n=1}^{\infty} \frac{1}{(n-1)!}\frac{d^nR}{d\tau^n}(0) \tag{5.25}$$

$$= \frac{1}{R_0}\sum_{n=0}^{\infty} \frac{1}{n!}\frac{d^n}{d\tau^n}\left(\frac{dR}{d\tau}\right). \tag{5.26}$$

The Taylor series of $\frac{dR}{d\tau}$ about $\tau = 0$, evaluated at $\tau = 1$ yields,

$$\bar{T} = \frac{1}{R_0}\frac{dR}{d\tau}(1). \tag{5.27}$$

With equation (5.27) it is possible to calculate the generation time of a stage-structure model based on the R_0 generating function (5.15). Now, we can also estimate the variance $\mathbf{Var}[\bar{T}]$ of the estimate $\bar{T}$. Consider the generating function for the random variable T (5.24),

$$g(\tau) = \sum_{n=1}^{\infty} \tau^n Q_n. \tag{5.28}$$

The first moment and variance, correspond to (Kot, 2001),

$$\mathbf{E}[T] = g'(1),\ \mathbf{Var}[T] = g''(1) + g'(1) - g'^2(1). \tag{5.29}$$

The estimated generation time (5.27) is an alternative to (5.14). The relation with (5.14) is as follows. Consider the *renewal equation*,

$$N_t = \sum_{i=1}^{\infty} R_i N_{t-i}, \tag{5.30}$$

with N_0 given and $N_i = 0, i < 0$. Consider a solution of the form $N_t = c\lambda^t$, and substituting in (5.30), yields the Euler-Lotka equation

$$1 = \sum_{i=1}^{\infty} R_i \lambda^{-i}. \tag{5.31}$$

Hence, the characteristic polynomial is given by $R(\lambda^{-1}) = 1$. Consider now the entire population reproducing at time $\tilde{T}$. Then,

$$R_i = \begin{cases} 0, i \neq \tilde{T} \\ 1, i = \tilde{T} \end{cases}. \tag{5.32}$$

The Euler-Lotka equation gives $1 = R_0 \lambda^{-\tilde{T}}$, therefore (5.14).

Using parameter estimates from Chapter 3, the total number of new flowering plants produced that are direct descendants of the original flowering plant, using equation (5.18), are shown in Figure 5.9. The average generation time applying (5.27) is $\bar{T} = 2.7318$ with variance $\mathbf{Var}[T] = 0.41711$. For scentless chamomile $\lambda = 19.37$ and $R_0 = 337.52$, using equation (5.14) to calculate generation time yields $\tilde{T} = 1.9643$.

5.5 Discussion

The goal of control of invasive species is to reduce population growth. In matrix models, calculation of λ to determine if the population is increasing, and how matrix entries affect λ to target the most sensitive transitions, is the basis of demographic analysis for control (McEvoy and Coombs, 1999). Here, because we can calculate an explicit formula for R_0, I propose to shift the focus and incorporate analysis of R_0 as a common practice for the design of control strategies. The analysis presented shows the applicability of the explicit R_0 formula for analyzing life cycle graphs and assisting in the design of control strategies. However, key to successful analysis of R_0 is the correct construction of the life cycle graph. In principle it is assumed that any stage class truly represents a particular survivorship and/or fecundity that is unique to that class, and that the time intervals are correct with respect to the life history of the organism.

As shown by Shea et al. (2005) with thistle, there are changes in the life history of organisms that make control strategies context-dependent, and classic demographic analysis (calculation of λ and the elasticity matrix) may yield different results for the same species in different regions, suggesting the need of more general control strategies. Although elasticity analysis is a very useful tool, the dependence on parameter estimates of transition entries make some of the predictions particular

to a region of space and time. Even when elasticities of λ to transitions are found numerically for control in a specific region, there might not be anything that can be done to control that transition, hence elasticity analysis may have no real consequences for management (Boyce et al., 2005). Life cycle analysis based on R_0 is not affected by specific parameter estimates and allows for the design of a more general control strategy. The main focus of R_0 is to find pathways that could be affected by specific control strategies. Key transitions to target could be transitions that are present in most pathways, so to have a larger effect on R_0

It is necessary to note that R_0 is the rate of increase per generation, as opposed to λ that is population increase in one time interval. The search for strategies that would reduce R_0 only a small portion may not be effective measures as they might not have any large effect on λ (Caswell, 2001). However, if strategies designed on R_0 can guarantee that R_0 will be substantially reduced, and will become less than one, then indeed, the control measure would be effective. As seen here, analysis of R_0 is useful in designing combined strategies that focus on pathways rather than individual transitions. There is already a general sense that combined strategies need to be used in order to have an effective biocontrol (Lym, 2005; McEvoy and Coombs, 1999). Also note that control agents are not explicitly included in this analysis, since the focus is on weaknesses of the organism to be controlled.

In this chapter I also derived a formula for the calculation of mean generation time $\bar{T}$ and its variance, an essential quantity in demographic analysis. The general definition of R_0-generating function (5.15) can be extended to the case with disjoint fecundity loops, by defining $R(\tau)$ to be the z-transform of the life cycle graph, with the substitution $\tau = z^{-1}$. This is subject to future research and analysis. The fact that variance of generation time can be estimated, might be useful to study the time at which the reproduction contribution to R_0 occurs in variable environments (Ellner, 1985). This is subject of future investigation.

Mean generation time and R_0 summarize complex life history schedules and determine intrinsic population growth rate. If indeed highly invasive species are "r-selected" (Rejmanek and Richardson, 1996; Davis, 2005), it is expected that these species have short generation times $\bar{T}$ with large R_0. Along with R_0, generation time calculation allows for the comparison of different species life histories, different modes of reproduction, and their effect in population dynamics and the control of invading organisms.

In summary analysis of life cycle graphs using R_0 proves useful because: i) its possible to obtain an analytic expression based on the life cycle, ii) generation time can be estimated, iii) the first and last reproduction times can be calculated, iv) analysis can be done directly on the graph, even when no explicit formula for R_0 is calculated (as shown in the vegetative reproduction example).

Bibliography

Benton, T. and A. Grant. 1999. Elasticity analysis as an important tool in evolutionary and population ecology. Trends in Ecology & Evolution **14**:467–471.

Boyce, M., L. Irwin, and R. Barker. 2005. Demographic meta-analysis: synthesizing vital rates for spotted owls. Journal of Applied Ecology **42**:38–49.

Brock, M., C. Weinig, and C. Galen. 2005. A comparison of phenotypic plasticity in the native dandelion *Taraxacum ceratophorum* and its invasive congener *t. officinale*. New Phytologist **166**:173–183.

Caswell, H. 2001. Matrix Population Models: Construction, Analysis, and Interpretation. 2nd edition. Sinauer Associates.

Caswell, H. and P. Werner. 1978. Transient-behavior and life-history analysis of teasel (*Dipsacus sylvestris* Huds). Ecology **59**:53–66.

Cochran, M. and S. Ellner. 1992. Simple methods for calculating age-based life-history parameters for stage-structured populations. Ecological Monographs **62**:345–364.

Cushing, J. 1998. An introduction to structured population dynamics. Society Industrial and Applied Mathematics.

Cushing, J. and Y. Zhou. 1994. The net reproductive value and stability in matrix population models. Natural Resource Modeling **8**:297–333.

Davis, H. 2005. r-selected traits in an invasive population. Evolutionary Ecology **19**:255–274.

De Kroon, H., A. Plaisier, and J. Vangroenendael. 1987. Density dependent simulation of the population-dynamics of a perennial grassland species, *Hypochaeris radicata*. Oikos **50**:3–12.

De Kroon, H., J. Van Groenendael, and J. Ehrlen. 2000. Elasticities: a review of methods and model limitations. Ecology **81**:607–618.

Ellner, S. 1985. Ess germination strategies in randomly varying environments .1. logistic-type models. Theoretical Population Biology **28**:50–79.

Govindarajulu, P., R. Altwegg, and B. Anholt. 2005. Matrix model investigation of invasive species control: Bullfrogs on Vancouver Island. Ecological Applications **15**:2161–2170.

Grotkopp, E., M. Rejmanek, and T. Rost. 2002. Toward a causal explanation of plant invasiveness: Seedling growth and life-history strategies of 29 pine (*Pinus*) species. American Naturalist **159**:396–419.

Hamilton, M., B. Murray, M. Cadotte, G. Hose, A. Baker, C. Harris, and D. Licari. 2005. Life-history correlates of plant invasiveness at regional and continental scales. Ecology Letters **8**:1066–1074.

Houllier, F. and J. Lebreton. 1986. A renewal-equation approach to the dynamics of stage-grouped populations. Mathematical Biosciences **79**:185–197.

Jongejans, E. and H. De Kroon. 2005. Space versus time variation in the population dynamics of three co-occurring perennial herbs. Journal of Ecology **93**:681–692.

Kiesecker, J. and A. Blaustein. 1997. Population differences in responses of red-legged frogs (*Rana aurora*) to introduced bullfrogs. Ecology **78**:1752–1760.

Kiesecker, J., A. Blaustein, and C. Miller. 2001. Potential mechanisms underlying the displacement of native red-legged frogs by introduced bullfrogs. Ecology **82**:1964–1970.

Kot, M. 2001. Elements of Mathematical Ecology. Cambridge University Press.

Lebreton, J. 2005. Age, stages, and the role of generation time in matrix models. Ecological Modelling **188**:22–29.

Lefkovitch, L. 1965. Study of population growth in organisms grouped by stages. Biometrics **21**:1–18.

Li, C. and H. Schneider. 2002. Applications of Perron-Frobenius theory to population dynamics. Journal of Mathematical Biology **44**:450–462.

Lloret, F., F. Medail, G. Brundu, I. Camarda, E. Moragues, J. Rita, P. Lambdon, and P. Hulme. 2005. Species attributes and invasion success by alien plants on Mediterranean Islands. Journal of Ecology **93**:512–520.

Lym, R. 2005. Integration of biological control agents with other weed management technologies: Successes from the leafy spurge (*Euphorbia esula*) IPM program. Biological Control **35**:366–375.

McEvoy, P. and E. Coombs. 1999. Biological control of plant invaders: Regional patterns, field experiments, and structured population models. Ecological Applications **9**:387–401.

McEvoy, P., C. Cox, and E. Coombs. 1991. Successful biological-control of ragwort, *Senecio jacobaea*, by introduced insects in Oregon. Ecological Applications **1**:430–442.

Mcintyre, S., T. Martin, K. Heard, and J. Kinloch. 2005. Plant traits predict impact of invading species: an analysis of herbaceous vegetation in the subtropics. Australian Journal of Botany **53**:757–770.

Muth, N. and M. Pigliucci. 2006. Traits of invasives reconsidered: Phenotypic comparisons of introduced invasive and introduced noninvasive plant species within two closely related clades. American Journal of Botany **93**:188–196.

Myers, J. and D. Bazely. 2003. Ecology and Control of Introduced Plants. Cambridge University Press.

Pico, F., N. Ouborg, and J. Van Groenendael. 2004. Influence of selfing and maternal effects on life-cycle traits and dispersal ability in the herb *Hypochaeris radicata* (Asteraceae). Botanical Journal of The Linnean Society **146**:163–170.

Rejmanek, M. and D. Richardson. 1996. What attributes make some plant species more invasive? Ecology **77**:1655–1661.

Sakai, A., F. Allendorf, J. Holt, D. Lodge, J. Molofsky, K. With, S. Baughman, R. Cabin, J. Cohen, N. Ellstrand, D. McCauley, P. O'Neil, I. Parker, J. Thompson, and S. Weller. 2001. The population biology of invasive species. Annual Review of Ecology and Systematics **32**:305–332.

Shea, K., D. Kelly, A. Sheppard, and T. Woodburn. 2005. Context dependent biological control of an invading thistle. Ecology **In press**.

Silvertown, J., M. Franco, I. Pisanty, and A. Mendoza. 1993. Comparative plant demography - relative importance of life-cycle components to the finite rate of increase in woody and herbaceous perennials. Journal of Ecology **81**:465–476.

Sutherland, S. 2004. What makes a weed a weed: life history traits of native and exotic plants in the USA. Oecologia **141**:24–39.

Wardle, G. 1998. A graph theory approach to demographic loop analysis. Ecology **79**:2539–2549.

Werner, P. 1975. Biology of canadian weeds .12. *Dipsacus sylvestris* Huds. Canadian Journal of Plant Science **55**:783–794.

Werner, P. and H. Caswell. 1977. Population-growth rates and age versus stage-distribution models for teasel (*Dipsacus sylvestris* Huds). Ecology **58**:1103–1111.

Chapter 6

Invasion with coupled map lattices: application to scentless chamomile

6.1 Introduction

When a non-native species is introduced and is established, the population starts growing, spreading and colonizing new regions (Ehler, 1998). Some of these exotic species are introduced on purpose, such as toads (*Bufo marinus*) to control sugarcane beetles, and later became pests (Knight, 2001). Some, like Canada thistle (*Crisium arvense*), a noxious weed introduced from Europe that has spread in Canada and the United States (McClay et al., 2002), are introduced by accident. Many are introduced as part of biological control efforts by weed and pest scientists to control other invasive species by means of their natural enemies, like the introduction of a gall midge (*Spurgia esulae*) to control leafy spurge (*Euphorbia esula* L.) (Lym, 2005).

Two fundamental aspects of invasion dynamics are population growth and population spread. The two related quantities (intrinsic growth rate and rate of spread) are essential to invasion theory. They have been the subject of study in mathematical models for invasions (Hastings et al., 2005), and the quantities are key control parameters in conservation management and biological control (Fagan et al., 2002; Shea, 2004; Neubert and Parker, 2004; Allen et al., 1996). Because of the long time and broad spatial scales at which invasions occur, the use of models is essential to understand the dynamics of invasions and design possible management and conservation strategies. The mathematical theory of invasions has much to offer in this respect (Fagan et al., 2002). One purpose of calculating the rate of spread is to use this to find ways to slow down the spread of invading organisms by biocontrol or other means (Fagan et al., 2002), and the prediction of invasion speed is essential in control and management of invading organisms and ecosystem management (Sharov and Liebhold, 1998; Sharov, 2004). In addition, models help to focus information

on vital variables while enhancing collaborations between theorists and empirical researchers (Shea, 2004)

There are several modelling strategies for population growth and spatial spread: partial differential equations, integro-difference equations, coupled map lattices, and cellular automata. Partial differential equations incorporate continuous space and time, integro-difference equations, discrete time and continuous space, and coupled map lattice, discrete time and space. For cellular automata, in addition to time and space being discrete, the state space is also discrete. Which modelling strategy is the best depends upon the dynamical characteristics of the system under analysis, and upon spatio-temporal scales. In the last two decades there has been an increase in the use of discrete models due to their ability to incorporate stochastic components and local inhomogeneities (Durrett and Levin, 1994), and because personal computers now allow for fast numerical computations.

Integro-difference equation (IDE) models are discrete-time and continuous-space models, that incorporate dispersal data directly using a kernel function (Kot et al., 1996). This dispersal kernel allows for the redistribution of individuals in continuous space. Mathematically an IDE is defined as

$$n_{t+1}(x) = \int_{-\infty}^{\infty} \underbrace{k(x,y)}_{\text{dispersal from } y \text{ to } x} \underbrace{f[n_t(y)]}_{\text{growth at } y} dy. \tag{6.1}$$

Here $n_t(x)$ is population density at time t location x and $f[n_t(y)]$ describes population growth. The dispersal kernel $k(x,y)$ is a probability density function describing the likelihood of dispersal to point x. These models have been widely used to study spatial dynamics and control of invasive species (e.g. Allen et al., 1996; Buckley et al., 2005; Kot et al., 1996)

Coupled map lattices (CMLs) are models where space and time are discrete, and whose structure is similar to IDEs. Some CMLs have been used to study host-parasitoid interactions (Hassell et al., 1991; Kean and Barlow, 2001; Bjornstad and Bascompte, 2001; Bonsall and Hassell, 2000), metapopulation level applications (Janosi and Scheuring, 1997) and applied biological control (Rees and Paynter, 1997; Rees and Hill, 2001). A coupled map lattice is a dynamical system where time and space are discrete, and the state variable is continuous (White and White, 2005; Kaneko, 1992).

As with integro-difference equations, a CML describes the growth and dispersal of the population, but now on a discrete lattice. Strictly, a CML only involves local interactions, meaning dispersal occurs in a local neighbourhood Ω. However, there is no restriction on how large Ω is. Consider the continuous spatial domain $\bar{X}$. A one-dimensional discrete regular lattice over $\bar{X}$ is defined as $X = \{x_{-\infty}, \ldots, x_0, \ldots, x_{-\infty}\}$, with $x_i = ih$, where h is the cell size (scale) of the lattice and i is an integer (Figure

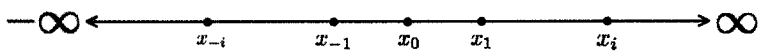

Figure 6.1: Definition of a lattice on the real line. Lattice points are located at regular intervals of distance h.

6.1) . Mathematically a CML can be defined,

$$n_{t+1}(x_i) = \sum_{x_j \in \Omega} \underbrace{k(x_i, x_j)}_{\text{dispersal from } x_j \text{ to } x_i} \underbrace{f[n_t(x_j)]}_{\text{growth at } x_j}, \tag{6.2}$$

where x_i, x_j are points in a one dimensional lattice, $n_t(x_i)$ is population at time t location x_i, $f[n_t(x_i)]$ is a map that models population growth and $k(x_i, x_j)$ is a discrete probability mass function for dispersal. In a spatially homogeneous environment, dispersal kernels that only depend on signed distance $x_d = x_i - x_j$ are called difference kernels. As an example of a difference kernel $k(x_d), x_d = x_i - x_j$, consider,

$$k(x_d) = \begin{cases} (1-u) \text{ if } x_d = 0 \\ \frac{u}{|\Omega|-1}, \text{ otherwise} \end{cases}, \tag{6.3}$$

where $|\Omega|$ is the number of cells in the neighbourhood Ω. Note that $u \in [0,1]$ and $\sum_\Omega k(x_d) = 1$. When $|\Omega| = 3$, this example is considered a classic CML model with nearest neighbour interaction. CMLs can be extended to a two-dimensional spatial lattice. Here the nearest neighbour interactions involve the central lattice point and eight neighbours so that $|\Omega| = 9$.

Some comparative studies show how results can be obtained using CMLs are similar to those found with other modelling structures like IDEs and individual based models (White and White, 2005; Brannstrom and Sumpter, 2005). As I will show here, analytical tools developed for IDEs can be used directly to study spread in discrete space for structured population models.

In this chapter I apply tools developed for calculation of wave speed and spread rate in integro-difference equations to coupled map lattices. To my knowledge, the application of these to CMLs is new. I use CMLs to study the population dynamics and spread of structured populations with applications to a particular invader, scentless chamomile (*Matricaria perforata*). I further analyze possible control strategies, and explore CMLs in heterogeneous landscapes and stochastic environments.

6.1.1 Scentless chamomile as a spatial invader

Scentless chamomile is an introduced annual, biennial or short-lived perennial plant that has become a widely distributed weed in cultivated areas in North America (Hinz,

1996; Hinz and McClay, 2000). Initially scentless chamomile spread slowly increasing its range only in the last decades (Hinz and McClay, 2000). The earliest records of scentless chamomile in Canada are in New Brunswick in 1876, Quebec in 1880, British Columbia in 1893, Saskatchewan in 1928 and Alberta in 1933 (Woo et al., 1991; Douglas et al., 1991). A single plant of this weed can produce up to 256,000 seeds per plant (McClay et al., 1995), and it grows in poorly drained low-lying areas (McClay et al., 1995; Woo et al., 1991), from which it spreads to adjacent fields (Hinz and McClay, 2000). Chamomile has small seeds that are dispersed on the ground and can be further spread by wind or water (Hinz and McClay, 2000).

In Chapter 3, a stage-structured model was developed, and transition values (survival and fecundity) were estimated from field data. I showed using elasticity matrices, that, in general, transition from rosettes to flowering plants and fecundity transitions to rosettes and to flowering plants contributed the most to population growth and would therefore be the most effective transitions to control. With additional data collected in Alberta, Canada, this chapter extends the matrix model to incorporate local spatial dynamics. This new approach allows us to analyze spread speed and potential control of this invader.

6.2 Discrete structured spatial models

6.2.1 Matrix integro-difference equations

Matrix population models have been shown to be an effective tool to study population growth and control (Shea and Kelly, 1998, 2004; Parker, 2000; McLeod and Saunders, 2001). Space can be incorporated in the matrix model formulation by extending a structured population across space, and considering dispersal between these locations in a continuous domain. As described by Neubert and Caswell (2000), the matrix integro-difference model is defined as

$$\mathbf{n}_{t+1}(x) = \int_{-\infty}^{\infty} [\mathbf{K}(x,y) \circ \mathbf{A}]\, \mathbf{n}_t(y)\, dy, \tag{6.4}$$

where $\mathbf{n}_t(x)$ is a vector of stages at time t and location x, $\mathbf{A}$ is the transition matrix as defined for matrix population models (Chapter 5, equation (5.1)), and $\mathbf{K}(x,y) = [k_{lm}(x,y)]$ is a dispersal matrix whose elements $k_{lm}(x,y)$ are kernels that describe dispersal as the individual moves from location y to x from stage m to stage l. Note that by definition, kernels k_{lm} in $\mathbf{K}$ are probability density functions. If difference kernels are assumed then $\mathbf{K}(x-y)$. The symbol "$\circ$" denotes Hadamard product which is element-wise multiplication. It is assumed that the $n \times n$ matrix $\mathbf{A}$ is non-negative and primitive, hence there is a real and positive dominant eigenvalue λ that corresponds to the population growth rate.

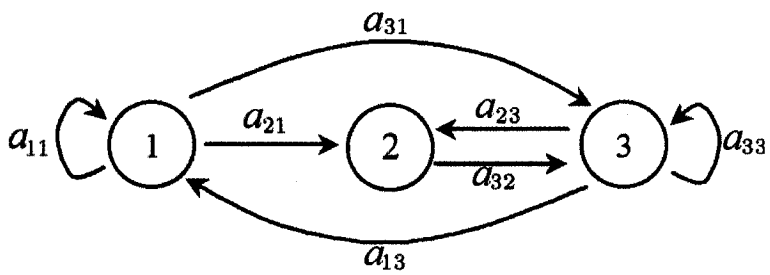

Figure 6.2: Life cycle graph of scentless chamomile as derived in Chapter 3. Node 1=seed bank, node 2=rosettes, node 3=flowering plants.

The matrix model developed in Chapter 3 provides a good example. Figure 6.2 describes the scentless chamomile life cycle graph. The projection interval for this model is 1 year. Nodes 1,2 and 3 correspond to seeds, rosettes and flowering plant stages. In the life cycle, seeds can germinate and produce either rosettes (stage without flowers) or flowering plants, or stay in the seed bank. Rosettes, can survive over winter producing a flowering plant next year. The projection matrix of scentless chamomile is given by

$$\mathbf{A} = \begin{bmatrix} a_{11} & 0 & a_{13} \\ a_{21} & 0 & a_{23} \\ a_{31} & a_{32} & a_{33} \end{bmatrix}, \tag{6.5}$$

and the dispersal matrix is given by difference kernels

$$\mathbf{K}(x-y) = \begin{bmatrix} \delta(x-y) & \delta(x-y) & k(x-y) \\ \delta(x-y) & \delta(x-y) & k(x-y) \\ \delta(x-y) & \delta(x-y) & k(x-y) \end{bmatrix}. \tag{6.6}$$

Here $k(z), z = x - y$ is the dispersal kernel describing the dispersal of seeds and the delta function $\delta(z)$ is used for transitions where no dispersal occurs. As can be seen from the third column of matrix $\mathbf{K}(z)$, seeds, produced by flowering plants, disperse and can remain as seeds, germinate to rosettes, or germinate to flowers in a single year.

A dispersal kernel for (6.6) can be defined using mechanistic principles, or can be obtained directly from data without assuming any particular shape (Lewis et al., 2005). Consider the example when relative frequencies of disperser f_j, are collected in two directions and at regular distances from a point source. The data can be written as, $\{(y_{-m}, f_{-m}), \ldots, (y_{-2}, f_{-2}), (y_{-1}, f_{-1}), (y_1, f_1), (y_2, f_2), \ldots, (y_m, f_m)\}$ where y_j is the location of the sample and f_j is the corresponding frequency (Figure 6.3). Using a linear interpolation function, a continuous difference kernel suitable for an integro-

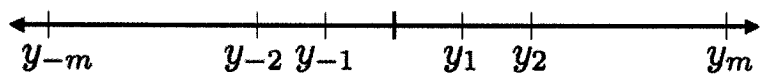

Figure 6.3: Relative frequencies of dispersal are collected in two directions and at regular distances y_i from a point source.

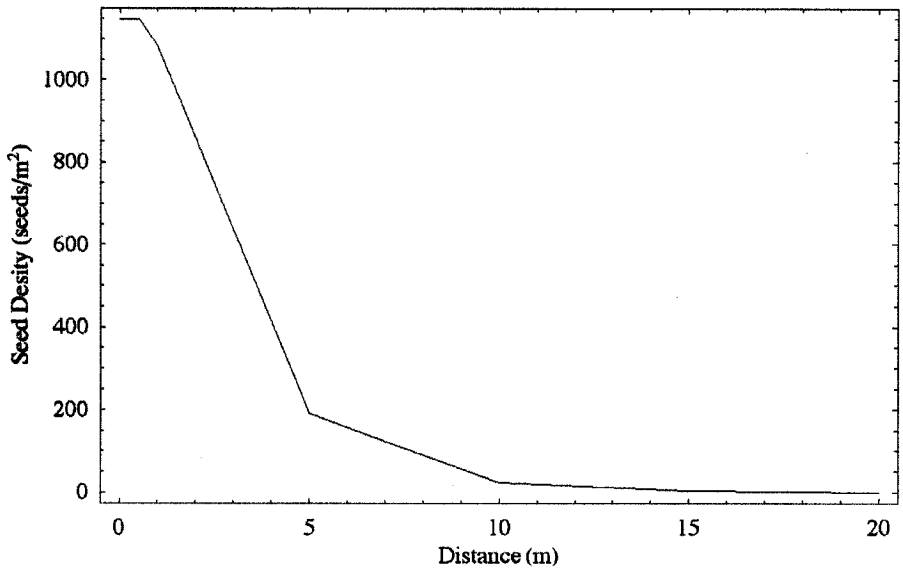

Figure 6.4: Linear interpolation of the scentless chamomile data obtained in Chapter 3. The data is obtained from the sum in all four cardinal directions, from seed traps collected in Vegreville, Alberta.

difference model can be defined in terms of $z = x - y$,

$$k(x,y) = k(z) = f_i + (f_i - f_{i-1})\frac{z - y_i}{y_i - y_{i-1}} \text{ with } y_{i-1} < z < y_i \tag{6.7}$$

(Figure 6.4).

6.2.2 Matrix coupled map lattice equations

Similar to a matrix IDE equation (6.4), a matrix CML equation with stage structure and difference kernels is described by

$$\mathbf{n}_{t+1}(x_i) = \sum_{x_j \in \Omega} \left[\tilde{\mathbf{K}}(x_i - x_j) \circ \mathbf{A}\right] \mathbf{n}_t(x_j). \tag{6.8}$$

Here $\mathbf{A}$ is the projection matrix as defined previously, $\mathbf{n}_t(x_i)$ is a vector of stages at time t location x_i and $\tilde{\mathbf{K}}$ is a matrix of discrete difference kernels. Each entry of $\tilde{\mathbf{K}}(x_i - x_j) = [\tilde{k}_{lm}(x_i - x_j)]$ must satisfy:

$$\sum_{i=-\infty}^{\infty} \tilde{k}_{lm}(x_i - x_j) = 1, \tag{6.9}$$

so that every disperser starting as x_j ends off at some x_i with probability one. The difference between matrix CML and matrix IDE is that the integral becomes a sum over discrete locations in space.

The kernel $\tilde{\mathbf{K}}$ can come from discretizing $\mathbf{K}$ (6.7) at any scale for use in terms of $x_d = x_i - x_j$,

$$\tilde{k}(x_d) = \int_{x_d - \frac{h}{2}}^{x_d + \frac{h}{2}} k(z)dz, -\infty < x_d < \infty. \tag{6.10}$$

For scentless chamomile, the discrete difference kernel $\tilde{\mathbf{K}}$ becomes,

$$\tilde{\mathbf{K}}(x_i, x_j) = \tilde{\mathbf{K}}(x_i - x_j) = \begin{bmatrix} \Delta(x_i - x_j) & \Delta(x_i - x_j) & \tilde{k}(x_i - x_j) \\ \Delta(x_i - x_j) & \Delta(x_i - x_j) & \tilde{k}(x_i - x_j) \\ \Delta(x_i - x_j) & \Delta(x_i - x_j) & \tilde{k}(x_i - x_j) \end{bmatrix}, \tag{6.11}$$

where $\Delta(x_i - x_j)$ is a discrete delta function defined as,

$$\Delta(x_i - x_j) = \delta_{ij} = \begin{cases} 1, \text{ if } i = j \\ 0, \text{ otherwise} \end{cases}. \tag{6.12}$$

Later in this chapter I will apply this model to scentless chamomile.

In two dimensions, a radially symmetric matrix of kernels $\mathbf{K}(\mathbf{x}, \mathbf{y}) = \mathbf{K}(r)$, $r = \sqrt{z_1^2 + z_2^2}$, $z_1 = x_1 - y_1$, $z_2 = x_2 - y_2$ is discretized for use in a CML. With dispersal from (x_{j_1}, x_{j_2}) to (x_{i_1}, x_{i_2}) equation (6.10) can be written in terms of $x_{d_1} = x_{i_1} - x_{j_1}$ and $x_{d_2} = x_{i_2} - x_{j_2}$ as

$$\tilde{\mathbf{K}}(\mathbf{x}_d) = \int_{x_{d_1} - \frac{h}{2}}^{x_{d_1} + \frac{h}{2}} \int_{x_{d_2} - \frac{h}{2}}^{x_{d_2} + \frac{h}{2}} \mathbf{K}(\sqrt{z_1^2 + z_2^2}) dz_1 \, dz_2. \tag{6.13}$$

See Figure 6.5.

6.3 Population spread rates

The way invasive species move across space, and how fast this occurs, is essential in the understanding invasion processes and how it can be controlled. With matrix IDEs, it is possible to calculate the rate of spread of a local population. As described below, the rate of spread, denoted c^*, is calculated as the minimum possible wave speed c of a moving wave front. In this section, I first describe how these two quantities can be calculated for matrix IDEs, and then show how these calculations hold for matrix CMLs.

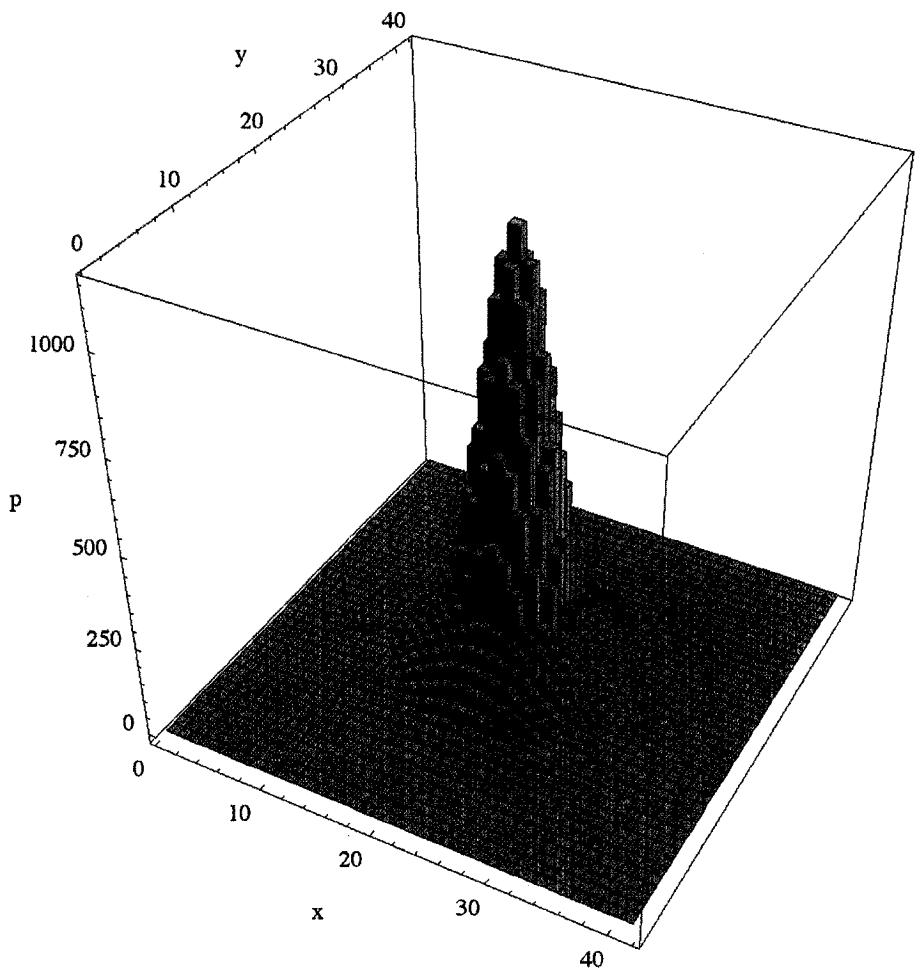

Figure 6.5: Two-dimensional kernel obtained from using equation (6.13) on the scentless chamomile data from Chapter 3.

6.3.1 Calculating the spread rate in a matrix IDE

A quantity that can be computed when space is included is the rate of spatial spread of a population that has been introduced locally. The spread rate c^* is defined for a locally introduced population as follows. An observer moving along a ray oriented away from the local introduction will asymptotically observe a population density of zero if the movement speed is faster than c^* and will asymptotically observe a positive population density if the speed is slower than c^*. A rigorous discussion and analysis of spread rates for structured population models can be found in Lui (1989).

Neubert and Caswell (2000) showed that the spread rate c^* can be related to the wave speed $c(s)$ for an exponentially declining population density $\mathbf{n}_t = \mathbf{w}e^{-s(x-ct)}$. Substitution into equation (6.4) with a difference kernel $\mathbf{K}(x,y) = \mathbf{K}(x-y)$,

$$\mathbf{w}e^{-s(x-ct)}e^{sc} = \int_{-\infty}^{\infty} [\mathbf{K}(x-y) \circ \mathbf{A}]\, \mathbf{w}e^{-s(y-ct)}dy \tag{6.14}$$

$$= \int_{-\infty}^{\infty} [\mathbf{K}(\xi) \circ \mathbf{A}]\, e^{s\xi}\mathbf{w}e^{-s(x-ct)}d\xi \tag{6.15}$$

$$= e^{-s(x-ct)} \int_{-\infty}^{\infty} [\mathbf{K}(\xi) \circ \mathbf{A}]\, e^{s\xi}d\xi\, \mathbf{w}, \tag{6.16}$$

where $\xi = x - y$. Hence,

$$\mathbf{w}e^{sc} = [\mathbf{M}(s) \circ \mathbf{A}]\, \mathbf{w} = \mathbf{H}(s)\mathbf{w}, \tag{6.17}$$

where $\mathbf{H}(s) = \mathbf{M}(s) \circ \mathbf{A}$ and $\mathbf{M}(s)$ is the moment generating function of the dispersal kernel:

$$\mathbf{M}(s) = \int_{-\infty}^{\infty} \mathbf{K}(\xi)e^{s\xi}d\xi. \tag{6.18}$$

The matrix $\mathbf{A}$ is non-negative and primitive and $\mathbf{M}(s)$ is positive. Hence $\mathbf{H}(s)$ is non-negative and primitive $n \times n$ matrix with eigenvalues $\rho_1(s), \rho_2(s), \ldots, \rho_n(s)$. By the Perron Frobenius theorem, the only eigenvalue corresponding to a non-negative eigenvector $\mathbf{w}$ is the dominant eigenvalue of $\mathbf{H}(s)$, $\rho_1(s)$. Hence, $e^{sc} = \rho_1(s)$ and a *dispersion relation*,

$$c(s) = \frac{1}{s} \ln\left(\rho_1(s)\right), \tag{6.19}$$

relates the speed of the wave c to the steepness of the wave s. The spread rate for the locally introduced population is given as:

$$c^* = \min_{s>0} c(s). \tag{6.20}$$

(Figure 6.6).

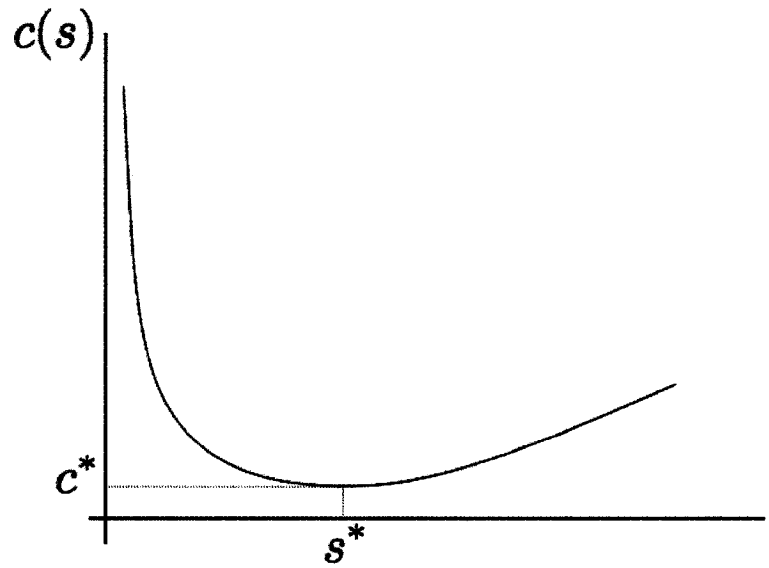

Figure 6.6: The rate of spread c^* is found by evaluating $c(s)$ at the steepness s^* that minimizes the wave speed function.

In summary, calculation of spread rate initially requires the transition matrix $\mathbf{A}$ and kernel matrix $\mathbf{K}$. The kernel matrix is transformed to give a matrix of moment generating functions $\mathbf{M}(s)$ by $\mathbf{A}$. This yields $\mathbf{H}(s) = \mathbf{A} \circ \mathbf{M}(s)$, whose dominant eigenvalue $\rho_1(s)$, is used in equations (6.19)-(6.20) to calculate the spread rate c^*. Neubert and Caswell (2000) give a detailed derivation linking c^* to the minimum of $c(s)$.

Some examples of application of (6.20) include Neubert and Parker's (2004), analysis of the spread of scotch broom (*Cytisus scoparius*), Buckley et al.'s (2005), analysis of invasion and spread of *Pinus nigra*, calculating the wave speed and determining control strategies to slow down the spread of this invader, and Jacquemyn et al.'s (2005), analysis of the effects of fire on the spread of the perennial tussock grass (*Molinia caerulea*) are studied.

Neubert and Caswell (2000) observed that c^* is a basic measure of invasiveness that summarizes detailed structured population dynamics and dispersal into a single statistic. They argued that it could be used to characterize invasiveness of a species, much as λ is used to summarize population growth rate. As with λ, formulae for the sensitivity and elasticity of c^* to the transition matrix entries can be derived. These are

$$\frac{\partial c^*}{\partial a_{ij}} = \frac{m_{ij}}{s^* \rho_1} \frac{\partial \rho_1}{\partial h_{ij}}, \tag{6.21}$$

for sensitivity and,

$$\frac{a_{ij}}{c^*}\frac{\partial c^*}{\partial a_{ij}} = \frac{1}{\ln \rho_1}\left[\frac{h_{ij}}{\rho_1}\frac{\partial \rho_1}{\partial h_{ij}}\right], \tag{6.22}$$

for elasticity. Equation (6.21) gives the absolute change in spread rate with respect to the projection matrix entries and (6.22) gives the relative change. Here s^* is the value where c^* is minimum and h_{ij} and m_{ij} are entries in $\mathbf{H}(s^*)$ and $\mathbf{M}(s^*)$ respectively (Figure 6.6). The quantity $\frac{\partial \rho_1}{\partial h_{ij}}$ is calculated using the same methods for calculating the sensitivity of growth rate λ, the dominant eigenvalue of $\mathbf{A}$ (see Caswell, 2001), that is,

$$\frac{\partial \rho_1}{\partial h_{ij}} = \frac{v_i(s^*)w_j(s^*)}{\langle \mathbf{w}(s^*), \mathbf{v}(s^*)\rangle}, \tag{6.23}$$

where $\mathbf{w}(s^*), \mathbf{v}(s^*)$ are the right and left eigenvectors of $\mathbf{H}(s^*)$, and $\langle \mathbf{w}(s^*), \mathbf{v}(s^*)\rangle$ is the scalar product of the two vectors.

For density-dependent projection matrices, the so-called *linear conjecture* states that the rate of spread of the matrix IDE model with density dependent projection matrix $\mathbf{A_n}$, is governed by its linearization around $\mathbf{n} = \mathbf{0}$ (Neubert and Caswell, 2000).

In other words, even if there are nonlinear interactions in the population, the rate of spread is given by the growth and dispersal behaviour of the leading edge of the invasion, where $\mathbf{n}$ is close to zero. Generally, this conjecture requires that there are no Allee effects at low population density. Some mathematical conditions under which the linear conjecture is known to hold are given in Lui (1989).

The matrix IDE approach thus allows spread rate speed and its sensitivity and elasticity to be determined analytically for discrete time and continuous space. In some cases, however, it may be advantageous to model space as discrete. For this, matrix CMLs are the better choice.

6.3.2 Calculating rate of spread in a matrix CML

CMLs can be considered a special case of matrix IDE, where space is discrete, therefore the dispersal kernel takes the shape of a function on a discrete lattice. To define wave speed, first we define the wave front and relate the discrete space CML with an associated exponential profile in a continuous space system (Figure 6.7). I then show the derivation of the wave speed formula for discrete systems

Similar to a matrix IDE, a wave speed formula can be derived for structured CML models. The derivation follows that of Neubert and Caswell (2000), but in this case we are dealing with discrete points on a lattice. Here, when deriving the wave speed, we are looking at a linear transition matrix in equation (6.4). In linear matrix CMLs

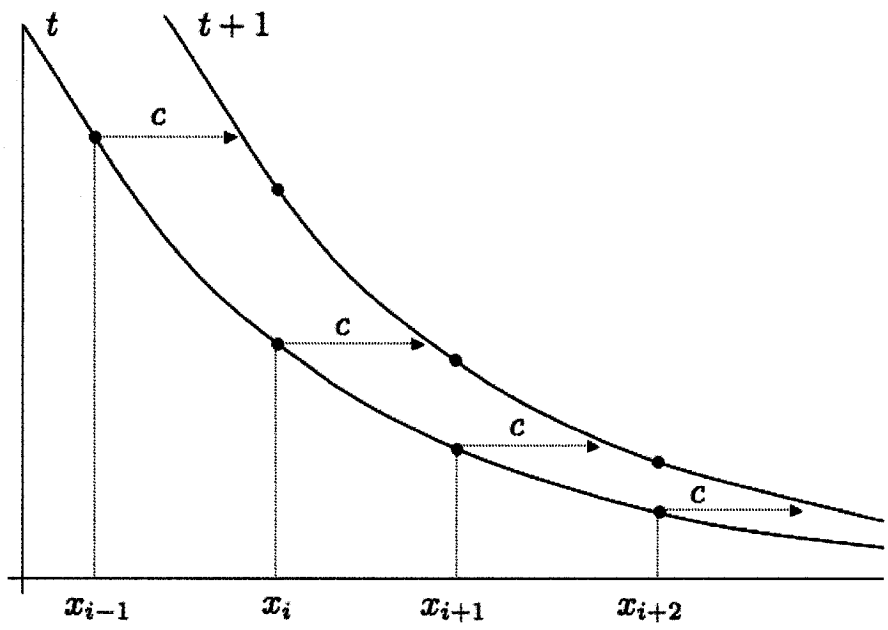

(a)

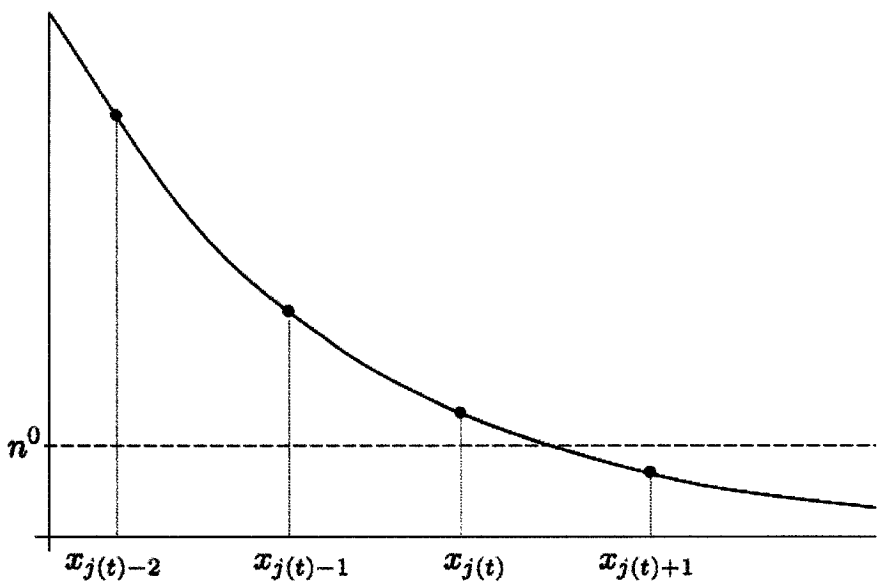

(b)

Figure 6.7: (a) Associated exponential profile that moves a distance $c \approx 0.9$ in one time step. n^0 is the detection threshold. (b) The detection threshold n^0 in the exponential profile is located between points $x_{j(t)}$ and $x_{j(t)+1}$.

the spread rate c^* of a locally introduced population can be calculated using the approach of Neubert and Caswell (2000) by evaluating the minimum possible wave speed c for an exponentially declining population density,

$$\mathbf{n}_t(x_i) = \mathbf{w}e^{-s(x_i - ct)}. \tag{6.24}$$

Substitution into (6.4) yields equation (6.19) where $\rho_1(s)$ is the largest eigenvalue of $\tilde{\mathbf{H}}(s) = \tilde{\mathbf{A}} \circ \tilde{\mathbf{M}}(s)$ and $\tilde{\mathbf{M}}(s)$ is the matrix of generating functions:

$$\tilde{\mathbf{M}}(s) = \sum_{-\infty}^{\infty} \tilde{\mathbf{K}}(x_j)e^{sx_j}. \tag{6.25}$$

Figure 6.7a shows the exponential profile and wave speed.

The spread on the lattice C_t, as calculated by the average rate of spatial extent of the spread over time, that is, $C_t = \frac{x_{j(t)}}{t}$, where $x_{j(t)}$, called spatial extent of spread, is the furthest point in the lattice where $n(x_{j(t)}) \geq n^0, n(x_{j(t)+1}) < n^0$ and n^0 is the critical level where a site is considered not empty (Figure 6.7b). Appendix 6.A shows that when the initial profile of the wave is exponentially decreasing with steepness s, it is possible to show that $C_t \to c(s)$ as $t \to \infty$, where $c(s)$ is the velocity of spread given in (6.19).

6.3.3 Calculating two-dimensional spread

A two dimensional CML is defined as follows:

$$\mathbf{n}_{t+1}(\mathbf{x}_i) = \sum_{\mathbf{x}_j \in \Omega} \left[\tilde{\mathbf{K}}(\mathbf{x}_i - \mathbf{x}_j) \circ \mathbf{A}\right] \mathbf{n}_t(\mathbf{x}_j), \tag{6.26}$$

where $\mathbf{n}_{t+1}(\mathbf{x}_i)$ now describes population density $\mathbf{n}_{t+1}$ in location $\mathbf{x}_j = [x_j \; y_j]^T$ in two dimensions, and $\tilde{\mathbf{K}}(\mathbf{x}_i - \mathbf{x}_j)$, as described earlier, is a matrix of kernels. Spread in two dimensions is calculated by considering only one direction, perpendicular to the wave front (Lewis et al., 2005).

It turns out that it is the marginal distribution of this two dimensional kernel that is needed for calculating population spread (see also Lewis et al., 2005). In this case the marginal distribution can be calculated by summing over one direction to give

$$\tilde{\mathbf{K}}(x_{d_1}) = \sum_{x_{d_2}=-\infty}^{\infty} \tilde{\mathbf{K}}(\mathbf{x}_d), \tag{6.27}$$

with $\mathbf{x}_d = [x_{d_1} \quad x_{d_2}]^T$, (Figure 6.8). The illustration in Figure 6.9 shows the reason why probabilities are summed in one direction when the kernel is used in

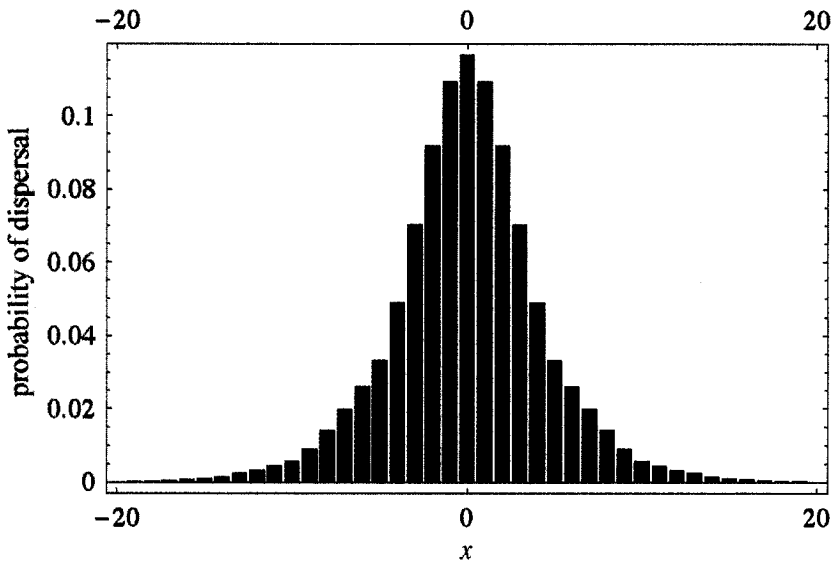

Figure 6.8: Marginalized kernel for scentless chamomile data. The marginal distribution is taken on the kernel in Figure 6.5.

one dimension to describe two-dimensional spread. Figure 6.8 shows the marginal distribution of the kernel in Figure 6.5.

Here we consider the case where spread is equal in all directions. Hence, equation (6.13) and Figure 6.8 pertain.

In summary, the marginal distribution of the kernel (equation (6.27) and Figure 6.8) is used in calculating the matrix of generating functions (6.27). From this the spread rate c^* is calculated from (6.19) -(6.20), where $\rho_1(s)$ is the dominant eigenvalue of $\tilde{\mathbf{H}}(s) = \mathbf{A} \circ \tilde{\mathbf{M}}(s)$.

6.3.4 Scentless chamomile rate of spread

Using the projection matrix in equation (6.5), and the kernel as defined in equation (6.7), it is possible to calculate the rate of spread for scentless chamomile. From Chapter 3, the estimated projection matrix for scentless chamomile is given by:

$$\mathbf{A}_1 = \begin{bmatrix} 0.08 & 0 & 36376.45 \\ 0.27 & 0 & 517 \\ 0.04 & 0.45 & 297.85 \end{bmatrix}, \mathbf{A}_2 = \begin{bmatrix} 0.08 & 0 & 1775.22 \\ 0.27 & 0 & 25.24 \\ 0.04 & 0.45 & 14.53 \end{bmatrix}. \quad (6.28)$$

Because of this large difference between years, rate of spread will be calculated for both.

Using equation (6.20) I calculated the rate of spread for scentless chamomile to be $c^* = 16.55$ m/yr for year 1 and $c^* = 11.32$ m/yr for year 2. The numerical simulations

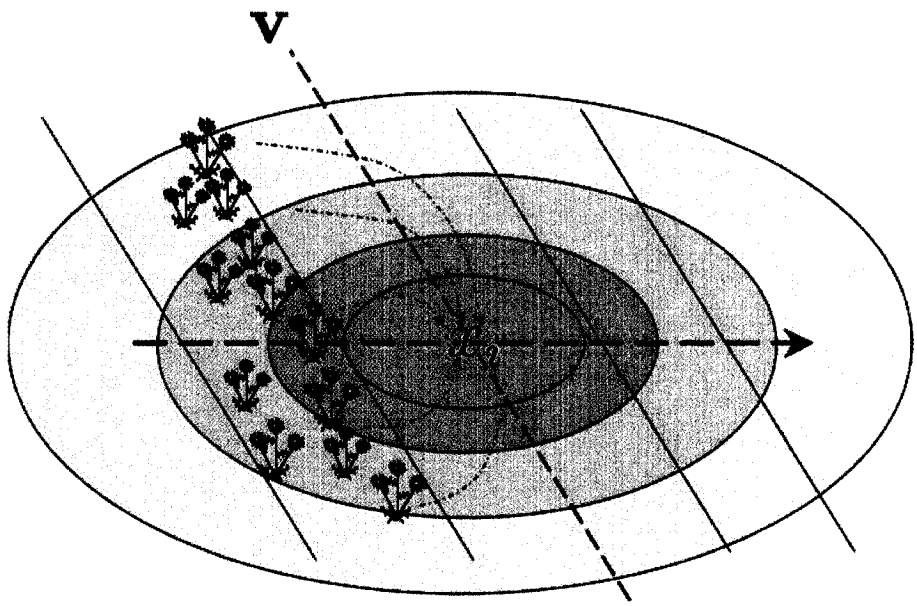

Figure 6.9: This figure shows why the marginal distribution of the kernel is taken when analyzing spread in one dimension. Suppose position x_i is being updated, then propagules will arrive to location x_i in a two dimensional system from all directions, with probability indicated by the concentric circles (the circles represent a kernel describing probabilities associated with points of origin $\mathbf{x}_j$ for a seed dispersing to $\mathbf{x}_i$, $k(\mathbf{x}_j, \mathbf{x}_i)$). If spread is taken only in the direction of the dashed line, contributions from locations below and above have to be considered. Hence, when the system is analyzed in one direction $\mathbf{u}$, the contributions in direction $\mathbf{v}$, have to be summed. A precise mathematical derivation is given in Lewis et al. (2005).

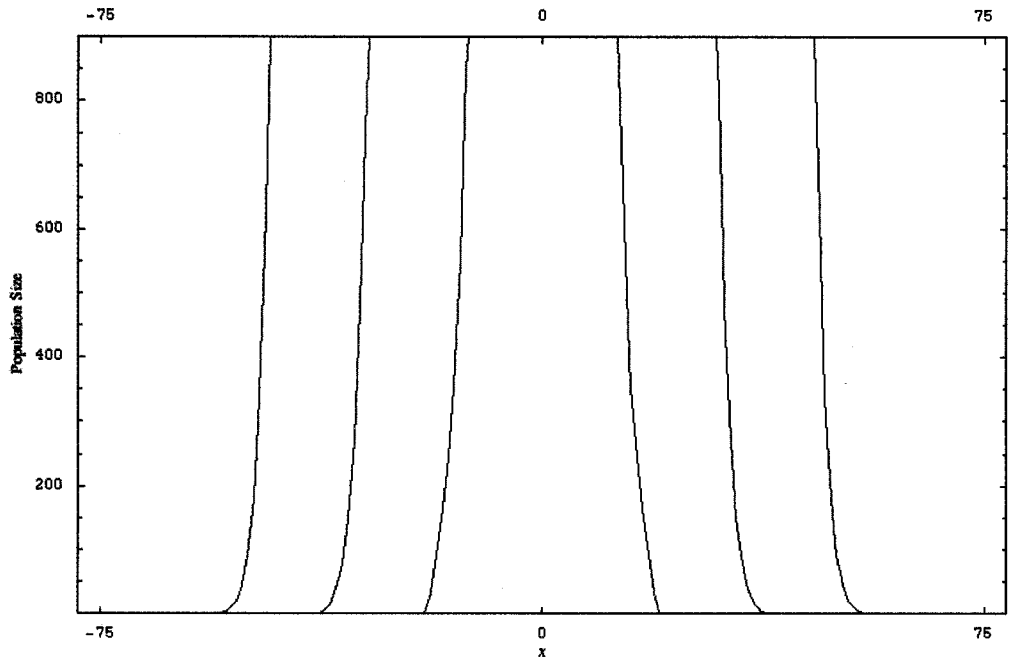

Figure 6.10: Numerical simulation showing the front wave moving over time, in a one-dimensional simulation of the spread of scentless chamomile.

Table 6.1: Estimated rate of speed for scentless chamomile. The calculations were done with data described in Chapter 3.

Method	c year 1	c year 2
Equation 6.20	$c^* = 16.55m/yr$	$c^* = 11.32m/yr$
Simulation in 1D	$c^* \approx 16.55m/yr$	$c^* \approx 11.32m/yr$
Bootstrap 90% CI	{16.43, 16.67 }	{10.33, 12.10 }

of the spread rate and the 90% confidence intervals are shown in Table 6.1. The confidence intervals were obtained from bootstrapping the sample of 86 seeds. Figure 6.10 shows the moving front in the one dimension numerical simulation. Elasticity to spread rate (Figure 6.11), was calculated using equation (6.22). These elasticities show that c^* is most sensitive to the flowering plant to flowering plant transition (a_{33}). As Figure 6.12 shows, although this transition has the most impact on c^*, a substantial reduction of fecundity is required to achieve large reductions in invasion speed. This indicates that control of scentless chamomile by reducing fecundity will unlikely be an effective control strategy, to control local growth (as seen in Chapter 3) or local spread, as shown here.

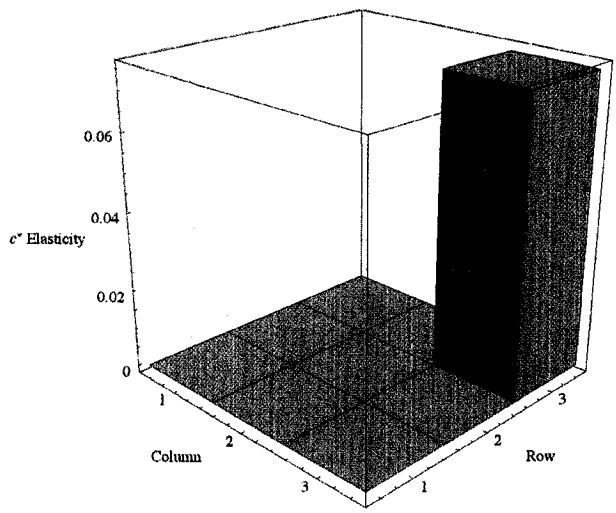

(a) Elasticity matrix year 1.

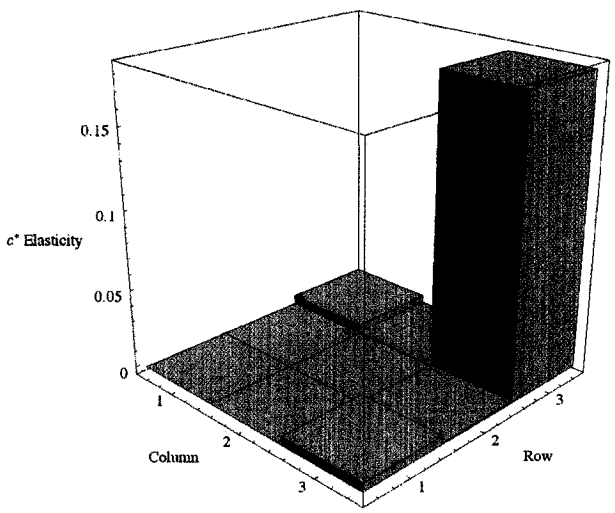

(b) Elasticity matrix year 2.

Figure 6.11: Elasticity of the wave speed c^* to entries in the transition matrix for (a) year 1 and (b) year 2. Column and row refer to column and row of the projection matrix (6.5). The numbers on the axes show the corresponding node number in Figure 6.2. The highest elasticity is in entry a_{33}.

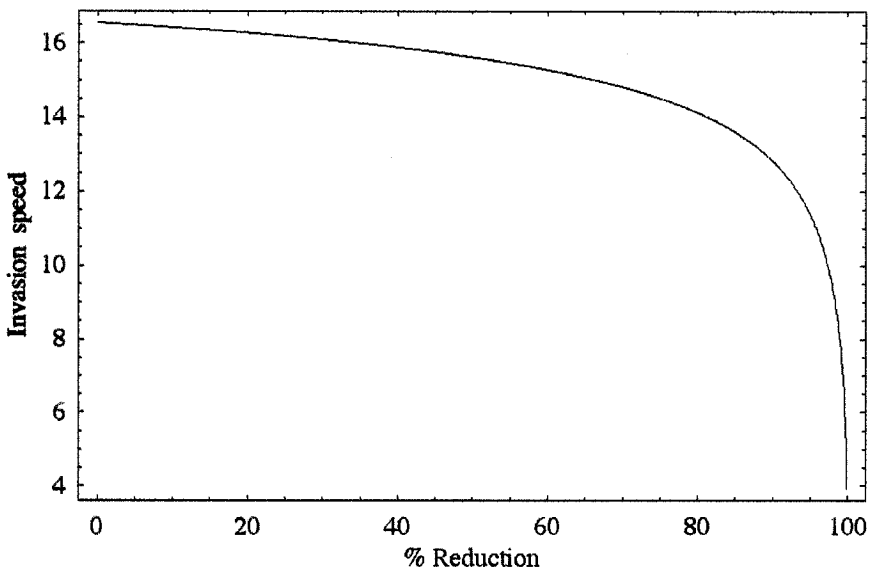

(a) Year 1

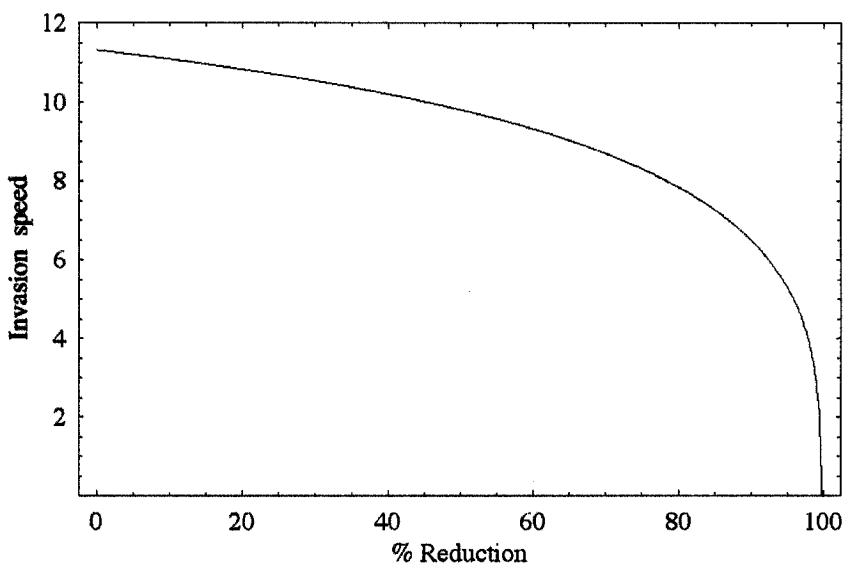

(b) Year 2

Figure 6.12: Reduction in invasion speed (m/year) as a function of percentage of fecundity reduction in scentless chamomile (transition a_{33}), for years 1 and 2.

6.4 Incorporating heterogeneous landscape

Coupled map lattice models provide a convenient and direct way of linking real landscape information with the population model. The basic equation for growth and spread (equation (6.26)) with a difference kernel can be written in two spatial dimensions and modified to include growth or establishment constraints

$$\mathbf{n}_{t+1}(\mathbf{x}_i) = \mathbf{P}(\mathbf{x}_i) \circ \sum_{x_j \in \Omega} [\mathbf{K}(\mathbf{x}_j - \mathbf{x}_i) \circ \mathbf{A}]\, \mathbf{n}_t(\mathbf{x}_j). \tag{6.29}$$

Here $\mathbf{P}(\mathbf{x}_i)$ is a vector whose entries contain the probability of establishment of propagules in each stage in location $\mathbf{x}_i = [x_i\ y_i]^T$. A landscape $\mathbf{P}$ can be defined directly from a raster layer in a GIS system, as I will show later with an example.

It is expected that any spatial constraints will change the wave speed depending on the ability of the dispersers to travel long or short distances, and thus disperse in a fragmented landscape (With, 2004). Consider, for example, an invading organism that spreads quickly, diluting local populations. It may reduce global populations in a landscape where patches are too small, failing to establish stable populations in local patches. Hence, spatial inhomogeneities could be of consequence when designing control strategies.

To investigate spread of scentless chamomile through the landscape, I ran simulations of scentless chamomile on a real landscape. To run simulations on a landscape, I simplified the scentless chamomile system to an unstructured population model of the form:

$$n_{t+1}(\mathbf{x}_i) = P(\mathbf{x}_i) \sum_{\Omega} k(\mathbf{x}_i - \mathbf{x}_j) \lambda_1 n_t(\mathbf{x}_j), \tag{6.30}$$

where λ_1, is the SC population growth rate for year 1, and $P(\mathbf{x}_i)$ is the growth constraint in location $\mathbf{x}_i$.

On the real landscape the discrete dispersal kernel was scaled using coarser 25m bin sizes in equation (6.10) (3 by 3 cells in the landscape). The distances in the lattice are calculated from the center of the lattice point to the center of the adjacent lattice point. To illustrate the applicability of a CML model at a landscape level, I simulated spread using the estimated kernel over a 25m resolution classified satellite image of The Vegreville-Edmonton region (Figure 6.13), involving the area were the parameter estimates of the matrix mode were obtained, and dispersal data was collected. The classified image (Figure 6.14a), shows pasture, cropland, forest, water bodies and infrastructure on a 25m pixel resolution. Chamomile can grow in croplands, pastures, and infrastructure (road edges) (Bowes et al., 1994). The probability of establishment p were obtained from habitat occupancy reported for scentless chamomile in Saskatchewan (Bowes et al., 1994, Table 2 in Balgonie 1985).

Based on occupancy probability, p for pastures was set to 0.6, cropland 0.024 and infrastructure 0.3. Results of the simulation are shown in Figures 6.14 and 6.15. The simulations show the spread after 50,150 and 300 iterations starting with an initial density of 1000 on a 25m^2 area. Assuming spread equal in all directions, the velocity of spread was calculated using $(1/t)(\sqrt{area/\pi})$. The rate of spread for the heterogeneous landscape is 15.25m/year compared to 22.25m/year in the numerical simulation without constraints. The difference between the calculated $c^* = 16.55$m/year, and the numerical simulation without constraints, 22.25m/year, is due to the rescaling of the kernel.

6.5 Environmental Stochasticity

The matrix IDE and matrix CML model described assume temporal invariance in population growth and spread. However, in many cases this assumption is unrealistic (Neubert and Parker, 2004). Strong resource dependencies change local population dynamics and as a consequence, the ability of organisms to spread (Dwyer and Morris, 2006; Fagan et al., 2005). Chamomile results show how growth rate differs substantially from one year to the next one (Chapter 3), and this difference also influences the rate of spread (Table 6.1)

The effect of these fluctuating environments can be incorporated by making population growth rate and the dispersal kernel a function of time (Neubert et al., 2000). For a CML,

$$\boldsymbol{\mathcal{N}}_{t+1}(x_i) = \sum_{j=-\infty}^{\infty} \left[\tilde{\mathbf{K}}_t(x_i - x_j) \circ \mathbf{A}_t\right] \boldsymbol{\mathcal{N}}_t(x_j). \tag{6.31}$$

Here $\tilde{\mathbf{K}}_t(x_d), x_d = x_i - x_j$ is a matrix whose elements are independent, and identically distributed (i.i.d.) discrete dispersal kernels, $\mathbf{A}_t$ are i.i.d. projection matrices, independent of the dispersal kernels for $t = 0, 1, 2, \ldots$, and $\boldsymbol{\mathcal{N}}_t(x_i)$ is a stochastic process describing the density of individuals at grid point x_i and time t. In other words, for a given time t and lattice point x_i, $\boldsymbol{\mathcal{N}}_{t+1}(x_i)$ is a vector of random variables describing the density of individuals from each stage.

Neubert et al. (2000) derived a formula to calculate the expected rate of spread and its variance for a stochastic IDE. Here I derive formulae that can be used for stochastic matrix CMLs. As in Section 6.3.1, $\tilde{\mathbf{H}}_t(s) = \tilde{\mathbf{M}}_t(s) \circ \tilde{\mathbf{A}}_t$ for $t = 1, 2, \ldots$, where $\tilde{\mathbf{H}}_t(s)$ is the matrix of generating functions for $\tilde{\mathbf{K}}_t$ (see equation (6.25)). As in the earlier section $\tilde{\mathbf{H}}_t(s)$ is a time-dependent non-negative and primitive matrix, with dominant eigenvalue $\rho_{1t}(s)$ and corresponding eigenvector $\mathbf{w}_{1t}(s)$. Appendix 6.B shows that the random variable describing the spread rate C_t is given by the spread

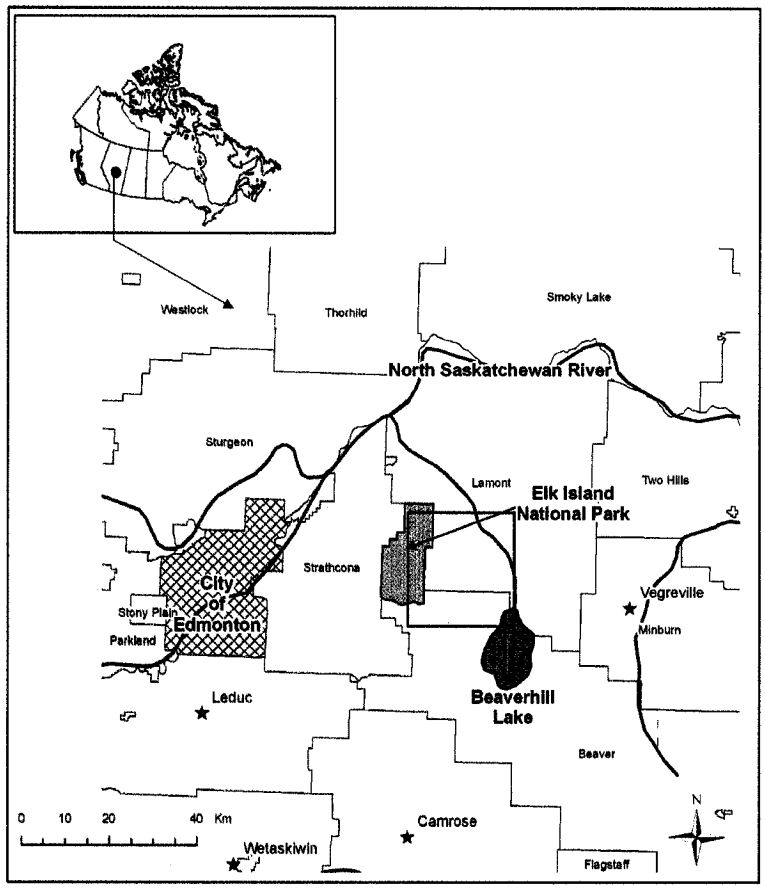

Figure 6.13: Map of the Edmonton-Vegreville region. The think line area indicates the subsection shown in Figure 6.14. Map taken from Young et al. (2006) and edited with authors permission.

(a) time 0

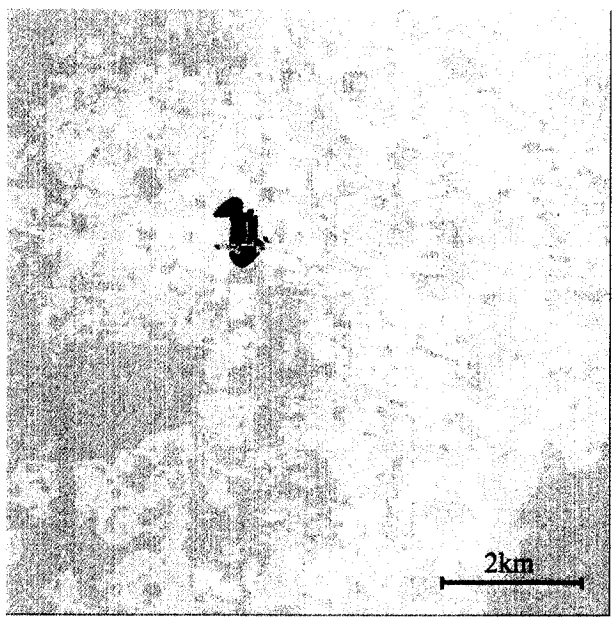

(b) time 50

Figure 6.14: Numerical simulations of equation (6.29) on a real landscape, the land uses classes correspond to, blue= water, dark green= forest, light green=pastures, yellow= cropland, light blue = infrastructure. (a) landscape corresponds to a subsection of figure 6.13, (b) simulation after 50 years. Shades of grey show scentless chamomile density

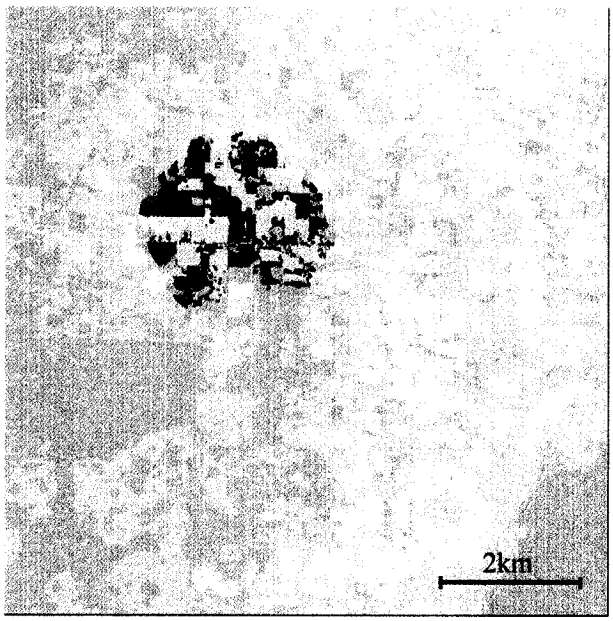

(a) time 150

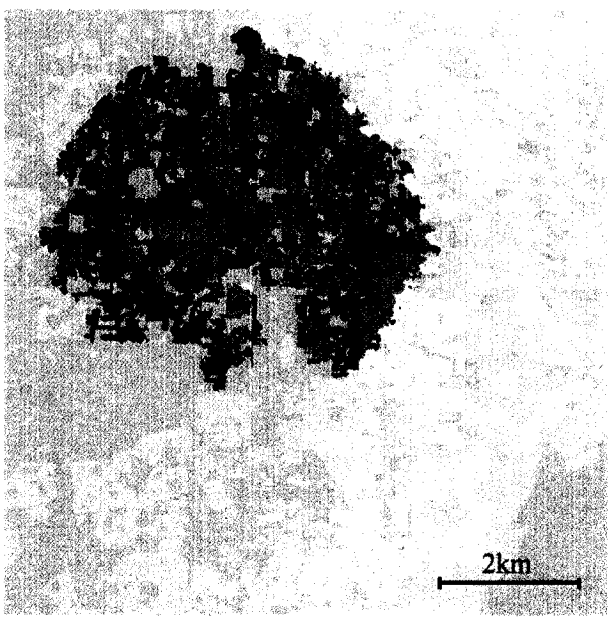

(b) time 300

Figure 6.15: (a) simulation of equation (6.29) parameterized for scentless chamomile after 150 iterations, (b) 300 iterations. Shades of grey show scentless chamomile density

rate $\mathcal{C}_t = \frac{x_{j(t)}}{t}$ is now a random variable. As $t \to \infty$,

$$\mathcal{C}_t = \frac{x_{j(t)}}{t} \to \frac{1}{s}\left(\frac{1}{t}\sum_{\tau=0}^{t-1}\ln(\rho_{1\tau}(s))\right), \tag{6.32}$$

$\mathcal{C}_t(s)$, the mean of (6.49) up to time t, is evaluated using the dominant eigenvalue $\rho_{1\tau}$ of the time-dependant matrix $\tilde{\mathbf{H}}_t(s)$. Because each eigenvalue is an iid random variable, and (6.32) calculates the mean of these from time $\tau = 0$ to $\tau = t-1$, the central limit theorem applies as $t \to \infty$. By the central limit theorem, $\mathcal{C}_t$ is normally distributed with mean

$$\mu(s) = E[\ln(\rho_{10})s^{-1}], \tag{6.33}$$

and variance

$$\sigma^2(s,t) = \frac{1}{t}\mathrm{Var}[\ln(\rho_{10})s^{-1}], \tag{6.34}$$

for large time t.

As shown in Neubert et al. (2000) for scalar integro-difference equations, the expected spread rate for stochastic matrix CMLs is calculated as,

$$\bar{c}^* = \min_{s>0}\mu(s) = \mu(s^*). \tag{6.35}$$

Consider the scentless chamomile example. In Chapter 3, I showed that fecundities were substantially different between year 1 and year 2, therefore there is one projection matrix for each year, $\mathbf{A}_1$ and $\mathbf{A}_2$ (6.28). As these were observed after two years I assume in the absence of any other information that they are equally likely to occur. The kernels are kept constant. For large times t the average speed and variance are given by $\mu(s^*)$ and $\sigma^2(s^*)$ where the mean is

$$\mu(s) = \frac{1}{2s}\left[\ln(\rho_1(\tilde{\mathbf{H}}_1(s))) + \ln(\rho_1(\tilde{\mathbf{H}}_2(s)))\right], \tag{6.36}$$

and the variance is,

$$\sigma^2(s,t) = \frac{1}{t}\left[\frac{1}{2s^2}\ln^2(\rho_1(\tilde{\mathbf{H}}_1(s))) + \ln^2(\rho_1(\tilde{\mathbf{H}}_2(s)))\right] - \mu^2(s), \tag{6.37}$$

and s^* is the wave steepness that minimizes (6.36)(see equation(6.35)). With

$$\tilde{\mathbf{H}}_1 = \mathbf{A}_1 \circ \begin{bmatrix} 1 & 1 & \tilde{\mathbf{M}}(s^*) \\ 1 & 1 & \tilde{\mathbf{M}}(s^*) \\ 1 & 1 & \tilde{\mathbf{M}}(s^*) \end{bmatrix}, \tilde{\mathbf{H}}_2 = \mathbf{A}_2 \circ \begin{bmatrix} 1 & 1 & \tilde{\mathbf{M}}(s^*) \\ 1 & 1 & \tilde{\mathbf{M}}(s^*) \\ 1 & 1 & \tilde{\mathbf{M}}(s^*) \end{bmatrix}, \tag{6.38}$$

the expected spread rate calculated using equation (6.35), is $\bar{c}^* = 14.29$ and its variance $\sigma^2(s^*,t) = \frac{196.9}{t}$. Figure 6.16 shows the calculated wave speed $\mathcal{C}_t$ and wave speed variance $\sigma^2(t)$, for 20 realizations of the numerical simulations. As seen in the Figure, $\mathcal{C}_t$ converges to the calculated $\bar{c}^*$ and the variance decreases according to (6.37) as time increases.

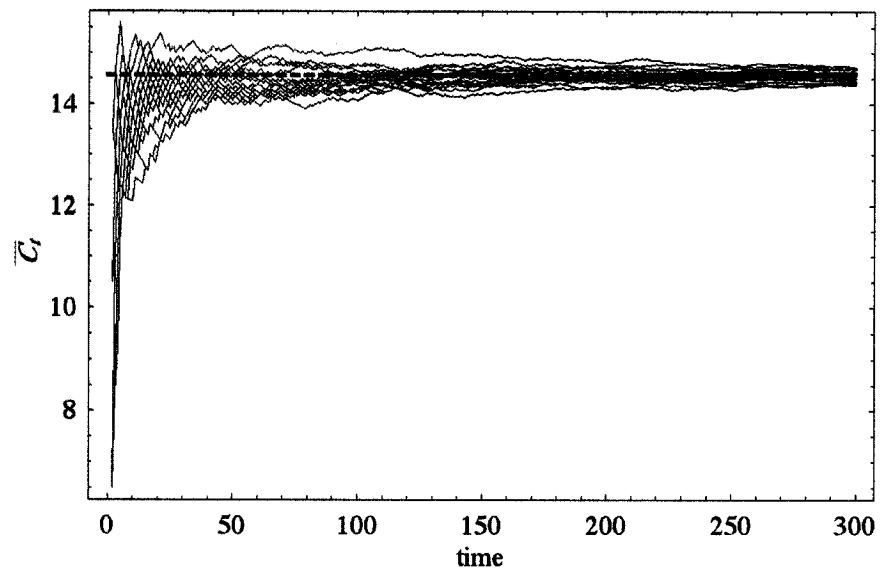

(a) Velocity of spread.

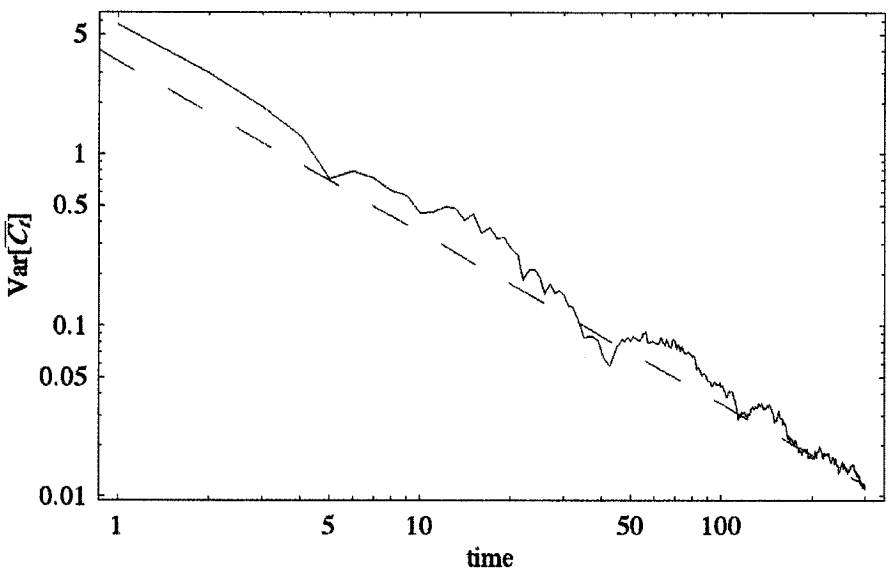

(b) Velocity of spread variance.

Figure 6.16: Estimated velocity of spread and variance for 20 realization of the stochastic model. The simulations were run 20 iterations. The dashed line indicates $\bar{c}$ obtained using equation (6.35).

Table 6.2: Rate of spread formulae

Symbol	Description	Formula	Source
$c(s)$	wave speed for matrix IDEs, and matrix CMLs	(6.19)	Neubert and Caswell (2000)(IDE) and this thesis (CML)
c^*	spread rate for matrix IDEs and matrix CMLs	(6.20)	Neubert and Caswell (2000)(IDE) and this thesis (CML)
C_t	average rate of spatial extent of spread fro matrix IDEs and matrix CMLs	(6.49)	Neubert and Caswell (2000)(IDE) and this thesis (CML)
$\mathcal{C}_t$	average rate of spatial extent of spread stochastic matrix CMLs	(6.32)	this thesis
$\bar{c}^*$	expected spread rate for stochastic matrix CMLs	(6.35)	this thesis

6.6 Discussion

In this chapter, I showed that the wave speed and rate of spread can be calculated for matrix CMLs in constant and stochastic environments in one and two dimensions. I also showed how heterogeneous landscape information can be incorporated to the CML model. Using scentless chamomile as an example, I showed how these methods can be applied.

6.6.1 Matrix coupled map lattices

Coupled map lattices are a convenient way of modelling spatial dynamics of invasive species. In these models population structure, age or stage structured, and spatial dynamics, using discrete kernels; can be incorporated to calculate vital quantities in biological invasion. The main result of this chapter is a CML framework for calculating rates of spread in constant, heterogeneous and stochastic environments. The methods shown here, calculation of rate of spread in stochastic and constant environments, are tools already developed for scalar and matrix IDEs (Kot et al., 1996; Neubert et al., 2000; Neubert and Caswell, 2000).

There are few examples of CMLs being used for biological invasions. In most cases, the CML have been used informally to incorporate heterogeneous landscape information and study distribution patterns, and not to calculate spread. Bjornstad and Bascompte (2001), for example, build a CML to understand how the self-

organizing spatial patterns emerge; and Rees and Paynter (1997), build a spatially explicit structured models that studies the ground covered by scotch broom. These models do not formulate the calculation of rate of spread, nor do they allow for analytical work due to their complexity. Individual based models have been a choice for modelling spread in heterogeneous environment, but their results are not amenable to general analysis,, like formal differential equations or integro-difference equation models (Hastings et al., 2005).

The formulae derived here are summarized in Table 6.2. The quantity c^* is the biologically relevant statistic. If an individual moves faster than c^*, it will outrun the invasion. On the other hand if it moves slower than c^* then it will fall behind. The calculation of c^* is done using the related wave speed quantity $c(s)$. This quantity describes the speed of a declining profile $n_t(x) \propto exp(-s(x-ct))$, where the speed is a function of the steepness of the wave s. The relation between c^* and $c(s)$ was initially investigated by Aronson and Weinberger (1978) for Fisher's equation. They showed that the rate of spread is obtained by minimizing $c(s)$ over all possible values of steepness s. The same holds for matrix IDEs (Neubert and Caswell, 2000), and it was assumed here that it holds for matrix CMLs. A rigorous mathematical proof of this is subject to future research.

The assumption that environments are constant over time is unrealistic. For that, $\mathcal{C}_t$, a random variable describing the average rate of spatial extent can be used. It is possible to calculate the mean and variance for $\mathcal{C}_t$, for large time.

6.6.2 Lessons for the design of control strategies

Matrix CMLs can be a useful tool for the design of control strategies, because they allow one to:

1. Calculate demographic parameters, λ, R_0, and rate of spread c^*.
2. Determine how fast a pest is spreading and what aspects of the life history of the invader should be target of control.
3. Establish how landscape heterogeneity, using real landscape information from GIS, affects the rate of spread of the invader.
4. Incorporate environmental stochasticity and study the effect of control strategies reducing spread.
5. Focus on measurable local dispersal data, rather than long-distance human-mediated dispersal.
6. Potentially use the CML model to optimize strategies in space and time to minimize c^* and λ with minimum effort.

Although matrix CMLs and other models of spatial dynamics, are a simplified representation of the invasion process, assuming the basic dynamic is well defined in these models, they can serve as useful tools to focus control of invasive species research.

6.6.3 Spread of scentless scentless chamomile

With the scentless chamomile data collected and presented in Chapter 3, I studied the local rate of spread of scentless chamomile in constant, stochastic and heterogeneous landscapes using the matrix CML formalism. For the scentless chamomile model, a linear interpolation function was used to calculate a discrete dispersal kernel. This kernel is straightforward to estimate from data, and does not assume any particular shape. Although this method of estimating the kernel is useful, the tails are short and the function does not allow for extrapolation to longer distances. Calculation of spread, using integro-difference models, have shown to be sensitive to the shape of the kernel (Kot et al., 1996). As shown below, this is also true for matrix CMLs.

The rate of local spread for scentless chamomile was calculated to be 11.35m/year in year 1 and 16.55m/year in year 2. At the rate of year 2 for example, scentless chamomile could cover 1 hectare in approximately 4 years. The average farm size in Alberta is around 393 hectares (Statistics Canada, 2001 census). Hence, if local dispersal is the only factor driving dispersal, it would take a long time to cover an entire field. Indeed, one of the shortcomings of the model is that it does not incorporate long-distance dispersal mediated by wind or water, or human mediated dispersal, which would make the kernel "fatter".

In the dispersal kernel measurement, the furthest measured dispersal distance was $d_{max} = 25$. To show the effect of fatter kernels, suppose that one seed is added to the sample at a d_{max} value of 20, 30 and 50m. The spread calculation was repeated for each augmented sample ($N = 86$ seeds) as d_{max}. The location of the 87^{th} seed, was moved. Figure 6.17 shows that the time it takes to cover 10 hectares of land decreases quickly, as d_{max} increases. This means that if, dispersing locally 50m is possible, scentless chamomile would have a coverage of 10 hectares in less than 4 years rather than approximately 11 years. This also indicates that, 1) the models is very sensitive to kernel shape, and 2) this model describes local spread, but longer tails are needed to explain faster spread long-distance spread. Despite these difficulties, this model serves as a model to test local dispersal hypothesis against long-distance dispersal (Clark, 1998).

As seen in Figure 6.14b, some disconnected patches were invaded by scentless chamomile through roads. Hence, landscape connectivity allows scentless chamomile to spread, even if in crops, the dominant class in the landscape, it has a low probability of occupancy.

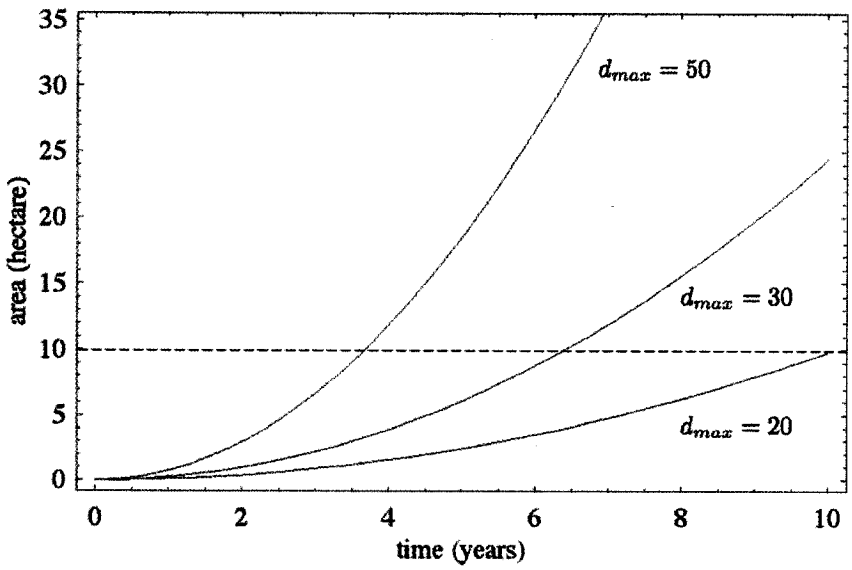

Figure 6.17: Time in years that 10 hectares of a farm are covered, if one seed is found at x distance form the source plant in scentless chamomile

Figure 6.15b shows a simulation after 500 years. From historical data (presented earlier), it is clear that local dispersal is not sufficient to explain scentless chamomile spread in Canada, and that human-mediated dispersal could be the factor missing. Human mediated long distance dispersal has been a major driving force in the spread of invasive organisms (Sakai et al., 2001). For example plant species of the family Acanthaceae in tropical islands, introduced as ornamental, have spread widely because of a long history of human mediated transport (Meyer and Lavergne, 2004). This type of dispersal can spread species across large and disconnected landscapes. However, although it can be incorporated as stochastic rare events, human mediated dispersal is complex and may not follow clear mechanisms. Ultimately, many of these human dispersal problems can be controlled in part with appropriate government policies, but they are not part of local control of population growth and spread. Therefore, the focus should be on local dispersal to optimize control strategies and slow local spread based on targeting life cycle transitions of the pest. The numerical simulation shown in Figures 6.14 and 6.15, show how scentless chamomile can spread in a heterogeneous landscape.

The large difference in the rate of spread between both years suggested that environmental stochasticity could have a large impact on rate of spread of scentless chamomile. The stochastic models showed an average asymptotic rate of spread $\bar{c} = 14.29$m/year. This is 14% slower than year 1 and 20% faster than year 2. The large variance Var$[\bar{c}]$ indicates that the difference between good year and bad year

could yield very different scenarios. While the estimate of the mean spread rate becomes more precise as invasion progresses, the spatial extent (how far the invasion front has moved) cannot be predicted (Neubert et al., 2000).

Elasticity analysis showed that flower to flower transition (a_{33}) has the most impact on reducing the rate of spread of scentless chamomile. However, a large reduction in fecundity is needed to have a substantial reduction in spread for both years (Figure 6.11). Elasticity analysis of λ indicated, that this transition should also be the target for control (Chapter 3). The seed weevil *Omphalapion hookeri*, targets flower heads and can potentially reduce fecundity (transitions a_{13}, a_{23}, a_{33}). Although this biological control agent has spread and established, they have a low impact on fecundity with less than 10% reduction (McClay and De Clerck-Floate, 1999). Other control agents, like the gall midge (*Rhopalomyia n. sp.*) (Hinz and Muller-Scharer, 2000) and the fungus *Colletotrichum sp.* (Peng et al., 2005), affect survival but not fecundity. Their impact on scentless chamomile in the field has not been quantified.

Demographic analysis of scentless chamomile has shown: 1) population growth rates are affected by flower to flower transitions, 2) local spread is also affected by flower to flower transitions 3) dispersal mechanisms like water and wind need to be incorporated in the model, 4) environmental stochasticity influences local spread, and 5) scentless chamomile high population growth rates, and the large reductions in fecundity needed to control it, suggests that combined strategies (mechanical, chemical and biological control) are needed to control this weed.

Appendix

6.A CML wave speed

When the initial profile of the wave is exponentially decreasing with steepness s, it is possible to show that $C_t \to c(s)$ as $t \to \infty$, where $c(s)$ is the velocity of spread given in (6.19). For an initial condition of the form:

$$\mathbf{n}_0(x_i) = \mathbf{n}^0 e^{-sx_i}, \tag{6.39}$$

any solution to (6.4) can be written in term of eigenvalues $\rho_i(s)$ and eigenvectors $\mathbf{w}_i(s)$ of $\mathbf{H(s)}$ as

$$\mathbf{n}_t(x_i) = \left[\beta_1 \rho_1(s)^t \mathbf{w}_1(s) + \beta_2 \rho_2(s)^t \mathbf{w}_2(s) + \ldots + \beta_n \rho_n(s)^t \mathbf{w}_n(s)\right] e^{-sx_i}. \tag{6.40}$$

Dividing by $\rho_1(s)^t$ we get,

$$\frac{\mathbf{n}_t(x_i)}{\rho_1(s)^t} = \left[\beta_1 \mathbf{w}_1(s) + \beta_2 \left(\frac{\rho_2(s)}{\rho_1(s)}\right)^t \mathbf{w}_2(s) + \ldots + \beta_n \left(\frac{\rho_n(s)}{\rho_1(s)}\right)^t \mathbf{w}_n(s)\right] e^{-sx_i}. \tag{6.41}$$

Because ρ_1 is the largest eigenvalue, as $t \to \infty$,

$$\frac{\mathbf{n}_t(x_i)}{\rho_1(s)^t} = \beta_1 \mathbf{w}_1(s) e^{-sx_i}, \tag{6.42}$$

where $\mathbf{w}_1(s)$ is the left eigenvector of $\mathbf{H}(\mathbf{s})$ and gives the stable stage distribution in the spreading population and s is the steepness of the advancing edge of the wave. Rearranging equation (6.42),

$$\mathbf{n}_t(x_i) = \beta_1 \mathbf{w}_1(s) e^{-sx_i} \rho_1(s)^t. \tag{6.43}$$

Without loss of generality, we consider any component n_t of $\mathbf{n}_t$ with corresponding eigenvector component w_1. Since we are dealing with a discrete lattice rather than the real line, at time t, n^0 lies somewhere between discrete points $x_{j(t)}$ and $x_{j(t)+1}$ Figure 6.7b. Hence,

$$\begin{gathered} n_t(x_{j(t)}) \le n^0 \le n_t(x_{j(t)+1}) \\ \beta_1 w_1(s) e^{-sx_{j(t)}} \rho_1(s)^t \le n^0 \le \beta_1 w_1(s) e^{-s(x_{j(t)+1})} \rho_1(s)^t, \end{gathered} \tag{6.44}$$

which can be rewritten,

$$e^{-sx_{j(t)}} \le \frac{n^0}{\beta_1 w_1(s)} \rho_1(s)^{-t} \le e^{-sx_{j(t)}} e^{-sh}. \tag{6.45}$$

Taking natural logarithms and dividing by s gives

$$-x_{j(t)} \le \frac{1}{s} \ln\left(\frac{n^0}{\beta_1 w_1(s)}\right) - \frac{t}{s} \ln(\rho_1(s)) \le -x_{j(t)} - h, \tag{6.46}$$

and dividing by $-t$ yields

$$\frac{x_{j(t)}}{t} \ge \frac{1}{st} \ln\left(\frac{n^0}{\beta_1 w_1(s)}\right) + \frac{\ln(\rho_1(s))}{s} \ge \frac{x_{j(t)}}{t} - \frac{h}{t}, \tag{6.47}$$

which can be rewritten,

$$\frac{1}{st} \ln\left(\frac{n^0}{\beta_1 w_1(s)}\right) + \frac{\ln(\rho_1(s))}{s} \le \frac{x_{j(t)}}{t} \le \frac{1}{st} \ln\left(\frac{n^0}{\beta_1 w_1(s)}\right) + \frac{\ln(\rho_1(s))}{s} + \frac{h}{t}. \tag{6.48}$$

As $t \to \infty$ the left and right quantities in the above equation approach $\frac{1}{s}\ln(\rho_1(s))$, the spread rate C_t is defined as,

$$C_t = \frac{x_{j(t)}}{t} \to \frac{1}{s} \ln(\rho_1(s)) = c(s), \tag{6.49}$$

as in equation (6.19).

6.B Wave speed for stochastic environment matrix CMLs

In this appendix I show that with an initial condition of the form $\mathbf{n}_0 = \mathbf{n}^0 e^{-sx}$, solutions to (6.31) can be written as a linear combination,

$$\boldsymbol{\mathcal{N}}_1(x_i) = [\beta_{10}\rho_{10}(s)\mathbf{w}_{10}(s) + \beta_{20}\rho_{20}(s)\mathbf{w}_{20}(s) + \ldots]\, e^{-sx_i} \tag{6.50}$$

$$\boldsymbol{\mathcal{N}}_2(x_i) = [\beta_{11}\rho_{10}(s)\rho_{11}(s)\mathbf{w}_{11}(s) + \beta_{20}\rho_{20}(s)\rho_{21}(s)\mathbf{w}_{21}(s) + \ldots]\, e^{-sx_i} \tag{6.51}$$

$$\vdots$$

$$\boldsymbol{\mathcal{N}}_t(x_i) = \left[\beta_{1t-1}\left(\prod_{\tau=0}^{t-1}\rho_{1\tau}(s)\right)\mathbf{w}_{1t-1}(s) + \ldots\right] e^{-sx_i}. \tag{6.52}$$

Dividing by $\prod_{\tau=0}^{t-1}\rho_{1\tau}(s)$, and since $\rho_{1\tau}(s)$ are the largest eigenvalues, as $t \to \infty$,

$$\boldsymbol{\mathcal{N}}_t(x_i) \to \beta_{1t-1}\mathbf{w}_{1t-1}(s)e^{-sx_i}\left(\prod_{\tau=0}^{t-1}\rho_{1\tau}(s)\right). \tag{6.53}$$

Without loss of generality, consider any component $\mathcal{N}_t$ of $\boldsymbol{\mathcal{N}}_t$ with corresponding eigenvector component $\mathbf{w}_{1t-1}(s)$. In the lattice at time t, n^0 lies somewhere between discrete points $x_{j(t)}$ and $x_{j(t)+1}$ (Figure 6.7). Hence,

$$\mathcal{N}_t(x_{j(t)}) \le n^0 \le \mathcal{N}_t(x_{j(t)+1}), \tag{6.54}$$

which can be written,

$$e^{-sx_{j(t)}} \le \frac{n^0}{\beta_{1t-1}w_{1t}(s)}\left(\prod_{\tau=0}^{t-1}\rho_{1\tau}(s)\right)^{-1} \le e^{-sx_{j(t)}}e^{-sh}. \tag{6.55}$$

Taking the natural logarithms and dividing by $-st$ yields,

$$\frac{1}{st}\ \ln\left(\frac{n^0}{\beta_{1t-1}w_{1t}(s)}\right) + \frac{1}{s}\left(\frac{1}{t}\sum_{\tau=0}^{t-1}\ln(\rho_{1\tau}(s))\right) \le \frac{x_{j(t)}}{t} \tag{6.56}$$

$$\le\ \frac{1}{st}\ln\left(\frac{n^0}{\beta_{1t-1}w_{1t}(s)}\right) + \frac{1}{s}\left(\frac{1}{t}\sum_{\tau=0}^{t-1}\ln(\rho_{1\tau}(s))\right) + \frac{h}{t}. \tag{6.57}$$

The spread rate $\mathcal{C}_t = \frac{x_{j(t)}}{t}$ is now a random variable. As $t \to \infty$,

$$\mathcal{C}_t = \frac{x_{j(t)}}{t} \to \frac{1}{s}\left(\frac{1}{t}\sum_{\tau=0}^{t-1}\ln(\rho_{1\tau}(s))\right), \tag{6.58}$$

$\mathcal{C}_t(s)$, the mean of (6.49) up to time t, evaluated using the dominant eigenvalue $\rho_{1\tau}$ of the time-dependant matrix $\tilde{\mathbf{H}}_t(s)$.

Bibliography

Allen, L., E. Allen, and S. Ponweera. 1996. A mathematical model for weed dispersal and control. Bulletin of Mathematical Biology **58**:815–834.

Aronson, D. and H. Weinberger. 1978. Multidimensional non-linear diffusion arising in population-genetics. Advances In Mathematics **30**:33–76.

Bjornstad, O. and J. Bascompte. 2001. Synchrony and second-order spatial correlation in host-parasitoid systems. Journal of Animal Ecology **70**:924–933.

Bonsall, M. and M. Hassell. 2000. The effects of metapopulation structure on indirect interactions in host-parasitoid assemblages. Proceedings of The Royal Society of London Series B-Biological Sciences **267**:2207–2212.

Bowes, G., D. Spurr, A. Thomas, D. Peschken, and D. Douglas. 1994. Habitats occupied by scentless chamomile (*Matricaria perforata* Merat) in Saskatchewan. Canadian Journal of Plant Science **74**:383–386.

Brannstrom, A. and D. Sumpter. 2005. Coupled map lattice approximations for spatially explicit individual-based models of ecology. Bulletin of Mathematical Biology **67**:663–682.

Buckley, Y., E. Brockerhoff, L. Langer, N. Ledgard, H. North, and M. Rees. 2005. Slowing down a pine invasion despite uncertainty in demography and dispersal. Journal of Applied Ecology **42**:1020–1030.

Caswell, H. 2001. Matrix Population Models: Construction, Analysis, and Interpretation. 2nd edition. Sinauer Associates.

Clark, J. 1998. Why trees migrate so fast: Confronting theory with dispersal biology and the paleorecord. American Naturalist **152**:204–224.

Douglas, D., A. Thomas, D. Peschken, G. Bowes, and D. Derksen. 1991. Effects of summer and winter annual scentless chamomile (*Matricaria perforata* Merat) interference on spring wheat yield. Canadian Journal of Plant Science **71**:841–850.

Durrett, R. and S. Levin. 1994. Stochastic spatial models - a users guide to ecological applications. Philosophical Transactions of The Royal Society of London Series **343**:329–350.

Dwyer, G. and W. Morris. 2006. Resource-dependent dispersal and the speed of biological invasions. American Naturalist **167**:165–176.

Ehler, L. 1998. Invasion biology and biological control. Biological Control **13**:127–133.

Fagan, W., M. Lewis, M. Neubert, C. Aumann, J. Apple, and J. Bishop. 2005. When can herbivores slow or reverse the spread of an invading plant? a test case from Mount St. Helens. American Naturalist **166**:669–685.

Fagan, W., M. Lewis, M. Neubert, and P. Van Den Driessche. 2002. Invasion theory and biological control. Ecology Letters **5**:148–157.

Hassell, M., H. Comins, and R. May. 1991. Spatial structure and chaos in insect population-dynamics. Nature **353**:255–258.

Hastings, A., K. Cuddington, K. Davies, C. Dugaw, S. Elmendorf, A. Freestone, S. Harrison, M. Holland, J. Lambrinos, U. Malvadkar, B. Melbourne, K. Moore, C. Taylor, and D. Thomson. 2005. The spatial spread of invasions: new developments in theory and evidence. Ecology Letters **8**:91–101.

Hinz, H., 1996. International Symposium on Biological Control of Weeds: Proceedings of the IX International Symposium on Biological Control of Weeds, Chapter scentless chamomile, a target weed for biological control in Canada: Factors influencing seedling establishment, pages 187–192 .

Hinz, H. and A. McClay. 2000. Ten years of scentless chamomile: Prospects for the biological control of a weed of cultivated land. Proceedings of the X International Symposium on Biological Control of Weeds pages 537–550.

Hinz, H. and H. Muller-Scharer. 2000. Influence of host condition on the performance of *Rhopalomyia n. sp* (Diptera: Cecidomyiidae), a biological control agent for scentless chamomile, *Tripleurospermum perforatum.* Biological Control **18**:147–156.

Jacquemyn, H., R. Brys, and M. Neubert. 2005. Fire increases invasive spread of molinia caerulea mainly through changes in demographic parameters. Ecological Applications **15**:2097–2108.

Janosi, I. and I. Scheuring. 1997. On the evolution of density dependent dispersal in a spatially structured population model. Journal of Theoretical Biology **187**:397–408.

Kaneko, K. 1992. Overview of coupled map lattices. Chaos **2**:279–282.

Kean, J. and N. Barlow. 2001. A spatial model for the successful biological control of *Sitona Discoideus* by *Microctonus Aethiopoides*. Journal of Applied Ecology **38**:162–169.

Knight, J. 2001. Alien versus predator. Nature **412**:115–116.

Kot, M., M. Lewis, and P. Van den driessche. 1996. Dispersal data and the spread of invading organisms. Ecology **77**:2027–2042.

Lewis, M., M. Neubert, H. Caswell, J. Clark, and K. Shea. 2005. A guide to calculating discrete-time invasion rates from data. Conceptual ecology and invasions biology, Springer.

Lui, R. 1989. Biological growth and spread modeled by systems of recursions .1. mathematical-theory. Mathematical Biosciences **93**:269–295.

Lym, R. 2005. Integration of biological control agents with other weed management technologies: Successes from the leafy spurge (*Euphorbia esula*) IPM program. Biological Control **35**:366–375.

McClay, A., R. Bourchier, R. Butts, and P. D.P., 2002. Biological control programmes in Canada, 1981-2000, Chapter *Cirsium arvense* (L.) Scopoli, Canada thistle (Asteraceae), pages 318–330 . CABI Pub.

McClay, A. and R. De Clerck-Floate. 1999. Establishment and early effects of *Omphalapion hookeri* (Kirby) (Coleoptera: Apionidae) as a biological control agent for scentless chamomile, *Matricaria perforata* Merat (Asteraceae). Biological Control **14**:85–95.

McClay, A., H. Hinz, R. De Clerck-Floate, and D. Peschken, 1995. The biology of Canadian weeds : contributions 62-83, Chapter *Matricaria perforata* Merat, scentless chamomile (Asteraceae), pages 395–402 . Agricultural Institute of Canada.

McLeod, S. and G. Saunders. 2001. Improving management strategies for the red fox by using projection matrix analysis. Wildlife Research **28**:333–340.

Meyer, J. and C. Lavergne. 2004. Beautes fatales: Acanthaceae species as invasive alien plants on tropical Indo-Pacific Islands. Diversity and Distributions **10**:333–U4.

Neubert, M. and H. Caswell. 2000. Demography and dispersal: Calculation and sensitivity analysis of invasion speed for structured populations. Ecology **81**:1613–1628.

Neubert, M., M. Kot, and M. Lewis. 2000. Invasion speeds in fluctuating environments. Proceedings of the Royal Society of London Series B-Biological Sciences **267**:1603–1610.

Neubert, M. and I. Parker. 2004. Projecting rates of spread for invasive species. Risk Analysis **24**:817–831.

Parker, I. 2000. Invasion dynamics of *Cytisus scoparius*: a matrix model approach. Ecological Applications **10**:726–743.

Peng, G., K. Bailey, H. Hinz, and K. Byer. 2005. *Colletotrichum sp*: A potential candidate for biocontrol of scentless chamomile (*Matricaria perforata*) in Western Canada. Biocontrol Science and Technology **15**:497–511.

Rees, M. and R. Hill. 2001. Large-scale disturbances, biological control and the dynamics of gorse populations. Journal of Applied Ecology **38**:364–377.

Rees, M. and Q. Paynter. 1997. Biological control of scotch broom: modelling the determinants of abundance and the potential impact of introduced insect herbivores. Journal of Applied Ecology **34**:1203–1221.

Sakai, A., F. Allendorf, J. Holt, D. Lodge, J. Molofsky, K. With, S. Baughman, R. Cabin, J. Cohen, N. Ellstrand, D. McCauley, P. O'Neil, I. Parker, J. Thompson, and S. Weller. 2001. The population biology of invasive species. Annual Review of Ecology and Systematics **32**:305–332.

Sharov, A. 2004. Bioeconomics of managing the spread of exotic pest species with barrier zones. Risk Analysis **24**:879–892.

Sharov, A. and A. Liebhold. 1998. Bioeconomics of managing the spread of exotic pest species with barrier zones. Ecological Applications **8**:833–845.

Shea, K. 2004. Models for improving the targeting and implementation of biological control of weeds. Weed Technology **18**:1578–1581.

Shea, K. and D. Kelly. 1998. Estimating biocontrol agent impact with matrix models: *Carduus nutans* in New Zealand. Ecological Applications **8**:824–832.

Shea, K. and D. Kelly. 2004. Modeling for management of invasive species: Musk thistle (*Carduus nutans*) in New Zealand. Weed Technology **18**:1338–1341.

White, S. and K. White. 2005. Relating coupled map lattices to integro-difference equations: dispersal-driven instabilities in coupled map lattices. Journal of Theoretical Biology **235**:463–475.

With, K. 2004. Assessing the risk of invasive spread in fragmented landscapes. Risk Analysis **24**:803–815.

Woo, S., A. Thomas, D. Peschken, G. Bowes, D. Douglas, V. Harms, and A. Mcclay. 1991. The biology of Canadian weeds .99. *Matricaria perforata* Merat (Asteraceae). Canadian Journal of Plant Science **71**:1101–1119.

Young, J. E., G. Sanchez-Azofeifa, S. Hannon, and R. Chapman. 2006. Trends in land cover change and isolation of protected areas at the interface of the southern boreal mixedwood and aspen parkland in Alberta, Canada. Forest Ecology and Management (***In Press***).

Chapter 7

Conclusion

In this dissertation I focused on matrix population models to study population growth and spread. The methodological tool presented here can prove useful in the study of the spread of invading organisms and their control. To my knowledge, the graph theoretic method for calculating R_0 (Chapter 4), generation time with generation function (Chapter 5) and rate of spread formulae for coupled map lattice models (Chapter 6), are new and have not been developed before.

In Chapter 3, I developed a new method for the calculation of the net reproductive rate, R_0. This method uses the graph representation of the life cycle of organisms without the need for matrix formalism, using Mason and Zimmermann's (1960) methods of graph reduction. The calculation of R_0 can also be done with the formula proposed by Cushing and Zhou (1994). The graph reduction method yields the same result. However, the method proposed here can be calculated directly from the graph, and yields a simplified equation.

The fact that an explicit formula for R_0 can be calculated allows for an analytical interpretation of life cycle pathways and their contribution to the population growth. Apart from being a practical tool, as shown in Chapters 5 and 6, the explicit R_0 reveals many aspects of the life history that can be analyzed in the context of control of invasive species. In the R_0 formula, all the pathways that contribute to reproduction like annual, biennial, perennial pathways, as well as vegetative reproduction, can be identified and their contributions to R_0 can be explored analytically.

In some cases, the use of R_0 to study the control of invading organisms has been suggested to be inappropriate (see Caswell, 2001; Levin et al., 1996). The fact that R_0 describes population growth *per generation* as opposed to λ that describes *per year* growth, does not determine how fast a population is growing. Thus, knowing the effects that particular life cycle events have on R_0 does not reveal effects on λ. I argue that, because of uncertainty of parameter estimation in matrix models, a safe strategy is to ensure that the population density of the invader will decrease over

time, therefore $\lambda < 1$. Since $\lambda < 1$ if and only if $R_0 < 1$, strategies can be designed using R_0, to find ways of reducing R_0 to be less than one.

As shown with Shea and Kelly's (1998) nodding thistle example in Chapter 4 and examples in Chapter 5, the same conclusion reached with elasticity analysis on λ, for specific parameter values, can be obtained in a much more general fashion for flexible parameter values using the analytical R_0 formula. The net reproductive rate can be use to complement demographic analysis based on the sensitivity and elasticity analysis.

Intrinsic growth rate and net reproductive rate are related throughout generation time (Caswell, 2001). In Chapter 5, I derived a formula for the calculation of the mean and variance of the generation time. Generation time, along with R_0, allows for the analysis of impacts of modes of reproduction and time of reproduction on invasiveness of organisms. This demographic quantity has been elusive for stage-structured models. Earlier methods were based on building a parallel age structure model to keep track of age (Cochran and Ellner, 1992; Lebreton, 2005). These methods are complicated and do not yield an analytical formula for generation time. The method proposed here, is simple and works on the stage structure life cycle graph. Further analysis is needed to explore the full potential of the quantities derived, specifically when applied to determine the evolutionary advantage of modes of reproduction and time of reproduction, and to the understanding of what makes some species more invasive than others.

Spread analysis of invading organisms has been well studied using diffusion equations and integro-difference equations (Shigesada and Kawasaki, 1997; Hastings et al., 2005). In Chapter 6, I showed that coupled map lattice models can also be used to calculate the rate of spread of populations, and derived formulae for calculating the rate of spread. Formulae for scalar and matrix CMLs, as well as stochastic environments, were also presented. The results of this thesis extend the work of Kot et al. (1996) on the rate of spread in integro-difference equation, Neubert et al. (2000) on integro-difference models in stochastic environments and Neubert and Caswell (2000) on matrix integro-difference equation.

The results show high intrinsic growth rates for scentless chamomile in Vegreville, Alberta, Canada. Scentless chamomile plasticity and profuse seed production make this weed difficult to control. As shown in Chapter 3, only large reductions in fecundity could have an impact on population growth and rate of spread. In Chapter 4, analysis of R_0 for scentless chamomile also indicates that fecundity should be the target for control. This is consistent with Hinz (1999), who obtained similar results for scentless chamomile in Europe.

Chapter 6 also indicates that, to control scentless chamomile spread, a large reduction in fecundity is needed. The rate of spread calculated, based on dispersal data obtained from Vegereville, is slow, and cannot explain long distance dispersal of

scentless chamomile across landscapes. The dispersal kernel used here only considers dispersal of scentless chamomile by seeds that fall on the ground, but does not consider wind or water dispersal.

The calculation of the true rate of spread is difficult. The tail of the kernel has large consequences to the rate of spread (Clark, 1998; Kot et al., 1996; Pielaat et al., 2006; Neubert and Caswell, 2000). Many studies reporting rate of spread for invading organisms, report a slow rate of spread when compared to the real distribution of the invading organism (e.g. Neubert and Parker, 2004; Garnier and Lecomte, 2006). In croplands, seeds could potentially be dispersed by mowing and tilling machines, and these dispersal mechanisms could disperse seeds further (see for example Bullock et al., 2003; Humston et al., 2005), making the tails of the kernel fatter, thus increasing the rate of spread.

Better calculation of the rate of spread for scentless chamomile should include a mechanistic model that include water and wind mediated dispersal in the kernel. Elasticity of life cycle entries on the rate of spread may yield a different result when fat tails are considered.

When studying scentless chamomile throughout this thesis, control agents were never considered. The focus was on what stages in the life history of scentless chamomile are better to target for control. This chapter also builds a model of scentless chamomile that could be used to optimize combined control strategies in space and time. Incorporating landscape information on heterogeneity, can be used to determine the distribution of control efforts over space and time.

In summary, the main results of this thesis are: 1) a method for the determination of an analytical R_0 formula based on the life cycle of an organism, 2) the theoretical implications of pathway contributions to the net reproductive rate and its application, 3) the calculation of a mean generation time and its variance, 4) the explicit formulation of unstructured or structured coupled map lattices and it application. 5) study of scentless chamomile control potential.

Bibliography

Bullock, J., I. Moy, S. Coulson, and R. Clarke. 2003. Habitat-specific dispersal: environmental effects on the mechanisms and patterns of seed movement in a grassland herb *Rhinanthus minor*. Ecography **26**:692–704.

Caswell, H. 2001. Matrix Population Models: Construction, Analysis, and Interpretation. 2nd edition. Sinauer Associates.

Clark, J. 1998. Why trees migrate so fast: Confronting theory with dispersal biology and the paleorecord. American Naturalist **152**:204–224.

Cochran, M. and S. Ellner. 1992. Simple methods for calculating age-based life-history parameters for stage-structured populations. Ecological Monographs **62**:345–364.

Cushing, J. and Y. Zhou. 1994. The net reproductive value and stability in matrix population models. Natural Resource Modeling **8**:297–333.

Garnier, A. and J. Lecomte. 2006. Using a spatial and stage-structured invasion model to assess the spread of feral populations of transgenic oilseed rape. Ecological Modelling **194**:141–149.

Hastings, A., K. Cuddington, K. Davies, C. Dugaw, S. Elmendorf, A. Freestone, S. Harrison, M. Holland, J. Lambrinos, U. Malvadkar, B. Melbourne, K. Moore, C. Taylor, and D. Thomson. 2005. The spatial spread of invasions: new developments in theory and evidence. Ecology Letters **8**:91–101.

Hinz, H., 1999. Prospects for the classical biological control of *Tripleurospermum perforatum* in North America. Ph.D. thesis, Freigurg-Schweiz University.

Humston, R., D. Mortensen, and O. Bjornstad. 2005. Anthropogenic forcing on the spatial dynamics of an agricultural weed: the case of the common sunflower. Journal Of Applied Ecology **42**:863–872.

Kot, M., M. Lewis, and P. Van den driessche. 1996. Dispersal data and the spread of invading organisms. Ecology **77**:2027–2042.

Lebreton, J. 2005. Age, stages, and the role of generation time in matrix models. Ecological Modelling **188**:22–29.

Levin, L., H. Caswell, T. Bridges, C. Dibacco, D. Cabrera, and G. Plaia. 1996. Demographic responses of estuarine polychaetes to pollutants: Life table response experiments. Ecological Applications **6**:1295–1313.

Mason, S. and H. Zimmermann. 1960. Electronic circuits, signals, and systems. Wiley.

Neubert, M. and H. Caswell. 2000. Demography and dispersal: Calculation and sensitivity analysis of invasion speed for structured populations. Ecology **81**:1613–1628.

Neubert, M., M. Kot, and M. Lewis. 2000. Invasion speeds in fluctuating environments. Proceedings of the Royal Society of London Series B-Biological Sciences **267**:1603–1610.

Neubert, M. and I. Parker. 2004. Projecting rates of spread for invasive species. Risk Analysis **24**:817–831.

Pielaat, A., M. Lewis, S. Lele, and T. de Camino-Beck. 2006. Sequential sampling designs for catching the tail of dispersal kernels. Ecological Modelling **190**:205–222.

Shea, K. and D. Kelly. 1998. Estimating biocontrol agent impact with matrix models: *Carduus nutans* in New Zealand. Ecological Applications **8**:824–832.

Shigesada, N. and K. Kawasaki. 1997. Biological invasions : theory and practice. 1st ed edition. Oxford University Press.